

THE UNIVERSITY OF CALGARY

POWER SYSTEM VOLTAGE STABILITY ASSESSMENT,
AND ENHANCEMENT BY VAR COMPENSATION

by

Oladiran Olugbolahan Obadina

A THESIS

SUBMITTED TO THE FACULTY OF GRADUATE STUDIES
IN PARTIAL FULFILLMENT OF THE REQUIREMENTS FOR THE
DEGREE OF DOCTOR OF PHILOSOPHY

DEPARTMENT OF ELECTRICAL ENGINEERING

CALGARY, ALBERTA

April, 1988

© Oladiran Olugbolahan Obadina 1988

Permission has been granted to the National Library of Canada to microfilm this thesis and to lend or sell copies of the film.

The author (copyright owner) has reserved other publication rights, and neither the thesis nor extensive extracts from it may be printed or otherwise reproduced without his/her written permission.

L'autorisation a été accordée à la Bibliothèque nationale du Canada de microfilmer cette thèse et de prêter ou de vendre des exemplaires du film.

L'auteur (titulaire du droit d'auteur) se réserve les autres droits de publication; ni la thèse ni de longs extraits de celle-ci ne doivent être imprimés ou autrement reproduits sans son autorisation écrite.

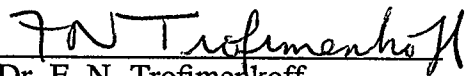
ISBN 0-315-42527-X

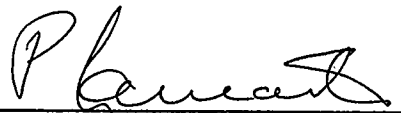
THE UNIVERSITY OF CALGARY
FACULTY OF GRADUATE STUDIES

The undersigned certify that they have read, and recommend to the Faculty of Graduate Studies for acceptance, a thesis entitled, "Power System Voltage Stability Assessement, and Enhancement by VAR Compensation", submitted by Oladiran O. Obadina in partial fulfillment of the requirements for the degree of Doctor of Philosophy.


Prof. G. J. Berg - Supervisor
(Dept. of Electrical Engineering)


Dr. N. D. Rao
(Dept. of Electrical Engineering)


Dr. F. N. Trofimenkoff
(Dept. of Electrical Engineering)


Dr. P. Lancaster
(Dept. of Mathematics and Statistics)


Dr. G. S. Christensen - External Examiner
(The University of Alberta)

Date: 1988-05-04

ABSTRACT

The main goal of this thesis is to develop analytical techniques for assessing power system security as far as static voltage stability is concerned and also for the planning of new volt-ampere-reactive (VAR) facilities to enhance security from voltage collapse.

A method of computing a practical voltage stability index, which serves to determine the voltage stability or otherwise of an operating point, is presented.

Simulation of a process that may lead to system voltage collapse is presented. The simulation is concerned with the action of the load-tap-changing (LTC) transformer following a system disturbance.

A new method of determining the voltage stability limit or critical state of a general multimachine power system is presented. In this method, the search for the stability limit is formulated as an optimization problem. The method accommodates device constraints or limitations in system equipment. A security index which may serve as a measure of the security of a given operating condition from voltage instability is defined.

A new method of planning shunt VAR compensation facilities is presented. The novel feature of this method is that the location and size of shunt VAR facilities are determined for the dual purpose of (i) achieving an acceptable system voltage profile, and (ii) achieving a specified degree of system security against voltage collapse. The

objective is also to minimize the total cost of the VAR installation.

ACKNOWLEDGEMENTS

I would like to express my gratitude to my Supervisor, Prof. Gunnar J. Berg, for his support, guidance and encouragement throughout this project.

Special thanks are also due to all my friends for their much needed moral support and encouragement during this project.

Financial assistance received from the Department of Electrical Engineering, University of Calgary, in the form of teaching assistanceships, is also gratefully acknowledged.

Finally, I would like to thank my wife, Ronke, and my children, Damola and Dotun, for their patience, understanding, and encouragement, without which I could hardly have completed this work.

Dedicated with love to
my wife, Ronke,
and
my children, Damola and Dotun;
-they are the salt of the earth.

TABLE OF CONTENTS

APPROVAL PAGE	ii
ABSTRACT	iii
ACKNOWLEDGEMENTS	v
DEDICATION	vi
TABLE OF CONTENT	vii
LIST OF TABLES	x
LIST OF FIGURES	xiii
LIST OF SYMBOLS	xv
1 INTRODUCTION	
1.1 BACKGROUND	1
1.2 LITERATURE SURVEY	4
1.2.1 Voltage Stability Conditions	5
1.2.2 Proximity Indicators	7
1.2.3 Control Strategies	9
1.2.4 Planning Network Reinforcement	9
1.3 OBJECTIVES AND CONTRIBUTIONS OF THE THESIS	10
1.3.1 Objectives of Thesis	10
1.3.2 Contributions of Thesis	11
1.4 SUMMARY OF THESIS CHAPTERS	12
2 POWER SYSTEMS VOLTAGE INSTABILITY	
2.1 INTRODUCTION	14
2.2 ANALYSIS OF VOLTAGE INSTABILITY -A SIMPLE EXAMPLE	15
2.3 REVIEW OF VOLTAGE STABILITY CONDITIONS	19
2.4 EVALUATION OF VOLTAGE STABILITY INDEXES	23
2.4.1 Applications	30
2.5 SIMULATION STUDY	35
2.5.1 LTC Transformer Tap Model	35
2.5.2 Load Model	36
2.5.3 Steps in the Simulation	37
2.5.4 Results of Simulation	38
2.6 CONCLUSIONS	43

3	DETERMINATION OF POWER SYSTEMS VOLTAGE STABILITY LIMIT	
3.1	INTRODUCTION	45
3.2	SIMPLE NETWORK	47
3.3	GENERAL FORMULATION	49
3.4	INCLUSION OF LOAD-VOLTAGE CHARACTER	59
3.5	SECURITY MARGIN	61
3.6	SOLUTION METHOD	62
3.6.1	Solution of QP Subproblem	67
3.6.2	Overall Algorithm	72
3.7	EXAMPLES OF APPLICATION	74
3.7.1	System One: 14-Bus Network	76
3.7.2	System Two: 28-Bus Network	86
3.8	CONCLUSIONS	93
4	IDENTIFICATION OF STRONG AND WEAK SPOTS IN A POWER SYSTEM FROM VOLTAGE STABILITY VIEWPOINT	
4.1	INTRODUCTION	96
4.2	METHOD ONE: RELATIVE VOLTAGE CHANGE METHOD	98
4.3	METHOD TWO: SENSITIVITY METHOD	100
4.3.1	Interpretation of the Lagrangian Multipliers	103
4.3.2	Evaluation of the Lagrangian Multipliers	107
4.4	NUMERICAL EXAMPLE	109
4.4.1	Radial System	110
4.4.2	14-Bus System	112
4.4.3	20-Bus System	117
4.5	CONCLUSIONS	121
5	VAR PLANNING FOR POWER SYSTEMS SECURITY	
5.1	INTRODUCTION	122
5.2	SECURITY	123
5.2.1	Concepts	123
5.2.2	Effects of VAR Compensation	126
5.3	SECURITY ASSESSMENT	128
5.4	VAR SUPPLY - FORMULATION	128
5.4.1	VAR Supply Costs	129
5.4.2	Voltage Magnitude Constraints	130
5.4.3	Security Margin Constraints	132
5.4.4	Overall Problem Formulation	134

5.5	A TWO-STAGE SOLUTION ALGORITHM	135
5.5.1	First Stage Solution	135
5.5.2	Second Stage Solution	136
5.5.3	Sensitivity Vectors	140
5.5.4	Steps in the Digital Solution	142
5.6	CONSIDERATION OF CONTINGENCIES	142
5.7	RESULTS	145
5.8	CONCLUSIONS	151
6	CONCLUSIONS AND RECOMMENDATIONS FOR FUTURE WORK	
6.1	INTRODUCTION	153
6.2	CONCLUSIONS	153
6.3	RECOMMENDATIONS FOR FURTHER WORK	155
	REFERENCES	157
	APPENDIX I	167
	APEENDIX II	171
	APPENDIX III	177

LIST OF TABLES

Table 2.1: Solution One: 28-Bus Network	33
Table 2.2: Solution Two: 28-Bus Network	34
Table 3.1: Load Distribution Vector (14-Bus Network)	76
Table 3.2: Generator Participation Factors (14-Bus Network)	76
Table 3.3: System Condition at the Voltage Stability Limit (Load MVA Independent of Bus Voltage)	79
Table 3.4: System Condition at the Voltage Stability Limit (With Line Outage)	81
Table 3.5: System Condition at the Voltage Stability Limit (Generator MW and MVAR Limits Ignored)	82
Table 3.6: System Condition at the Voltage Stability Limit (With Line Outage and Generator Limits Ignored)	84
Table 3.7: System Condition at the Voltage Stability Limit (Impedance Load Representation)	85
Table 3.8: Load Distribution Vector (28-Bus Network)	88
Table 3.9: Generator Participation Factors (28-Bus Network)	88
Table 3.10: System Condition at the Stability Limit (28-Bus Network) (Load MVA Independent of Bus Voltage)	89
Table 3.11: System Condition at the Stability Limit (28-Bus Network) (With Line Outage)	92
Table 4.1: Line and Transformer Data (Radial Network)	111
Table 4.2: Initial and Limiting System States (Radial Network)	112

Table 4.3: Bus Strength Indexes (Radial Network)	112
Table 4.4: Initial and Limiting System States (14-Bus Network)	113
Table 4.5: Bus Strength Indexes (14-Bus Network)	113
Table 4.6: Area Strength Indexes (14-Bus Network)	117
Table 4.7: Initial and Limiting System States (20-Bus Network)	118
Table 4.8: Bus Strength Indexes (20-Bus Network)	119
Table 4.9: Area Strength Indexes (20-Bus Network)	119
Table 5.1: Contingency List	146
Table 5.2: Specified Security Limits	146
Table 5.3: System Voltages and SM Before VAR Allocation	147
Table 5.4: VAR Support Parameters	148
Table 5.5: Result of Solution of First Stage Subproblem	149
Table 5.6: Result After Solution of Second Stage Subproblem	150
Table 5.7: System Voltages and SM After VAR Allocation	151
Table III.1: Initial Operating Condition of the 14-Bus Network	179
Table III.2: Regulated Bus Data	179
Table III.3: Line and Transformer (14-Bus Network)	180
Table III.4: Cost of Generation	180
Table III.5: Initial Operating Condition of the 28-Bus Network	183
Table III.6: Regulated Bus Data	184
Table III.7: Cost of Generation (28-Bus Network)	184

Table III.8: Line and Transformer (28-Bus Network)	185
Table III.9: Initial Operating Condition of the 20-Bus Network	186
Table III.10: Regulated Bus Data (20-Bus Network)	188
Table III.11: Line and Transformer (20-Bus Network)	189

LIST OF FIGURES

Figure 2.1: Simple System	18
Figure 2.2: At-Load Voltage Variation (pf=0.93)	18
Figure 2.3: Voltage Stability Index Versus MVA Load	31
Figure 2.4: System Studied for Simulation	39
Figure 2.5a: Time-Domain Response of the Receiving End (Bus 2) Voltage ($Y_c = 0$)	40
Figure 2.5b: Time-Domain Response of the Total MVA Demand ($Y_c = 0$)	40
Figure 2.6a: Time-Domain Response of the Receiving End (Bus 2) Voltage ($Y_c = 3.0$ pu)	41
Figure 2.6b: Time-Domain Response of the Total MVA Demand ($Y_c = 3.0$ pu)	41
Figure 3.1: Flowchart of the SQP Algorithm	73
Figure 3.2a: Voltage Versus MVA Load At Bus 3 (pf Constant)	78
Figure 3.2b: Voltage Versus MVA Load at Bus 12 (pf Constant)	78
Figure 3.3: SM Versus Load Exponent (14-Bus System)	87
Figure 3.4a: Voltage Versus MVA Load At Bus 4 (pf Constant)	91
Figure 3.4b: Voltage Versus MVA Load at Bus 5 (pf Constant)	91
Figure 3.5: SM Versus Load Exponent (28-Bus System)	94
Figure 4.1: 4-Bus Radial Network	111

Figure 4.2: Areas of the AEP 14-Bus Network	116
Figure 4.3: Areas of the 20-Bus Network	120
Figure 5.1: Simple System	124
Figure 5.2: At-Load Voltage Variations	124
Figure 5.3: Simple System with Compensation	127
Figure 5.4: At-Load Voltage Variations Including Compensation	127
Figure 5.5: Flowchart of Basic Solution Method	143
Figure 5.6: Flowchart of VAR Support Planning Considering Contingencies	144
Figure III.1: AEP 14-Bus Network	178
Figure III.2: 28-Bus Network	182
Figure III.3: 20-Bus Network	187

LIST OF SYMBOLS

$[\cdot]^T$	Transpose of a matrix
$[\cdot]^{-1}$	Inverse of a matrix
$\ \cdot\ _2$	Euclidean norm of a matrix
$\bar{\cdot}$	Complex quantity
$\underline{\cdot}$	Vector quantity
V_i	Voltage magnitude at bus i
δ_i	Voltage angle at bus i
\bar{Y}_{ij}	Complex ij^{th} element of the bus admittance matrix
P_i	Real power injection at bus i
Q_i	Reactive power injection at bus i
S_i	MVA power injection at bus i
β	Load distribution vector
γ	Vector of Generator participation factors.
J_L	Set of all load buses
J_G	Set of all generator buses
$\underline{\lambda}$	Vector of Lagrange multipliers
q_{ci}	New capacitive VAR at bus i

q_{ri}

New inductive VAR at bus i

CHAPTER 1

INTRODUCTION

1.1 BACKGROUND

Electric power systems are an integral part of all industrially developed societies. The electricity generated and transmitted by these power systems has proven to be a most convenient, flexible, clean, safe, efficient, and useful form of energy. At the present time, a lack of electricity is newsworthy. Electricity is so vital in the lives of people that its unavailability causes inconvenience, loss of production, and danger to many individuals, including those who are hospitalized. A prolonged blackout could lead to social disorder, and even national tragedy [1].

The blackout problem of an electric power system has traditionally been associated with the steady state and transient stability problems. Steady state and transient instability are the phenomena involved in connection with the loss of a major portion of a grid due to the inability of certain generators to maintain synchronism in the face of small and large disturbances respectively [2]. These types of instability are, generally speaking, well understood today. System stability is being preserved to a greater extent than ever by the advent of faster and more effective stabilizers [3], and more reliable protection systems [4].

In recent years a category of instability, usually termed voltage instability or collapse, has been responsible for several major blackouts world-wide. There have been reported cases of voltage instability phenomena in France [5], Belgium [6], the United States [7], Japan [8], and recently in the Ontario Hydro system in Canada [9].

As frequency is a critical parameter in the balance between real (MW) generation and real (MW) load throughout the power system, so transmission voltage levels reflect the balance between the supply and demand of reactive power. While frequency is uniform throughout the power system, voltage levels can vary markedly across a transmission network, designed to operate at a particular voltage level. As a result, it is generally accepted that the voltage instability problem, which is associated with the inability of a power system to maintain bus voltage magnitudes, is due to a deficit of reactive power at certain buses in the network [10,11]. The actual process of collapse may therefore be triggered by some form of disturbance, resulting in significant changes in the reactive power balance in the system.

The operating environment of many present-day power systems substantially increases the vulnerability of the system to reactive deficit problems and therefore difficulties in maintaining system voltage profiles. Several factors have contributed to this situation. There is increasing difficulty in obtaining power plant sites in the vicinity of major power consumers. Also, the exploitation of hydro power resources has proceeded spectacularly to a point where remote, large generation

plants have been developed [1]. As a result, electrical power is often transported through high capacity lines over long distances from generation to consumer. Furthermore, the strengthening of transmission networks has been curtailed in general by high costs, and in particular cases by the difficulty of acquiring right-of-way [12]. This has resulted in increased loading and exploitation of the older circuits.

Other factors include the relative decrease in the reactive power outputs of generating units, and shifts in power flow patterns associated with changing fuel costs and generator availability [12].

Literature on voltage collapse problems reveals that system voltage collapse can take several forms [13,14]. In some cases, phase angle and frequency remained constant while voltage continued to decay to a critical value causing protection equipment to react and effectively dismantle the network. This form of voltage collapse is associated with the instability of the slow secondary voltage control equipment (load-tap-changing (LTC) transformer, capacitor switching, and load shedding). It occurs when the system does not have enough capacity to supply the load. Because the collapse process occurs over a relatively long period of time (several seconds to several minutes), it is generally referred to as being static rather than dynamic. In other cases, frequency and angle swings accompany the voltage decay. This dynamic mechanism of voltage collapse is related to the transient stability of post-contingency conditions [15,16].

The incidents of voltage collapse are of serious concern to the electric utility industry, which is actively pursuing the development of computer-aided procedures to avert the process or minimize its effect.

Procedures that are being considered include:

- (i) Procedure to determine the voltage stability or otherwise of a given or anticipated operating condition.
- (ii) Procedure to assess the margin of an operating condition to voltage collapse.
- (iii) Control methods to move the system to a more secure operating condition if security is in jeopardy.
- (iv) Planning network reinforcement for improved security to collapse.

In response to these concerns, research efforts are made today in many countries to clarify voltage instability or collapse, and to develop new planning criteria and on-line security monitoring and control tools that may help in averting blackouts [5-45].

1.2 LITERATURE SURVEY

In the literature, the static and dynamic mechanisms of voltage collapse have been studied separately. This is because of the time scale separation between the dynamic changes in frequency and those in voltage due to the secondary voltage control equipment.

This thesis is concerned with the static mechanism of voltage collapse. Existing literature may be categorized on the basis of the concerns listed in Section 1.1 above. Literature on the dynamic mechanism is just beginning to emerge [38,43].

1.2.1 Voltage Stability Conditions

Some work has been reported on defining and establishing voltage stability criteria, i.e., criteria that may be used to determine whether or not an operating condition is stable from voltage stability viewpoint. These voltage stability criteria are based on the natural cause-effect relationships that exists at load buses in the power system under normal (stable) conditions. Also, some of the criteria are based on the qualitative study of the simple two-bus power system.

In [40], Concordia defined voltage instability as being manifested by the fact that when the load impedance decreases (i.e., more load is added), the resulting voltage decrease is so large that the load power consumption does not increase, or even decreases. This stability criterion was applied to and demonstrated for the simple two-bus system. However, it is not readily applicable to a practical system since loads are generally not of the impedance type.

In [22] and [42], it is suggested that an operating condition is stable from the voltage viewpoint if every load bus voltage increases when a source voltage increases or when a shunt capacitor is switched in at a load bus. Mathematical conditions are derived based on this definition. The mathematical conditions require that for voltage stability the reduced Jacobian matrix of the load flow

equations must be nearly equal to an M-matrix. A matrix with non-positive off-diagonal elements is referred to as an M-matrix if it is non-singular, and elements of its inverse are all nonnegative. Unfortunately, it is apparent that this condition may not be sufficient.

As noted in [25], transformer taps are a major contributing factor in system voltage collapse. In [8,30,37], voltage instability is characterized in association with the slow tap-changing transformer dynamics. Stability conditions are derived in terms of allowable transformer taps settings using eigenvalue analysis. These methods requiring eigenvalue analyses are not easily applicable in practice.

In [32] Borremans et. al. proposed a criterion for voltage stability of a given operating condition. The criterion states that for an operating point, voltage stability is ascertained when at that operating point, an elementary increase of reactive demand is met by a finite increase in reactive power generation. Analytical computation of an index, which is defined on the basis of this criterion, for the simple two-bus system was presented in the paper. In order to generalize this criterion to a general power network the paper suggested the use of two load flow computations. Even though this criterion seems quite practicable, the generalization requiring two load flow computations may be quite time consuming for most power systems.

1.2.2 Proximity Indicators

A number of indices have been proposed to assess the proximity of a operating condition to voltage collapse. Some of the proposed indices are based on the observation by several investigators that the Jacobian matrix of the load flow equations is singular at the voltage stability limit or the collapse point [13,34].

Tamura et. al. [13] were one of the first to observe a relation between the singularity of the Jacobian matrix and static voltage stability limit. Kwatny et. al. [34] studied the stability limit problem as a static divergence or bifurcation characterized by the disappearance of an equilibrium point. Beyond this point, solutions to the load flow equations cannot be obtained.

In [14], Tiranuchit et. al. suggested the use of the minimum singular value of the Jacobian matrix of the load flow equations as a security index, and derived static control strategies based on this index. Kessel et. al. [31] developed a voltage stability index based on the feasibility of solution to the load flow equations at each bus. In [33], Jarjis et. al. used a generalized eigenvalue approach to determine supporting hyperplanes of the feasibility region. The method serves to indicate the stability margin of an operating point.

One common drawback of all these methods is that the operating constraints on system equipment (e.g. MW and MVAR limits of system generating units) are not taken into consideration. As noted by Edwin et. al. (discussion to [31]), production capabilities of generating units are important considerations, moreso since voltage collapse is considered to be a reactive power problem.

In [18], Venikov et. al. suggested the use of repeated load flow computations, as power injections are increased, to determine the voltage stability limit. Having determined the stability limit, the margin to collapse is then available. However, besides being computationally very demanding, this approach may be inadequate due to the unreliable behaviour of the Newton-Raphson method of load flow analysis in the vicinity of the voltage stability limit. This behaviour is linked to the singularity of the Jacobian at the voltage stability limit, and the existence of close multiple load flow solutions around that limit.

Flatabo et. al. [26] suggested the use of a combination of load flow analysis and sensitivity parameters in order to reduce the computation time and circumvent the numerical ill-conditioning known to occur as the voltage stability limit is approached. Another possible short-cut to the repeated load flow calculations is the quadratic extrapolation method proposed in [32]. These methods are inherently approximate and may yield unrealistic results:

Another approximate method is suggested by Barbier et. al. [25] to evaluate the condition at the voltage stability limit. Other approximate methods have been suggested which are derived from the study of the simple two-bus power system. Details of these may be found in [32,44]. Again, these methods being approximate, may yield unrealistic results.

1.2.3 Control Strategies

In comparison to the subject on proximity indicators, not much has appeared in the literature as regards control strategies to improve system security against voltage collapse. As noted previously, Tiranuchit et. al. [14] suggested control strategies using the minimum singular value of the Jacobian of the load flow equations as an index. In [45], Kirschen et. al. suggested a method of rescheduling generators' MW power output to correct voltage violations using linear programming. Methods such as LTC transformer tap blocking and generator MW output rescheduling are also suggested in [25].

It is noted in [34], that a control strategy should identify the weakest or critical bus in a transmission system. Knowledge of this is useful since the collapse process may be initiated from this critical bus. The critical bus may be the most effective location to apply emergency countermeasures (for example, load shedding) in order to save the rest of the system.

Kessel et. al. [31] proposed a method of identifying the system critical bus based on certain indices which measure the proximity of the load at each bus to the feasibility limit. Again, these indices do not take the limits of system equipment into consideration and may therefore yield unrealistic results.

1.2.4 Planning Network Reinforcement

As mentioned previously, the problem of voltage collapse is usually precipitated by reactive power deficiency. It is therefore apparent that the security of the

power system against collapse may be improved at the planning stages by locating adequate shunt VAR compensation equipment at key buses in the network.

Much work has been reported in the literature on the problem of planning shunt VAR facilities for maintaining voltage magnitudes within specified limits. Some of this work is reported in references [46] to [55]. However, as noted by many investigators [19,28], voltage magnitudes alone is not a good enough indicator of the proximity of an operating condition to collapse. Therefore, shunt VAR sources need to be planned for purposes of voltage collapse prevention as well as voltage magnitude considerations.

In [8] and [14], methods are presented for identifying the most beneficial locations to install shunt capacitors for the purpose of improving system security as far as voltage collapse is concerned. It is clear that just identifying the best location is not sufficient. The size and locations of VARs needed to meet a minimum specified security requirement, while minimizing costs, should be determined.

1.3 OBJECTIVES AND CONTRIBUTIONS OF THE THESIS

1.3.1 Objectives of Thesis

As already pointed out, most of the work and methods related to assessing the margin of an operating condition to the collapse point do not take the operational limits of system equipment into consideration. In particular, the MW and MVAR production capabilities of system generators, and the limits of transformer tap set-

tings are of importance since the problem of voltage collapse is usually a reactive power problem.

The main objectives of this thesis are as follows:

- (i) To develop a method of assessing the margin of an operating condition to voltage collapse, taking into consideration the operational limits of system equipment.
- (ii) To develop a method of identifying electrically weak buses in a transmission system. As mentioned previously, knowledge of the system's weakness is essential for effective control purposes.
- (iii) To develop a method of planning shunt VAR sources (static capacitors and inductors , synchronous condensers) for purposes of strengthening the network thereby improving security as far as voltage collapse is concerned.

1.3.2 Contributions of Thesis

The main contributions of this thesis may be summarized as follows:

- (i) The voltage stability conditions proposed in [32] is generalized for application to practical size power systems.
- (ii) A method of determining the voltage stability limit of a general power system accurately and directly is proposed. The methodology takes the operational limits of system equipment into account, and its applications illustrated by examples. A security margin to collapse is subsequently defined.

- (iii) Two methods of identifying the system's weakest bus are proposed.
- (iv) A method of planning shunt VAR compensation facilities for improved (specified) system voltage security is proposed.

1.4 SUMMARY OF THESIS CHAPTERS

In Chapter 2, an analysis of a simple two-bus power system is presented in order to provide an insight into the problem of voltage instability. A method to determine the voltage stability condition proposed in [32] for a practical size power system is presented. The method uses sensitivity parameters computed at the given operating point. It does not require repeated load flow computations. Application of the method to a 28-bus network is given.

Simulation of a process that may lead to voltage collapse is presented. The simulation study is concerned with the action of the LTC transformer following a system disturbance. It also takes into account the load-voltage characteristics of the exponential type.

In Chapter 3, a method is presented to determine the voltage stability limit or critical point of a multimachine power system. The problem is formulated as a nonlinear optimization problem. With this formulation, the limits on system equipments are taken into consideration. The formulation also accommodates consideration of the system's load-voltage characteristics. The solution of the optimization problem using the sequential quadratic programming algorithm is discussed. A security margin which may serve as a measure of the system's security from

collapse is defined. Results of applications of the method to two example systems are presented and discussed.

In Chapter 4, two methods to identify the system's weakest spot are presented. The methods take advantage of the approach described in Chapter 3 for determining the voltage stability limit. The first method is based on the voltage change at each bus as the system condition changes from an initial point to the voltage stability limit. The other method is based on sensitivity information computed at the voltage stability limit. The two methods give practically identical results when applied to three example systems.

In Chapter 5, a new method of planning VAR compensation facilities for the purpose of improving system voltage profile and security is presented. The objective is also to minimize the total cost of the VAR installation. The problem is formulated as a mixed-integer nonlinear programming (MINP) problem. A two-stage algorithm to obtain a near-optimal solution is presented. An algorithm to consider contingency situations is also presented. Results of application of the method are presented and discussed.

In Chapter 6, the main conclusions on the work reported in the thesis are given together with some suggestions for further research in this area.

CHAPTER 2

POWER SYSTEMS VOLTAGE INSTABILITY

2.1 INTRODUCTION

The phenomena of voltage instability or collapse may take several forms. It is characterized by progressive falling bus voltages, and it has occurred in connection with several major blackouts throughout the world. The main problem arises because of inability of the network to meet a demand for reactive power, required to sustain satisfactory voltage levels. The collapse process may be aggravated by the load-voltage characteristics. For example, the induction machine loads, which often constitute 60-70 percent of the total system loads [57], have the characteristics that, below a certain voltage level, the reactive demand increases as supply voltage decreases. This causes a further decrease in voltage.

As mentioned in Chapter 1, this thesis is concerned with the static aspect of voltage collapse. This form of voltage instability is associated with the instability of the slow secondary voltage control equipment (load tap-changing (LTC) transformer, capacitor switching, load shedding). Owing to its slow nature, this process is classed as being static. Within this context, it is desirable to know, amongst other things, whether a proposed operating condition is stable from the voltage stability viewpoint. In other words, given a projected system state,

identified, e.g., in terms of a solution to the load flow equations, it is desirable to know whether the systems voltage controllers would function in a stable mode.

In the next section, an analysis of a simple power system is presented in order to give insight into the problem of voltage instability and collapse. In section 2.3, a brief review of some of the methods proposed to assess the voltage stability of a power system is given. In section 2.4, the evaluation of a voltage stability condition is presented. Simulation of a process that may lead to system voltage collapse is presented in section 2.5.

2.2 ANALYSIS OF VOLTAGE INSTABILITY -A SIMPLE EXAMPLE

In order to provide insight into the problem of voltage instability considered, a simple power system will be examined first. The condition for voltage stability will be derived.

Figure 2.1 shows the simple system including an impedance load, $\bar{Z}_R = Z_R \angle \phi$, supplied by a constant voltage source, \bar{V}_1 , through a transmission line of impedance $\bar{Z}_L = Z_L \angle \xi$ and a LTC transformer of turns ratio $t : 1$. It is assumed that the LTC transformer is used to regulate the voltage at the receiving end.

Letting

$$\bar{Z} = \frac{\bar{Z}_L}{\bar{Z}_R} = Z \angle \theta,$$

it can be shown that,

$$V_R = \frac{t V_1}{[(t^2 + Z \cos \theta)^2 + (Z \sin \theta)^2]^{1/2}} \quad (2.1)$$

where, V_R is the magnitude of the receiving end voltage.

Normal operation of the LTC transformer involves turns ratio adjustment corresponding to a change in V_R . If V_R drops, t is decreased, thereby raising V_R . Thus $\Delta t < 0$ requires $\Delta V_R > 0$ for stable operation. However, if $\Delta t < 0$ results in $\Delta V_R < 0$, the receiving end voltage will be reduced further, indicating voltage collapse. Therefore, for voltage-stable operation of this system, a necessary condition is that,

$$\frac{dV_R}{dt} < 0 \quad (2.2)$$

Combining equations (1) and (2) we find the corresponding condition,

$$Z < t^2 \quad (2.3)$$

Hence for voltage stability,

$$\frac{|Z_L|}{|Z_R|} < t^2 \quad (2.4)$$

Assuming for example that the operating value of t is equal to 1 (the nominal

value), equation (2.4) reduces to

$$\frac{|Z_L|}{|Z_R|} < 1 \quad (2.5)$$

For normal stable operation $|Z_R| > |Z_L|$. However, it may turn out that $|\bar{Z}_R| < |\bar{Z}_L|$ due to a system disturbance causing line outage (increasing source impedance), or due to excessive real and/or reactive power pickup at the load end (decreasing $|\bar{Z}_R|$).

Figure 2.2 shows the variation of V_R against MVA demand S_R , at constant power factor. Point A (where $V_R = V_R^{crit}$) represents the critical system state. The upper segment ($V_R > V_R^{crit}$) is considered the stable operating region, satisfying equation (2.5). The broken line is a similar plot for a higher sending end voltage V_1 . It can be seen that in the stable region, increasing the sending end voltage increases the receiving end voltage whereas, in the unstable region, increasing the sending end voltage actually reduces the receiving end voltage. It should also be observed that for an initial operating point in the unstable region, a load shedding action (reducing MVA load or increasing Z_R) causes further reduction in the receiving end voltage.

The critical point corresponds to the condition $|\bar{Z}_L| = |\bar{Z}_R|$ which is the condition under which the maximum available power is obtained at the receiving

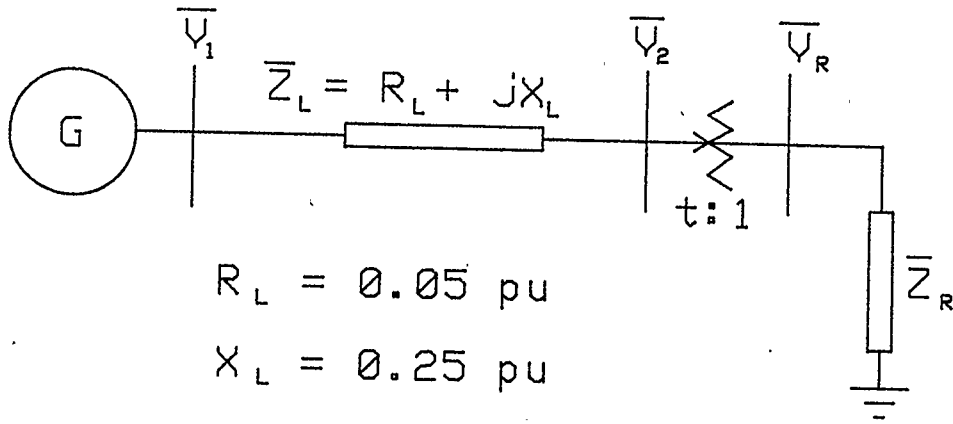


Figure 2.1: Simple System

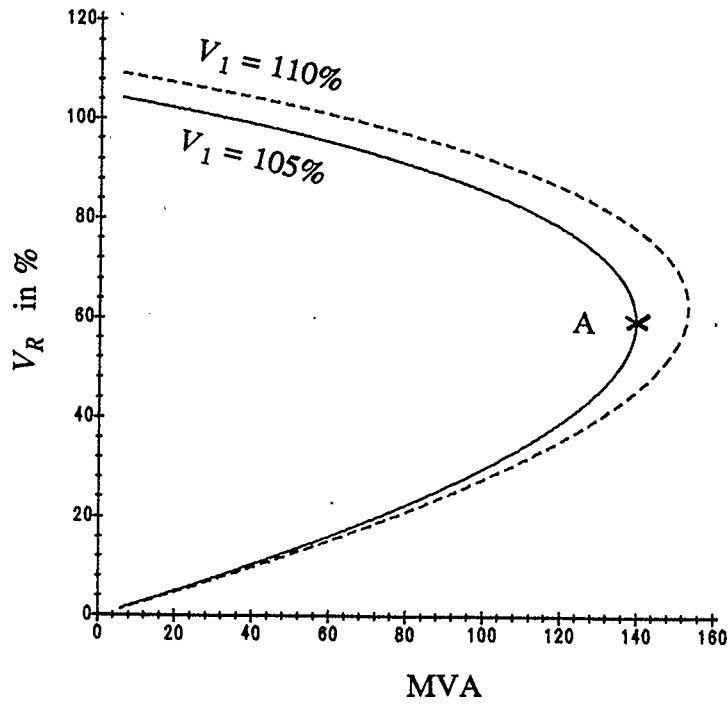


Figure 2.2: At-Load Voltage Variations
($pf = 0.93$)

end. This power is

$$\bar{S}_R^{\max} = P_R^{\max} + jQ_R^{\max} = \frac{1}{4} \frac{e^{j\phi}}{\cos^2\left(\frac{\xi - \phi}{2}\right)} \frac{V_1^2}{Z_L} \quad (2.6)$$

The corresponding load voltage, which is the minimum stable voltage at the load terminal, is

$$\bar{V}_R^{\text{crit}} = \frac{e^{j\left(\frac{\phi - \xi}{2}\right)}}{2 \cos\left(\frac{\xi - \phi}{2}\right)} \bar{V}_1 \quad (2.7)$$

It will be useful to know not only that the system is operating on the stable portion of the curve but also how close it is to the the voltage stability limit or critical point.

2.3 REVIEW OF POWER SYSTEMS VOLTAGE STABILITY CONDITIONS

Several conditions for the voltage stability of an operating point have been proposed. Venikov [42] suggested a criterion using the model for a simple system where power is transmitted from one bus through a transmission line to the load bus. The receiving end voltage is stable from voltage standpoint if the voltage at the receiving end, V_R , increases as the sending end voltage V_1 increases, i.e.,

$$\frac{dV_1}{dV_R} > 0$$

Abe et. al. [22] generalized this idea to multigenerator multiload systems and deduced that the power system is stable from the voltage stability viewpoint if the voltage at every load bus increases when any of the source voltages increases, or when a static capacitor is switched on at a load bus. It is then shown that for this condition to hold, the reduced Jacobian matrix of the load flow equations should be nearly equal to an M-matrix. A matrix B with non-positive off-diagonal elements is an M-matrix if B is non-singular, and elements of B^{-1} are all nonnegative.

In [8], Abe et. al. included the dynamics of the load tap changers with the power flow equations. Stability of an operating point is analysed. Stability conditions are derived based on the eigenvalues of the set of linearized dynamic system equations.

In [30] Liu et. al. studied system voltage stability via linearized dynamical equations of the LTC transformer taps and steady state decoupled reactive power equations. A set of conditions for voltage stability is derived for a hyperbox of tap settings and load bus voltages, using eigenvalue analysis.

Medanic et. al. [37] proposed an approach to modeling, analysis and design of slow distributed voltage control schemes. A nonlinear discrete type dynamical model governed by the LTC transformer taps as control tools is studied. Conditions are derived to predict when the LTC based scheme may be poorly coordi-

nated and not be able to maintain voltages.

Tamura et. al. [13] suggested that voltage instability is related to the multiple power flow solutions. It was noted in [13] that close multiple voltage solution pairs are likely to occur under heavy loading conditions, and that the individual solutions of the pair have different features from the standpoint of stability. When there is a pair of multiple power flow solutions where one is stable while the other is unstable, the effect of voltage control that is beneficial to the stable solution may be detrimental to the unstable solution.

Kwatny et. al. [34] suggested that bifurcation theory may provide an appropriate tool for the analysis of multiple power flow solutions. They have studied voltage instability along this line. It is shown in [34] that an equilibrium point is stable if it is strictly causal and stable in the sense of Liapunov.

The above methods are of theoretical interest and not easily applicable in practice.

In [32], Borremans et. al. proposed a criterion for the voltage stability of a given operating condition. The criterion states that for an operating point, voltage stability is ascertained when at that operating point an elementary increase of reactive power demand is matched by a finite increase of reactive power generation. If an index VS (voltage stability) is defined,

$$VS = \left. \frac{dQ_R}{dQ_G} \right|_{\Delta P_R=0}$$

where Q_G is the sum of the generated reactive powers, and P_R and Q_R are the real and reactive demands, Borremans stability condition may be stated,

$$VS > 0 \quad (2.8)$$

The paper [32] discusses analytical computations of the index, VS, for a simple two-bus power network. Borresman et. al. suggest that with a power flow analysis program, it is possible to evaluate the VS indexes for all load buses in a practical size power network. First, a power flow analysis gives Q_G for the base case. Then a reactive power variation, ΔQ_{Li} , is imposed at a given bus i (or similar simultaneous variations at load buses in an area). A second power flow analysis gives the change ΔQ_G corresponding of the reactive power generated by the generators, the synchronous condensers (taking into account their physical limitations), shunt capacitors and line charging. The ratio $\Delta Q_{Li}/\Delta Q_G$ can then be evaluated. Borremans approach appears attractive because it is conceptually simple, and practical in its implementation. However, the method requires two power flow solutions and may be quite time consuming for most power systems.

In the next section, a new method is presented for computing the VS indexes at all buses (and areas) in a power network. The method requires one power flow analysis. Sensitivity analysis is then performed around the solution point to com-

pute the VS indexes and hence determine the stability or otherwise of the that solution point.

2.4 EVALUATION OF SYSTEM VOLTAGE STABILITY INDEXES

The method discussed in this section may be considered a generalization and extension of the approach proposed by Borremans et. al. [32].

Under a steady state condition, a power balance is maintained in the network, i.e., at an equilibrium point, the total power supply must equal the total load demand plus the total transmission losses. This applies for both the real and reactive components of power.

The reactive power balance may be expressed,

$$Q_{GT} = \sum_{i \in J_L} Q_{Li} + q \quad (2.9)$$

where Q_{GT} is the sum of all reactive sources, including, generating units, synchronous condensers, static shunt capacitors and line charging, Q_{Li} is the reactive power demand at bus i , q is the total reactive losses, and J_L is the set of all load buses.

Consider a small change in the reactive demand at bus i , ΔQ_{Li} . For a stable steady state condition to be maintained, it is required that,

$$\Delta Q_{GT} = \Delta Q_{Li} + \Delta q \quad (2.10)$$

From equation (2.10), we have,

$$\frac{\Delta Q_{Li}}{\Delta Q_{GT}} \bigg|_{\substack{\Delta P=0 \\ \Delta Q_{Lj}=0, j \neq i}} = \frac{1}{1 + \frac{\Delta q}{\Delta Q_{Li}}} \quad (2.11)$$

In the limit, as the changes becomes arbitrarily small, we have,

$$VS_i = \frac{\partial Q_{Li}}{\partial Q_{GT}} = \frac{1}{1 + \frac{\partial q}{\partial Q_{Li}}} \quad (2.12)$$

where VS_i is the voltage stability index for bus i . For voltage stability, it is required that,

$$VS_i > 0, \quad i \in J_L \quad (2.13)$$

From equation (2.12), it appears that VS_i may be computed if $\frac{\partial q}{\partial Q_{Li}}$ is available. The evaluation of $\frac{\partial q}{\partial Q_{Li}}$ will be discussed later.

The voltage stability index can also be defined for a region or a complete system.

For a region R, with J_R as the set of load buses, let

$$Q_R = \sum_{i \in J_R} Q_{Li}$$

An expression similar to equation (2.10) may be written with respect to this region, i.e.,

$$\Delta Q_{GT} = \Delta Q_R + \Delta q$$

A voltage stability index may then be defined for this region,

$$VS_R = \frac{\Delta Q_R}{\Delta Q_{GT}} = \frac{1}{1 + \frac{\Delta q}{\Delta Q_R}} \quad (2.14)$$

Again, a stable operating condition requires that

$$VS_R > 0 \quad (2.15)$$

In order to evaluate VS_R , the ratio $\Delta q/\Delta Q_R$ is required.

The change in the total reactive losses due to changes in reactive demands may be expressed,

$$\Delta q = \sum_{i \in J_R} \frac{\partial q}{\partial Q_{Li}} \Delta Q_{Li} \quad (2.16)$$

Assuming equal small increments in the reactive demands, ΔQ_{Li} , at all load buses in the region, we have,

$$\Delta Q_{Li} = \frac{\Delta Q_R}{n_R} \quad (2.17)$$

where n_R is the number of load buses in the region.

Combining equations (2.16) and (2.17),

$$\frac{\Delta q}{\Delta Q_R} = \frac{1}{n_R} \sum_{i \in J_R} \frac{\partial q}{\partial Q_{Li}} \quad (2.18)$$

Combining equations (2.18) and (2.14), we have,

$$VS_R = \frac{1}{1 + \frac{1}{n_R} \sum_{i \in J_R} \frac{\partial q}{\partial Q_{Li}}} \quad (2.19)$$

It is apparent from equations (2.12) and (2.19) that in order to evaluate the the voltage stability index, the gradient of the reactive loss with respect to the reactive demand (real demand remaining constant) is required.

The losses in the network, $p + jq$, equal the algebraic sum of all powers into the network [58], i.e.,

$$\bar{s} = p + jq = \sum_{i=1}^N \sum_{j=1}^N \bar{V}_i (\bar{Y}_{ij} \bar{V}_j) \quad (2.20)$$

where

N is the number of buses

$\bar{V}_i = V_i / \underline{\delta}_i$ is the complex bus voltage at bus i

$\bar{Y}_{ij} = G_{ij} + jB_{ij}$ is the $(ij)^{th}$ element of the bus admittance matrix.

The system reactive loss can therefore be expressed,

$$\begin{aligned} q &= \frac{\bar{s} - \bar{s}'}{2j} \\ &= - \sum_{i=1}^N \sum_{j=1}^N V_i V_j B_{ij} \cos(\delta_i - \delta_j) \end{aligned} \quad (2.21)$$

where \bar{s}' is the complex conjugate of \bar{s} .

From equation (2.21), the change in the reactive losses with respect to the system voltages may be expressed,

$$\Delta q = \sum_{i=1}^{N-1} \frac{\partial q}{\partial V_i} \Delta V_i + \sum_{i=1}^{N-1} \frac{\partial q}{\partial \delta_i} \Delta \delta_i \quad (2.22)$$

where the N^{th} bus is assumed to be the slack bus.

The power injection equations for each bus in the network may be expressed,

$$\begin{aligned} P_i &= \sum_{j=1}^N V_i V_j Y_{ij} \cos(\delta_i - \delta_j - \phi_{ij}) \\ Q_i &= \sum_{j=1}^N V_i V_j Y_{ij} \sin(\delta_i - \delta_j - \phi_{ij}), \quad i = 1, 2, \dots, N-1 \end{aligned} \quad (2.23)$$

where ϕ_{ij} is the angle of the admittance \bar{Y}_{ij} .

The sensitivity of the real injections, P_i , and the reactive injections, Q_i , around a given operating point may be expressed by the following matrix equation,

$$\begin{bmatrix} \Delta \underline{P} \\ \Delta \underline{Q} \end{bmatrix} = \begin{bmatrix} \frac{\partial P}{\partial \delta} & \frac{\partial P}{\partial V} \\ \frac{\partial Q}{\partial \delta} & \frac{\partial Q}{\partial V} \end{bmatrix} \begin{bmatrix} \Delta \underline{\delta} \\ \Delta \underline{V} \end{bmatrix} \quad (2.24)$$

where

$$\Delta \underline{P}^T = [\Delta P_1 \dots \Delta P_{N-1}]$$

$$\Delta \underline{Q}^T = [\Delta Q_1 \dots \Delta Q_{N-1}]$$

$$\Delta \underline{V}^T = [\Delta V_1 \dots \Delta V_{N-1}]$$

$$\Delta \underline{\delta}^T = [\Delta \delta_1 \dots \Delta \delta_{N-1}]$$

Equation (2.24) is the well-known matrix equation used in the Newton-Raphson method of load flow analysis. The matrix,

$$\begin{bmatrix} \frac{\partial P}{\partial \delta} & \frac{\partial P}{\partial V} \\ \frac{\partial Q}{\partial \delta} & \frac{\partial Q}{\partial V} \end{bmatrix}$$

is the Jacobian matrix. By inverting the Jacobian matrix, the equivalent inverse relation [59]

$$\begin{bmatrix} \Delta\delta \\ \Delta V \end{bmatrix} = \begin{bmatrix} \frac{\partial\delta}{\partial P} & \frac{\partial\delta}{\partial Q} \\ \frac{\partial V}{\partial P} & \frac{\partial V}{\partial Q} \end{bmatrix} \begin{bmatrix} \Delta P \\ \Delta Q \end{bmatrix} \quad (2.25)$$

is obtained. From equation (2.25) the sensitivity of the respective bus voltage magnitudes and angle with respect to active and reactive demand is obtained, i.e.,

$$\Delta V_i = \sum_{j \in J_R} \frac{\partial V_i}{\partial Q_{Lj}} \Delta Q_{Lj}$$

$$\Delta\delta_i = \sum_{j \in J_R} \frac{\partial\delta_i}{\partial Q_{Lj}} \Delta Q_{Lj}, \quad i = 1, 2, \dots, N-1 \quad (2.27)$$

Combining equations (2.22) and (2.27),

$$\Delta q = \sum_{j \in J_R} \sum_{i=1}^{N-1} \left[\frac{\partial q}{\partial V_i} \frac{\partial V_i}{\partial Q_{Lj}} + \frac{\partial q}{\partial\delta_i} \frac{\partial\delta_i}{\partial Q_{Lj}} \right] \Delta Q_{Lj} \quad (2.28)$$

In summary, the terms $\frac{\partial q}{\partial V}$ and $\frac{\partial q}{\partial\delta}$ at the operating point are calculated using equation (2.21). The terms involving $\frac{\partial V}{\partial Q}$ and $\frac{\partial\delta}{\partial Q}$ are calculated from the inverted Jacobian (equation (2.25)). The loss gradient defined by equation (2.18) can thus be expressed as

$$\frac{\Delta q}{\Delta Q_R} = \frac{1}{n_R} \sum_{j \in J_R} \sum_{i=1}^{N-1} \left[\frac{\partial q}{\partial V_i} \frac{\partial V_i}{\partial Q_{Lj}} + \frac{\partial q}{\partial \delta_i} \frac{\partial \delta_i}{\partial Q_{Lj}} \right] \quad (2.29)$$

Having evaluated the gradient of the the reactive losses with respect to the reactive loads, the voltage stability (VS) indexes in equations (2.12) and (2.19) can be determined. Results of applications of this method are shown in the next section.

2.4.1 Applications

The voltage stability indexes, VS, have been evaluated for two example systems using the method presented above. The first system is the simple two-bus system shown in figure 2.1. The second system is a 28-bus network [29] which includes six generating units and thirty-two transmission lines. Data for the second system is given in Appendix III.

2-Bus System

For the two bus example, the voltage stability index VS_R is evaluated for each operating point as the MVA load is increased (load impedance Z_R reduced). Figure 2.3 shows a plot of VS_R against the receiving end power. VS_R is positive for the stable operating region, zero at the voltage stability limit, and negative in the unstable region. The value of the index at the respective operating points is as expected.

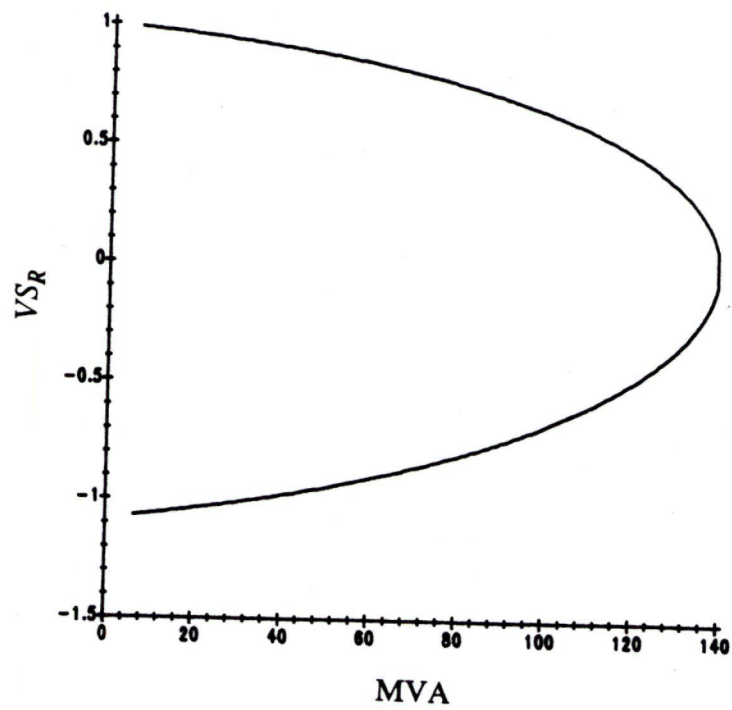


Figure 2.3: Voltage Stability Index Versus MVA Load (2-Bus System)

28-Bus System

Using the method proposed in reference [60], two voltage solutions are determined for the specified load conditions in the 28-bus system. The voltage stability indices VS_i were computed at each load bus using the method presented above. The system voltage stability index VS_R has also been determined for each operating condition. Tables 2.1 and 2.2 show the two solutions and their respective voltage stability indexes.

It will be observed that for solution one, $VS_i > 0$ for all system load buses. Also, the system voltage stability index $VS_{R,1} > 0$. This means that solution 1 is a 'voltage stable solution'. On the other hand, solution 2 represents an unstable operating condition from a voltage viewpoint since $VS_i < 0$ for most of the load buses. Also, the system voltage stability index $VS_{R,2}$ is negative. It is interesting to note that solution 2 with bus voltages that approach normal operating levels is unstable.

Although the VS_R indexes could be used to determine whether or not an operating point is voltage stable, it may not be appropriate or satisfactory in assessing the margin of the operating point from the collapse point. This is because as the system load increases, system generators reach their VAR limits at different points causing discontinuities in the magnitude of the index. The problem of evaluating the margin of an operating point from the stability limit is addressed in Chapter 3.

Table 2.1: Solution One - 28-Bus Network

Bus	Bus Voltage		$\frac{\partial q}{\partial Q_{Lj}}$	VS_j
	Mag.	Ang*		
1	1.0500	0.0	-	-
2	0.9830	-48.8	1.955	0.338
3	0.9782	-52.7	1.894	0.346
4	0.9817	-51.3	1.812	0.356
5	0.9800	-55.7	1.870	0.349
6	0.9971	-22.7	0.456	0.687
7	0.9914	-14.6	0.485	0.673
8	0.9967	-21.8	0.505	0.664
9	0.9971	-11.1	0.357	0.737
10	0.9732	-36.4	1.404	0.416
11	0.9800	-39.0	1.584	0.387
12	0.9975	-25.7	0.396	0.716
13	0.9818	-17.7	0.747	0.572
14	0.9773	-26.5	1.124	0.471
15	0.9675	-33.8	1.423	0.413
16	0.9643	-31.8	1.421	0.413
17	1.0010	-11.5	0.461	0.685
18	0.9923	-13.6	0.481	0.675
19	0.9999	-6.0	0.368	0.731
20	0.9637	-48.9	1.953	0.339
21	0.9606	-44.0	1.876	0.348
22	0.9606	-45.8	1.943	0.339
23	0.9621	-42.0	1.897	0.345
24	1.0500	-8.3	-	-
25	1.0500	6.3	-	-
26	1.0500	-22.7	-	-
27	1.0500	-19.5	-	-
28	1.0500	-29.8	-	-

$$VS_{R,1} = 0.454$$

* in degrees

Table 2.2: Solution Two - 28-Bus Network

Bus	Bus Voltage		$\frac{\partial q}{\partial Q_{Lj}}$	VS_j
	Mag.	Ang*		
1	1.0500	0.0	-	-
2	0.8582	-54.7	-3.579	-0.388
3	0.8534	-59.8	-3.526	-0.396
4	0.8620	-58.0	-3.437	-0.410
5	0.8500	-63.7	-3.668	-0.375
6	0.9800	-23.5	-0.300	1.428
7	0.9763	-15.2	-0.231	1.300
8	0.9782	-22.5	-0.312	1.454
9	0.9876	-11.6	-0.100	1.111
10	0.8985	-39.5	-2.159	-0.863
11	0.8900	-42.6	-2.592	-0.628
12	0.9822	-27.1	-0.303	1.435
13	0.9538	-18.4	-0.647	2.831
14	0.9272	-28.6	-1.410	-2.441
15	0.8945	-36.7	-2.289	-0.776
16	0.8952	-34.2	-2.034	-0.967
17	0.9857	-12.0	-0.281	1.390
18	0.9776	-14.1	-0.220	1.282
19	0.9911	-6.4	-0.075	1.081
20	0.8481	-54.9	-3.471	-0.405
21	0.8554	-48.8	-3.160	-0.463
22	0.8500	-51.1	-3.257	-0.443
23	0.8587	-46.4	-3.061	-0.485
24	1.0500	-8.9	-	-
25	1.0500	5.9	-	-
26	1.0500	-24.2	-	-
27	1.0500	-21.8	-	-
28	1.0190	-32.7	-	-
$VS_{R,2} = -1.215$				

* in degrees

2.5 SIMULATION STUDY

In this section, the simulation of a process that may lead to voltage collapse in a transmission system is presented. This simulation focuses on the action of the LTC transformer taps following a system disturbance. Load-voltage character of the exponential type has also been incorporated. Modeling of the load and the transformer tap action is therefore an important part of the simulation study. The respective models will be discussed next.

2.5.1 LTC Transformer Tap Model

An LTC transformer is a control tool used to maintain local voltages within desirable limits. It is activated when the controlled bus voltage deviates from allowable limits.

Let the nominal tap position of the LTC in the line connecting buses i and j (controlling bus i) be denoted by $n_{i,j}^0$. Let the corresponding nominal voltage at bus i be V_i^0 , and the allowable voltage deviation be ΔV_i . When the operating condition in the system changes, each LTC transformer in the system will change its tap position if necessary to maintain the local voltage within the given limits. The change will take the form of one or more discrete equal-valued changes in tap position, separated by the duration of the LTC transformer duty cycle.

Based on this operation, the slow dynamics associated with the changes in the tap positions may be expressed as the following discrete equation [37]:

$$n_{i,j}^{(k+1)} = n_{i,j}^{(k)} - d_i f(V_i - V_i^o) \quad (2.30)$$

where k is the step count and d_i is the stepsize in the change of the tap position during one operating cycle of the LTC transformer. $f(V_i - V_i^o)$ is the control function governing the operation of the LTC transformer and is given by,

$$f(V_i - V_i^o) = \begin{cases} 1 & \text{if } V_i - V_i^o > \Delta V_i \text{ for } t \geq t_{di} \\ 0 & \text{if } |V_i - V_i^o| \leq \Delta V_i \text{ for } t \leq t_{di} \\ -1 & \text{if } V_i - V_i^o < -\Delta V_i \text{ for } t \geq t_{di} \end{cases} \quad (2.31)$$

where t is time, and t_{di} is the duty cycle of the LTC controlling bus i .

Thus if $|V_i - V_i^o| \leq \Delta V_i$ or $t < t_{di}$ no LTC tap action results. If $|V_i - V_i^o| > \Delta V_i$ for a period greater than the transformer duty cycle time, t_{di} , the tap ratio is changed according to equation (2.30).

2.5.2 Load Model

For this study, a general static load model is used in which the MVA load at a particular bus is an exponential function of the bus voltage. The load

characteristics are given by,

$$P_{Li} = P_{oi} V_i^{pi} \quad (2.32)$$

$$Q_{Li} = Q_{oi} V_i^{qi} \quad (2.33)$$

where P_{oi} and Q_{oi} are the prescribed active and reactive loads at rated (nominal) voltage, pi and qi are constants which reflect the dependence of active and reactive demand on voltage at bus i .

2.5.3 Steps in the Simulation

A computer program has been developed to simulate the action of the LTC transformer following a system fault. The main steps in the simulation algorithm are,

STEP 1: Solve the system load flow equations for the initial (base case) condition.

STEP 2: Initiate disturbance and solve load flow equations with taps fixed at pre-disturbance positions.

STEP 3: Increase time, t .

STEP 4: Change tap positions using equation (2.30)

STEP 5: Solve the load flow equations with taps fixed at positions determined in STEP 4.

STEP 6: If the time t is greater than maximum time, STOP, otherwise, return to STEP 2.

In solving the load flow equations, the load voltage characteristics are taken into consideration.

2.5.4 Results of Simulation

The simulation study was performed on a representative system shown in figure 2.4. The system represents a load area with local generation available to serve a portion of the load. The load area is thereby dependent on transfer of power over a transmission system.

The purpose of the LTC transformer T_1 is to maintain the (low) secondary voltage, V_R , within $\pm 1\%$ of nominal value. The tap controller is set to operate only when the secondary voltage, V_R , exceeds the prescribed allowed range and remains in this range for a period longer than $t_{d1} = 10$ seconds.

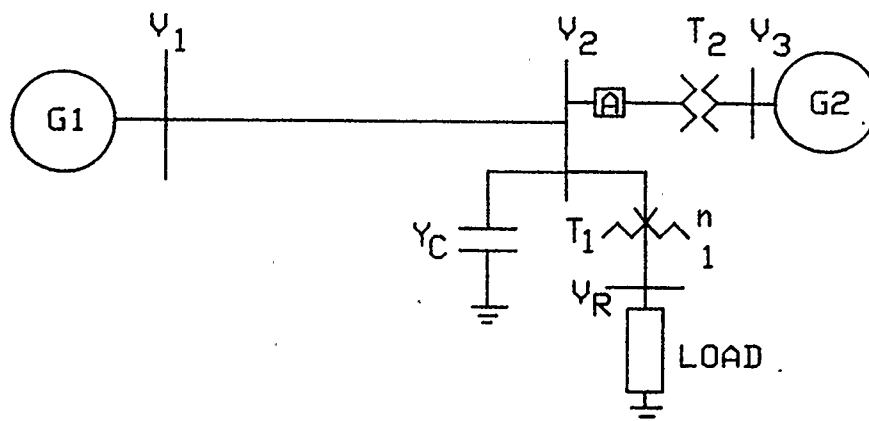


Figure 2.4: System Studied for Simulation

The system load is represented as shown in equations (2.32) and (2.33). In this study, the real and reactive power voltage exponents are assumed equal, i.e.,

$$k = p_i = q_i$$

Three different values of k are considered.

The disturbance chosen was to trip the local generator (by opening of breaker A). The time domain responses illustrating the effect of the disturbance and subsequent action by the LTC transformer with $Y_C = 0$, and $Y_C = 3.0$ per unit are shown in figures 2.5 and 2.6. Time domain responses are obtained for values of load exponents k of 0.6, 0.8 and 1.0.

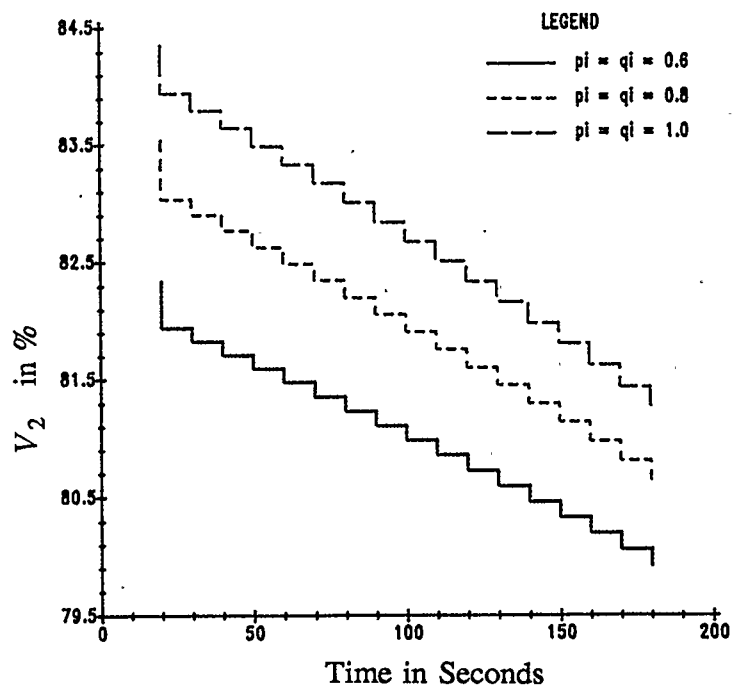


Figure 2.5a: Time-Domain Response of the Receiving End Voltage V_2
($Y_C = 0$)

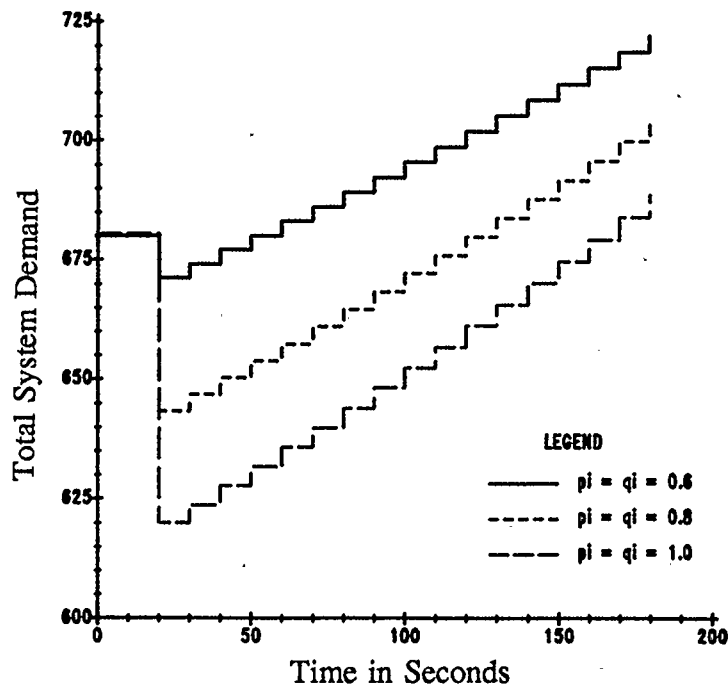


Figure 2.5b: Time-Domain Response of the Total System MVA Demand
($Y_C = 0$)

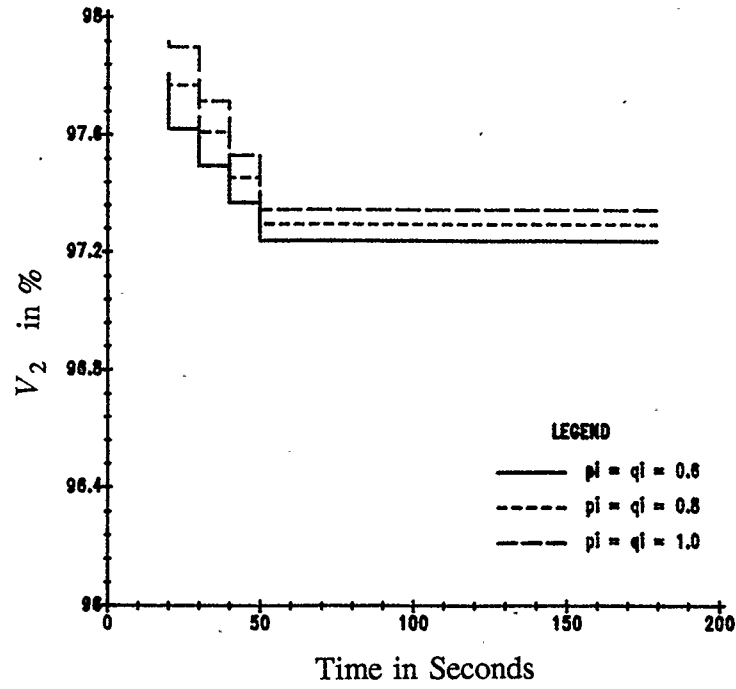


Figure 2.6a: Time-Domain Response of the Receiving End Voltage V_2 ($Y_C = 3.0$ p.u.)

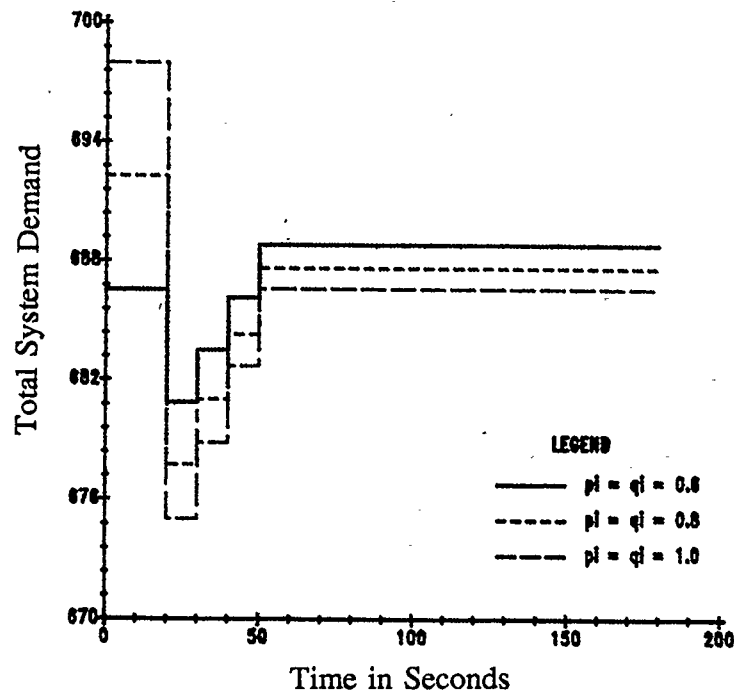


Figure 2.6b: Time-Domain Response of the Total System MVA Demand ($Y_C = 3.0$ p.u.)

Figure 2.5a shows the time response of the voltage at bus 2, V_2 . Figure 2.5b shows the time response of the total system MVA demand. The total MVA demand is the sum of the load MVA and the MVA losses.

Immediately following the disturbance at time, $t = 20$ seconds, excessive voltage decline results in reduction in load and in the total system demand. The LTC starts operating to increase V_R . As V_R increases, the MVA load at the bus increases. Hence more power is drawn through the already heavily loaded transmission line. The increasing total system demand (figure 2.5b) results in further decline in the receiving end voltage V_2 (figure 2.5a). However, the LTC continues to operate to increase the secondary voltage, V_R , resulting in further increase in system demand and decrease in V_2 . In this example, the process continues until the LTC runs through its boosting tap range. It may however happen, in some other instance, that the increased system demand exceeds the maximum transmissible power of the network, resulting in system voltage collapse.

It is apparent from figure 2.5 that less voltage dependent loads (loads with smaller k) result in larger increase in the system demand and greater decline in the receiving end voltage V_2 as the LTC operates to raise V_R . Such stiff loads may therefore make the system more susceptible to imminent voltage collapse.

The effect of capacitive compensation is investigated by assuming now that $Y_C = 3.0$ per unit. and repeating the simulation study. Figure 2.6a and 2.6b show the time domain responses of the receiving end voltage V_2 and the total

demand for the same disturbance, initiated at $t = 20$ seconds.

From figure 2.6 it may be observed that after three tap downs, the LTC transformer is able to bring the load voltage V_R to the desired range. The LTC action ceases, and a steady equilibrium of the tap is maintained from time $t = 50$ seconds. It is therefore apparent that the addition of VAR compensating equipment improves the security of the system against voltage collapse.

2.6 CONCLUSIONS

In order to provide insight into the voltage collapse problem, a simple 2-bus power system has been analysed. Stability conditions are derived for the simple system based on the action of the at-load LTC transformer.

A method to determine a practical voltage stability index for a network of realistic size has been presented. The method may be incorporated into a Newton-Raphson load flow analysis program to assess the voltage stability or otherwise at a particular operating point.

A simulation study has been presented to demonstrate a process that may lead to system voltage collapse. Using a simple but typical example system, time domain responses of receiving end voltage and total system demand following a disturbance indicate that loads which are less voltage dependent may be more severe from voltage stability standpoint. Also, results for the example system show that VAR compensation may be an effective way to improve the system security

against collapse.

CHAPTER 3

DETERMINATION OF VOLTAGE STABILITY LIMIT IN MULTIMACHINE POWER SYSTEMS

3.1 INTRODUCTION

In order to prevent the occurrence of voltage instability in an electric power system, it is of interest to determine the systems' voltage stability limits (or critical states) for normal as well as contingency conditions. Knowing the critical states, indications of systems security from voltage collapse are available.

In [18], Venikov proposed the use of the convergence in the Newton-Raphson (*NR*) load flow calculations to estimate the stability limit. An initial (stable) operating condition is changed by increasing the demand (vector) in finite steps along a specified trajectory. At each step the system state is determined by the corresponding load flow solution. The process is continued up to the point where the *NR* method diverges, or the modified *NR* method "suspends". Besides being computationally intensive, this method may be inadequate due to the unreliable behavior of the *NR*-based load flow solution methods in the vicinity of the voltage stability limit. This behavior has been linked to the singularity of the Jacobian matrix at the voltage stability limit and the existence of close multiple load flow solution around that limit [13].

To reduce the computational requirement and circumvent the numerical ill-conditioning likely to occur with the repeated load flow method near the voltage stability limit, Flatabo et. al. [26] proposed the use of a combination of load flows and sensitivity parameters. Boresman et. al. [32] proposed a quadratic extrapolation method as a possible short cut to the repeated load flow approach. These methods are inherently approximate and may yield unrealistic results.

The methods of Jarjis et. al. [33], Mercede et. al. [15], and Liu et. al. [30] characterise the voltage stability region using different approaches. One common drawback of all these method is that the operational limits of system components, e.g., transformer tap settings and generator MW and MVAR limits, are not taken into consideration. For example, it is well known that when a generator reaches its VAR limit, the terminal voltage can no longer be maintained at constant value. As a result, the system performance pattern changes. It therefore seems inadequate to evaluate the margin of an operating point to the critical point without taking the operational limits of system components, particularly the generator VAR limits, into account. More often than not the voltage collapse problem may be considered to be a reactive power problem. It is to be expected that ignoring generator capability limits would yield larger but unrealistic voltage stability regions.

Kessel et. al. [31] developed a voltage stability index based on the feasibility of solution of the power flow equations for each node. In [14], Tiranuchit et. al. proposed the use of the minimum singular value of the Jacobian matrix of the power flow equations as a global voltage stability index. Again, these methods

ignore the generator limits. The indices may not therefore represent the condition of the network close to and at the critical point.

In this chapter, a new method of determining the critical state directly and accurately is proposed. The operational limits of system equipment (e.g MW and MVAR limits of generators, and transformer tap settings) are taken into account. Knowing the critical state, a voltage security margin is defined which may serve as a measure of the security of a given operating condition from voltage instability or collapse.

3.2 SIMPLE NETWORK

For the simple two-bus network (figure 2.1), the condition for stability of the receiving end voltage was shown in Chapter 2 of this thesis to be (equation (2.5))

$$\frac{|\bar{Z}_L|}{|\bar{Z}_R|} < 1$$

where

$\bar{Z}_R = Z_R \angle \phi$ is the load impedance, and

$\bar{Z}_L = Z_L \angle \xi$ is the impedance of the transmission line.

The critical point corresponds to the condition when $|\bar{Z}_L| = |\bar{Z}_R|$. This is the condition under which the maximum available power is obtained at the receiving end. The unstable condition, $|\bar{Z}_L| > |\bar{Z}_R|$, might occur due to system distur-

bance causing line outage (increasing source impedance), or due to excessive real and/or reactive power pickup at the load end (decreasing $|\bar{Z}_R|$).

The load MVA at the critical point may be expressed as (equation (2.6)),

$$\bar{S}_R^{\max} = \frac{1}{4} \frac{e^{j\phi}}{\cos^2\left(\frac{\xi - \phi}{2}\right)} \frac{V_1^2}{Z_L}$$

The corresponding load voltage, which is the minimum stable voltage at the load terminal, may be expressed (equation (2.7))

$$\bar{V}_R^{\text{crit}} = \frac{e^{j\left(\frac{\phi - \xi}{2}\right)}}{2 \cos\left(\frac{\xi - \phi}{2}\right)} \bar{V}_1$$

The theory used to analyse the simple network may be extended to the multinode case with ideal voltage sources [61]. The above results cannot however be applied simply to multimachine power system networks owing to the fact that synchronous generators are not ideal voltage sources. The voltage angles at the sources depend on the real power delivered by the machines. Moreover, when a machine field current reaches its upper limit, the automatic voltage regulator (AVR) becomes inoperative and the machine model has to be modified. Also, the load demand is normally given in terms of MW and MVAR rather than impedance.

In the next section, the general problem formulation associated with the proposed method is presented. Also presented are modifications to the general formulation to take into consideration the voltage dependence of system loads. For this purpose, exponential static load/voltage characteristics are assumed.

3.3 GENERAL FORMULATION

Consider a power system with N buses. Let buses 1 to M be load buses and buses $M + 1$ to N be generator buses. It is assumed that the slack bus is the N^{th} bus. In the steady state, the system is described by the power flow equations, i.e.

$$P_i = \sum_{j=1}^N V_i V_j Y_{ij} \cos (\delta_i - \delta_j - \phi_{ij}) \quad (3.1)$$

$$Q_i = \sum_{j=1}^N V_i V_j Y_{ij} \sin (\delta_i - \delta_j - \phi_{ij})$$

$$i = 1, \dots, N - 1 \quad (3.2)$$

where

P_i and Q_i are the net real and reactive power entering bus i

V_i / δ_i is the i^{th} bus complex voltage,

Y_{ij} / ϕ_{ij} is the $(i, j)^{th}$ entry of the network bus admittance matrix.

The apparent power demand (MVA) at a load bus i is determined as,

$$S_i = (P_i^2 + Q_i^2)^{1/2} = \left[\sum_j^N \sum_k^N V_i^2 V_j V_k Y_{ij} Y_{ik} \cos(\delta_k - \delta_j + \phi_{ik} - \phi_{ij}) \right]^{1/2}, \quad i \in J_L \quad (3.3)$$

where

$$J_L = \{1, 2, \dots, M\}$$

The total system *MVA* demand is therefore

$$S_{TOTAL} = \sum_{i \in J_L} S_i \quad (3.4)$$

As noted in the previous section, the critical point corresponds to the maximum load power, i.e., the state when the network delivers maximum *MVA* power, subject to a given load distribution, to the load points. This can be expressed,

$$S_{TOTAL}^{critical} = \text{maximum} \left(\sum_{j \in J_L} S_j \right)$$

For a given network, the maximum total load depends on the distribution and power factors of the initial *MVA* loads, and on the expected (given) pattern of increase from the initial values. It also depends on the capabilities of the generators. Hence for the multimachine system, the value of $S_{TOTAL}^{critical}$ is subject to constraints which may be enumerated as follows;

- (a) **Distribution Constraints:** These constraints describe and enforce the pattern (or direction) of increase of the *MVA* demand vector \underline{S} , where

$$\underline{S}^T = [S_1, S_2, \dots, S_M] \quad (3.5)$$

In the proposed method of analysis, it is required that the distribution pattern of the *MVA* demand be specified. A vector $\underline{\beta}$ has been introduced for this purpose. β_i is a per unit value representing the relative increase in the load at bus i with respect to the corresponding system total load increase, i.e.,

$$S_i^{new} = S_i^{initial} + \beta_i \Delta S_{TOTAL} \quad (3.6)$$

where

$S_i^{initial}$ is the initial known *MVA* demand at bus i , and

S_i^{new} is the new *MVA* demand at this bus after an increase ΔS_{TOTAL} in the total *MVA* load of the system.

From equation (3.6), a load distribution constraint equation is written for bus i

as

$$\beta_i \sum_{j \in J_L} S_j - S_i = \beta_i \sum_{j \in J_L} S_j^{initial} - S_i^{initial}$$

Letting

$$C_i = \beta_i \sum_{j \in J_L} S_j^{initial} - S_i^{initial},$$

we have

$$\beta_i \sum_{j \in J_L} S_j - S_i = C_i. \quad (3.7)$$

- (b) *MW* and *MVAR* limits on Generators: To determine the system critical state exactly, it is necessary to take the power production capabilities of the system generating units into consideration. These constraints limit the *MW* and *MVAR* outputs from systems generators to their respective specified limits. The constraints are specified as follows,

$$P_i^{\min} \leq P_i \leq P_i^{\max}$$

$$Q_i^{\min} \leq Q_i \leq Q_i^{\max}, \quad i = M + 1, \dots, N - 1. \quad (3.8)$$

- (c) *Generator MW Participation*: As the load increases, the *MW* output of each generating unit is increased from the base point to "participate" in the load change. For this purpose, the participation factors of the generating units need to be specified in a vector γ^o , where γ_i^o is the specified participation factor of generator i .

The total system demand P_D is expressed as

$$P_D = \sum_{j \in J_L} P_j + P_{losses}, \quad (3.9)$$

where

P_{losses} is the system total MW loss.

The participation of generating unit i , ΔP_i , for an increase in total system demand, ΔP_D , may be expressed as

$$\Delta P_i = \gamma_i^o \Delta P_D. \quad (3.10)$$

Let

$$\Delta P_i = P_i - P_i^{initial}$$

and

$$\Delta P_D = P_D - P_D^{initial}$$

where

$P_D^{initial}$ and $P_i^{initial}$ are the initial total system MW demand and initial MW output of generator i respectively.

We obtain, from equation (3.10),

$$f_i = \gamma_i P_D - \gamma_i P_D^{initial} - P_i + P_i^{initial} = 0, \quad (3.11)$$

$$i = M+1, \dots, N-1$$

$$\gamma_i = \gamma_i^0 \quad \text{when} \quad P_i^{\min} \leq P_i \leq P_i^{\max}$$

and

$$\gamma_i \leq \gamma_i^0 \quad \text{when} \quad P_i = P_i^{\max}$$

where

P_i^{\min} and P_i^{\max} are the minimum and maximum MW limits of generating unit i .

The participation factors may be chosen to reflect economic consideration [62].

This is shown in Appendix I.

(d) Specified Power Factor of Incremental MVA Load: The power factor of the load increase at each load bus may be assumed to remain constant at a specified value. This optional constraint set which allows control with the power factor of the load increase is enforced by the following requirement,

$$\Delta P_i = pf_i \Delta S_i$$

where

ΔS_i is the MVA load increase at bus i .

ΔP_i is the MW load increase at bus i .

pf_i is the power factor of load increase at bus i .

Putting

$$\Delta P_i = P_i - P_i^{initial}$$

and

$$\Delta S_i = S_i - S_i^{initial},$$

constraint equations may be written for each load bus as

$$P_i - pf_i S_i = -pf_i S_i^{initial} + P_i^{initial}.$$

Setting

$$K_i = -pf_i S_i^{initial} + P_i^{initial},$$

we have,

$$P_i - pf_i S_i = K_i, \quad i \in J_L \quad (3.12)$$

In some reports on voltage collapse problems [19,26,30], only the reactive component of the load increased while the MW component remained constant. Such situations might be studied using the method that is proposed here by setting the power factors pf_i (equation (3.12)) to zero.

- (e) Limits on Controlled Voltages and LTC Transformer taps.

In summary, the problem of determining the voltage stability limit of a general multimachine power network is formulated as an optimization problem, i.e.,

maximize

[Total *MVA* demand]

subject to:

- (a) distribution constraints at load buses
- (b) *MVAR* and *MW* limits on generators
- (c) generators' *MW* participation
- (d) specified power factor of (incremental) *MVA* demand
- (e) limits on controlled voltages and *LTC* transformer taps

The variables of this optimization problem are voltage angles at all buses except the slack bus, voltage magnitudes at all buses, *LTC* transformer taps, and generator participation factors. The voltage magnitude at a generator bus is allowed to vary within specified limits if the generator *VAR* limit is not exceeded. Also, a tap-changer controlled voltage is allowed to vary within specified limits if the tap setting is not at its limit.

It should be noted that other constraints such as power transfer capability of certain lines may be included in this formulation.

In mathematical terms, the formulation may be expressed as the following non-linearly constrained optimization problem, *NCPI*;

minimize

$$-S_T = [- \sum_{j \in J_L} S_j(\underline{V}, \underline{\delta}, \underline{t}, \underline{\gamma})] \quad (3.13)$$

subject to:

$$(1) \beta_i S_T(\underline{V}, \underline{\delta}, \underline{t}, \underline{\gamma}) - S_i(\underline{V}, \underline{\delta}, \underline{t}, \underline{\gamma}) = C_i, \quad i \in J_L$$

$$(2) Q_i^{\min} \leq Q_i(\underline{V}, \underline{\delta}, \underline{t}, \underline{\gamma}) \leq Q_i^{\max} \quad i = M + 1, \dots, N - 1$$

$$(3) P_i^{\min} \leq P_i(\underline{V}, \underline{\delta}, \underline{t}, \underline{\gamma}) \leq P_i^{\max} \quad i = M + 1, \dots, N - 1$$

$$(4) f_i(\underline{V}, \underline{\delta}, \underline{t}, \underline{\gamma}) = 0 \quad i = M + 1, \dots, N - 1$$

$$(5) P_i(\underline{V}, \underline{\delta}, \underline{t}, \underline{\gamma}) + K_i Q_i(\underline{V}, \underline{\delta}, \underline{t}, \underline{\gamma}) = 0 \quad i \in J_L$$

$$(6) \gamma_i \leq \gamma_i^0 \quad i = M + 1, \dots, N - 1$$

$$(7) V_i^{\min} \leq V_i \leq V_i^{\max} \quad i \in J_C$$

$$(8) t_i^{\min} \leq t_i \leq t_i^{\max} \quad i = 1, \dots, n_t$$

where

$$\underline{V}^T = [V_1, \dots, V_N]$$

$$\underline{\delta}^T = [\delta_1, \dots, \delta_{N-1}]$$

$$\underline{t}^T = [t_1, \dots, t_{n_t}]$$

$$\underline{\gamma}^T = [\gamma_{M+1}, \dots, \gamma_{N-1}]$$

J_c is the set of voltage-controlled buses

n_t is the number of *LTC* transformers.

The solution of this optimization problem is the system state at the critical point (stability limit) and the corresponding value of the total *MVA* load. It should be noted that for a given network, the system critical state thus obtained is particular to the initial load MW and MVAR distribution, the choice of the load MVA distribution vector $\underline{\beta}$, the generating unit participation factors as specified in $\underline{\gamma}$, MW and MVAR production limits, and the distribution and size of VAR compensation facilities. It should be noted also that the above formulation treats the load *MVA* as being independent of the bus voltage. In Section 3.4 below, a modification to the above formulation is proposed which takes the voltage dependence of the loads into consideration. This will allow a study of the effects of the load-voltage characteristics on the voltage stability limit.

3.4 EXTENSION OF BASIC FORMULATION TO INCLUDE VOLTAGE DEPENDENCE OF LOADS

A general static load model in which the MVA loading at a particular bus i is a function of the per unit bus voltage, V_i , is given as [63]

$$P_{Li} = P_{oi} V_i^{p_i} \quad (3.14)$$

$$Q_{Li} = Q_{oi} V_i^{q_i} \quad (3.15)$$

where P_{oi} and Q_{oi} are the prescribed active and reactive loads at rated (nominal) voltage, p_i and q_i are constants which reflect the load-voltage characteristics at bus i . P_{Li} and Q_{Li} are the MW and MVAR demands at bus i .

The power flow equations at load nodes are now written,

$$g_i = P_{oi} V_i^{p_i} + \sum_{j=1}^N V_i V_j Y_{ij} \cos(\delta_i - \delta_j - \phi_{ij}) = 0 \quad (3.16)$$

$$h_i = Q_{oi} V_i^{q_i} + \sum_{j=1}^N V_i V_j Y_{ij} \sin(\delta_i - \delta_j - \phi_{ij}) = 0, \quad (3.17)$$

$$i \in J_L$$

In order to include the voltage dependence of the loads in the determination of

the voltage stability limit, equations (3.16) and (3.17) are included as constraints in the *NCP1*. It should be noted that P_{oi} and Q_{oi} are allowed to increase according to a prescribed pattern governed by the vector $\underline{\beta}$ mentioned above. P_{oi} and Q_{oi} are therefore treated as variables in the optimization problem. The problem of determining the critical point including the voltage dependence of the loads may thus be formulated as a non-linear optimization problem, (*NCP2*):

minimize

$$-S_T = [- \sum_{j \in J_L} S_j(\underline{V}, \underline{\delta}, \underline{t}, \underline{\gamma}, \underline{P}_o, \underline{Q}_o)] \quad (3.18)$$

subject to:

$$(1) \beta_i S_T(\underline{V}, \underline{\delta}, \underline{t}, \underline{\gamma}, \underline{P}_o, \underline{Q}_o) - S_i(\underline{V}, \underline{\delta}, \underline{t}, \underline{\gamma}, \underline{P}_o, \underline{Q}_o) = C_i$$

$$i \in J_L$$

$$(2) Q_i^{\min} \leq Q_i(\underline{V}, \underline{\delta}, \underline{t}, \underline{\gamma}, \underline{P}_o, \underline{Q}_o) \leq Q_i^{\max} \quad i = M + 1, \dots, N - 1$$

$$(3) P_i^{\min} \leq P_i(\underline{V}, \underline{\delta}, \underline{t}, \underline{\gamma}, \underline{P}_o, \underline{Q}_o) \leq P_i^{\max} \quad i = M + 1, \dots, N - 1$$

$$(4) f_i(\underline{V}, \underline{\delta}, \underline{t}, \underline{\gamma}, \underline{P}_o, \underline{Q}_o) = 0 \quad i = M + 1, \dots, N - 1$$

$$(5) P_i(\underline{V}, \underline{\delta}, \underline{t}, \underline{\gamma}, \underline{P}_o, \underline{Q}_o) + K_i Q_i(\underline{V}, \underline{\delta}, \underline{t}, \underline{\gamma}, \underline{P}_o, \underline{Q}_o) = 0, \quad i \in J_L$$

- (6) $g_i(\underline{V}, \underline{\delta}, \underline{t}, \underline{\gamma}, \underline{P}_o, \underline{Q}_o) = 0 \quad i \in J_L$
- (7) $h_i(\underline{V}, \underline{\delta}, \underline{t}, \underline{\gamma}, \underline{P}_o, \underline{Q}_o) = 0 \quad i \in J_L$
- (8) $\gamma_i \leq \gamma_i^o \quad i = M + 1, \dots, N - 1$
- (9) $V_i^{\min} \leq V_i \leq V_i^{\max} \quad i \in J_C$
- (10) $t_i^{\min} \leq t_i \leq t_i^{\max} \quad i = 1, \dots, n_t$

where

$$\underline{P}_o^T = [P_{o1}, P_{o2}, \dots, P_{oM}]$$

$$\underline{Q}_o^T = [Q_{o1}, Q_{o2}, \dots, Q_{oM}]$$

Again, the solution to this optimization problem is the system critical state.

3.5 SECURITY MARGIN

Having determined the system critical state, a security or stability margin, SM , can be defined as

$$SM = \frac{\sum_{j \in J_L} S_j^{limit} - \sum_{j \in J_L} S_j^{initial}}{\sum_{j \in J_L} S_j^{limit}} \quad (3.19)$$

where

S_j^{limit} is the MVA demand at bus j at the critical point, and

$S_j^{initial}$ is the MVA demand at bus j at the initial operating condition.

This index gives an explicit indication of the distance to voltage collapse in terms of uncontrollable variables, namely, the system load. As noted by several investigators [17,26], a measure in terms of load power margin may be the best indication of system security from collapse. For a stable (feasible) initial operating condition, SM takes on value between 0 and 1. $SM = 0$ occur at the voltage stability limit. A negative value of SM means no acceptable operating point exists for the specified initial system load.

3.6 SOLUTION METHOD

Without loss of generality, the nonlinear programming problems NCP1 and NCP2 may be stated compactly as follows:

minimize

$$f(\underline{x}) \tag{3.20}$$

subject to:

$$(1) \quad g_j(\underline{x}) = 0, \quad j = 1, \dots, m_e$$

$$(2) \quad g_j(\underline{x}) \geq 0, \quad j = m_e + 1, \dots, m$$

$$(3) \quad \underline{x}^l \leq \underline{x} \leq \underline{x}^u$$

where

\underline{x} is an n -dimensional vector of variables,

\underline{x}^l and \underline{x}^u are the lower and upper limits on \underline{x} respectively, and

all functions are continuously differentiable.

Numerous methods and software packages exist today for solving this class of optimization problem [64]. In this thesis, the nonlinear programming problems are solved using the sequential quadratic programming (SQP) algorithm [65]. Software routines developed by the Numerical Algorithms Group (NAG) based on the SQP algorithm are used [66]. The SQP algorithm outlined below follows the derivation in reference [65].

In order to establish the sufficient conditions for optimality, let

$$\underline{h}(\underline{x}) = 0 \tag{3.21}$$

be the vector of the constraint functions that are active (i.e. binding or exactly

satisfied) at the optimal point. The Lagrangian function may be defined as,

$$L(\underline{x}, \underline{\lambda}) = f(\underline{x}) - \underline{\lambda}^T \underline{h}(\underline{x}) \quad (3.22)$$

where

$\underline{\lambda}$ is a vector of Lagrangian multipliers.

Taking the first derivative of $L(\underline{x}, \underline{\lambda})$ with respect to \underline{x} and equating to zero, the stationary point of equation (3.22) may be obtained as the solution of

$$g(\underline{x}^*) = J^T(\underline{x}^*) \underline{\lambda} \quad (3.23)$$

where

\underline{x}^* is the optimal solution of problem (3.23)

$J(\underline{x}^*)$ is the Jacobian matrix of \underline{h} at \underline{x}^*

Equation (3.23) is the first order Kuhn-Tucker optimality condition. When this condition holds, \underline{x}^* is a minimum of the Lagrangian function within the subspace defined by the vectors of the active constraint gradients. This property suggests that \underline{x}^* can be defined as a solution of a linearly constrained subproblem, whose objective is related to the Lagrangian function, and whose linear constraints are chosen so that minimization occurs only within the desired subspace.

The property of the optimum is used to pose a simple subproblem with quadratic objective function and linear constraints. This class of optimization prob-

lems is called a quadratic program (QP). The objective function is a quadratic approximation of the Lagrangian function. The constraints are the linearized constraints of the original problem.

The QP subproblem can now be defined as:

minimize

$$\frac{1}{2} \Delta \underline{x}_k^T B_k \Delta \underline{x}_k + \nabla f(\underline{x}_k)^T \Delta \underline{x}_k \quad (3.24)$$

subject to:

$$\nabla g_j(\underline{x}_k)^T \Delta \underline{x}_k + g_j(\underline{x}_k) = 0, \quad j = 1, \dots, m_e$$

$$\nabla g_j(\underline{x}_k)^T \Delta \underline{x}_k + g_j(\underline{x}_k) \geq 0, \quad j = m_{e+1}, \dots, m$$

$$\underline{x}^l - \underline{x}_k \leq \Delta \underline{x}_k \leq \underline{x}^u - \underline{x}_k,$$

where

k is the iteration number

\underline{x}_k is the value of \underline{x} at the k^{th} iteration

B_k is a positive definite quasi-Newton approximation of the Hessian of the augmented Lagrangian function of problem (3.23).

B_k is updated at each iteration using the Broyden-Fletcher-Goldfarb-Shanno formula [65].

The SQP algorithm to solve (3.23) generates a sequence $\underline{x}_1, \underline{x}_2, \underline{x}_3, \dots$ that converges to the optimal solution \underline{x}^* . Each previous estimate is improved upon by taking a step α_k in a direction $\Delta \underline{x}_k$ such that,

$$\underline{x}_{k+1} = \underline{x}_k + \alpha_k \Delta \underline{x}_k. \quad (3.25)$$

The scalar function α_k is determined by a line search procedure to produce a sufficient decrease in the augmented Lagrangian merit function. The direction of movement, $\Delta \underline{x}_k$, is found by solving the QP subproblem (3.24).

It should be noted that the constraint equations in problem (3.20) are the load flow equations, and the matrix of the linearized equations in problem (3.24) is the Jacobian matrix in the Newton-Raphson load flow solution method. However, because the constraint equations of problem (3.24) are not solved but handled by the Lagrangian method, the problem of singularity of the load flow Jacobian matrix at the voltage stability limit is avoided.

The SQP-based algorithm may be summarized by the following steps:

STEP 1: Check termination criteria, if \underline{x}^k satisfies the optimality conditions, the algorithm terminates with \underline{x}^k as solution.

STEP 2: Solve the QP subproblem (3.24).

STEP 3: Update the estimate of the solution and go back to STEP 1.

The QP problem (3.24) is solved using another iterative procedure, discussed in the next section.

3.6.1 Solution of QP Subproblem

Letting $\Delta \underline{x}_k = \underline{z}^*$, the iterative procedure to solve the QP subproblem generates a sequence of feasible iterates $\underline{z}_1, \underline{z}_2, \dots, \underline{z}^*$. Let \underline{z}_i denote the estimate of the solution at the i^{th} iteration. The next iterate is defined by

$$\underline{z}_{i+1} = \underline{z}_i + \rho_i \underline{p}_i \quad (3.26)$$

where

\underline{p}_i is an n -dimensional search direction, and

ρ_i is a scalar step length.

At each iteration, only a subset of the constraint set in problem (3.27), called the working set, is needed to evaluate the search direction. The working set consists of load flow constraints that are binding, i.e., exactly satisfied at the current point. These constraints include,

- (a) MVAR generation at a limit
- (b) MW generation at a limit

- (c) voltages at a limit
- (d) transformer taps at a limit
- (e) load distribution constraints.

Let A_i denote the matrix of coefficients of the constraints in the current working set, i.e., the i^{th} iteration, with t_i linearly independent rows. Under this condition, the QP subproblem (3.24) can be expressed as

minimize

$$\underline{c}^T \underline{z} + \frac{1}{2} \underline{z}^T B \underline{z}$$

subject to:

$$A_i \underline{z} = \underline{b} \quad (3.27)$$

Given a feasible point \underline{z}_i , the step \underline{p}_i from \underline{z}_i to \underline{z}^* is the solution of the n -dimensional problem,

minimize

$$(B \underline{z}_i + \underline{c}) \underline{p}_i + \frac{1}{2} \underline{p}_i^T B \underline{p}_i \quad (3.28)$$

subject to:

$$A_i \underline{p}_i = 0$$

The constraint equation

$$A_i p_i = 0$$

implies that the step p_i from a feasible point to any other feasible point must be orthogonal to the rows of A_i .

If Z_i is a matrix whose columns form a basis for the set of vectors orthogonal to the rows of A_i , i.e.,

$$A_i Z_i = 0,$$

then Z_i is a matrix of n rows and $n-t_i$ columns, and p_i can be written,

$$p_i = Z_i p_z, \quad (3.29)$$

for any $(n-t_i)$ -dimensional vector p_z .

The solution of problem (3.28) is obtained by computing the $(n-t_i)$ -dimension vector p_z which is the solution of the unconstrained problem:

$$\underset{p_z}{\text{minimize}} \quad (B_{z_i} + \underline{c})Z_i p_z + \frac{1}{2} p_z^T Z_i^T B Z_i p_z \quad (3.30)$$

The solution to problem (3.30) is given by,

$$p_z = -(Z_i^T B Z_i)^{-1} Z_i^T (B_{z_i} + \underline{c})$$

From equation (3.29), the search direction p_i can be expressed as,

$$p_i = -Z_i(Z_i^T B Z_i)^{-1} Z_i^T (B z_i + \underline{c}) \quad (3.31)$$

The algorithm to solve problem (3.24) is based on developing a working set which is a prediction of the correct active set. The correct active set of the problem is not known a priori. Since the prediction of the active set could be wrong, the algorithm includes a procedure for testing whether the current prediction is correct, and altering it if it is not.

The algorithm to solve the QP problem involves the following steps:

- STEP 1: Determine a feasible point of the QP problem.
- STEP 2: Test for convergence. If conditions for optimality are satisfied, STOP.
- STEP 3: If necessary, delete constraints from the current working set. This is done on the basis of the Lagrangian multiplier estimates.
- STEP 4: Compute a feasible search direction p_i using equation (3.29).
- STEP 5: Compute a step length ρ_i .
- STEP 6: If necessary, add a constraint to the working set. If ρ_i is a step to the constraint r , constraint r is added to the next working set and the associated quantities are updated.

STEP 7: Update estimate of solution (using equation (3.26)) and return to STEP 2.

An essential feature of the algorithm is that all iterates are feasible, i.e., if the initial point \underline{z}_0 is feasible, all subsequent iterates, \underline{z}_i , are also feasible.

In STEP 1, an initial feasible point is found by solving the following linear programming problem:

minimize

$$F(\underline{z}) = - \sum_{j \in J_V} (a_j \underline{z} - b_j) \quad (3.32)$$

subject to:

$$a_j \underline{z} - b_j \geq 0, \quad j \in J_V$$

where J_V is the set of indices identifying constraints that are violated at \underline{z} .

The function $F(\underline{z})$ is a linear function, and is equal to the sum of infeasibilities at \underline{z} . It should be noted that $F(\underline{z})$ is zero at any feasible point.

In STEP 2, a test for convergence is conducted. If the current solution satisfies the optimality conditions, the algorithm terminates.

In STEP 3, a decision is taken whether to continue minimizing in the subspace defined by the current working set, or to modify the current working set. This is done on the basis of the Lagrangian multiplier estimates. The Lagrangian multiplier, η_j , corresponding to an inequality constraint j in the working set, is

said to be optimal if $\eta_j \leq 0$ when the associated constraint is at the upper bound, or if $\eta_j \geq 0$ when the associated constraint is at the lower bound. If a multiplier is non-optimal, the objective function can be reduced by deleting the corresponding constraint from the working set.

In STEP 4, the feasible direction p_i is computed. The step length along the feasible direction is computed in STEP 5. In order to retain feasibility, it is necessary to ensure that the step length does not violate any constraint that is not in the working set. If $z_i + p_i$ is feasible, ρ_i is taken as unity; otherwise, ρ_i is set to the step along p_i to the nearest constraint which is added to the working set in STEP 6. The estimate of the solution is updated in STEP 7.

3.6.2 Overall Algorithm

The overall algorithm to solve the nonlinear programming problem by the SQP method is summarized in the flowchart shown in figure 3.1. Equation (3.25) represents the outer loop. The inner loop corresponds to equation (3.26).

The NAG routines used to solve the optimization problems require that the first derivatives of the problem functions (the objective function and the constraint functions) with respect to all the variables be provided. The evaluated derivatives for NCP1 are shown in Appendix II.

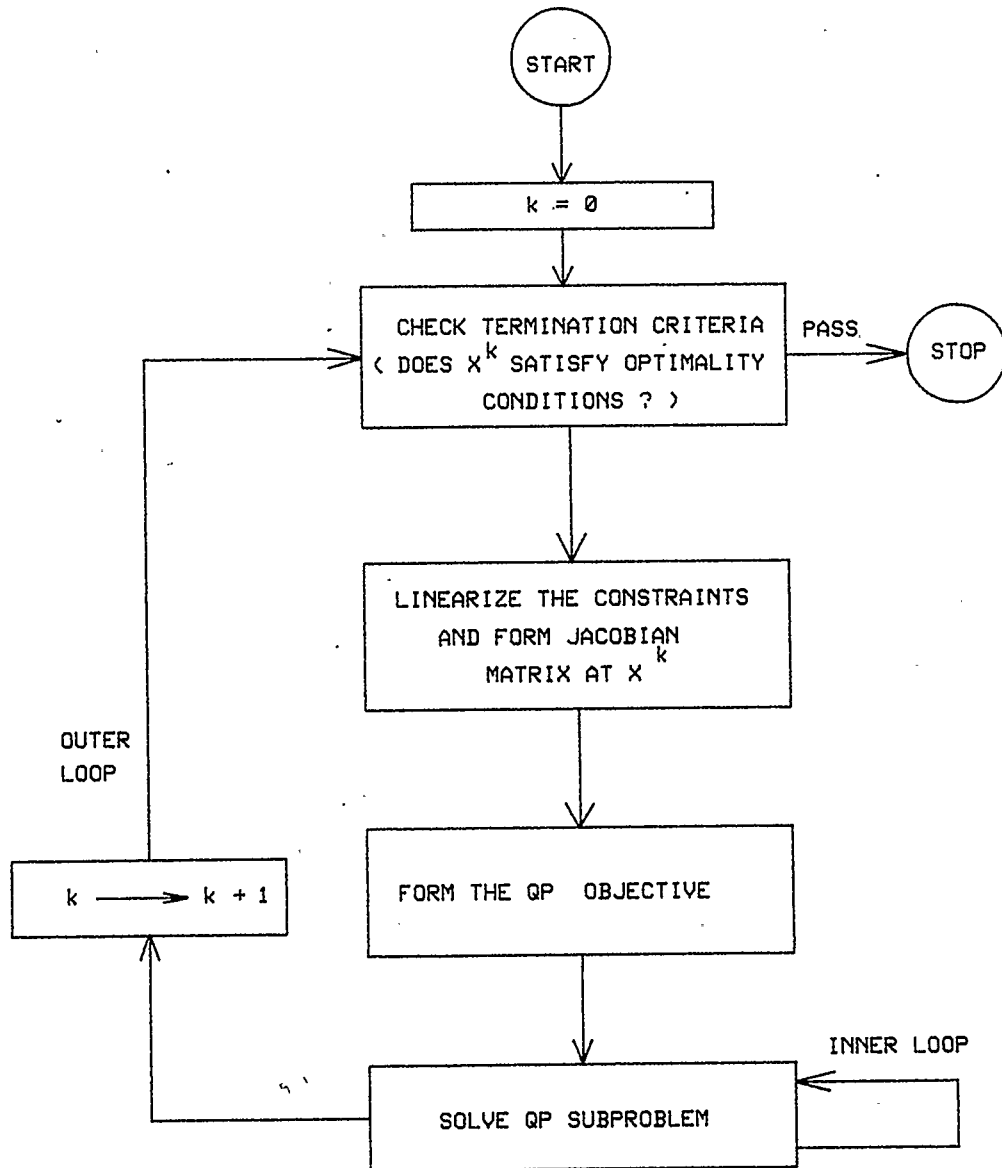


Figure 3.1: Flowchart of Basic SQP Algorithm

3.7 EXAMPLES OF APPLICATION OF THE PROPOSED METHOD

The method proposed in this chapter has been applied to evaluate the voltage stability limit and security margin, SM , of two power systems: The AEP 14-bus network (figure III.1) [67] and a 28-bus network (figure III.3) [29]. The AEP 14-bus network includes two generators, three synchronous condensers and twenty transmission lines/transformers. The 28-bus network includes six generating units and thirty-two transmission lines. The data for these systems are shown in Appendix III.

In the two examples, the elements of the distribution vector, $\underline{\beta}$, are chosen to be

$$\beta_i = \frac{S_i^{initial}}{\sum_{j \in J_L} S_j^{initial}}, \quad i \in J_L \quad (3.33)$$

In practice, the elements of $\underline{\beta}$ should be chosen to correspond to the expected relative increase in the demands at each bus. This information may be obtained from the load forecasts.

It should be noted that

$$\sum_{i \in J_L} \beta_i = 1.$$

$\beta_i = 0$ implies that the MVA demand at bus i remains unchanged in the scenario

to be investigated.

For the given initial system demand, the system generation may be distributed on the basis of economic allocation or dispatch. As the system load changes, the output of certain generating units must be changed, i.e., they must participate in the load change in order that the new load be served at the most economical operating point. It is shown in Appendix I that this may be achieved, approximately, by choosing the participation factors for each generating unit as follows [62] :

$$\gamma_i^o = \frac{1/F_i''}{\sum_{j=M+1}^N \left[\frac{1}{F_j''} \right]} \quad (3.34)$$

where

$$F_i'' = \frac{d^2 F_i(P_i)}{dP_i^2}$$

and

$F_i(P_i)$ is the cost function of the generating unit i .

In evaluating the systems security margins, it is assumed that the load power factors remain constant at the initial values specified by the initial bus loads.

3.7.1 System One : 14-Bus Network (Fig. III.1)

For this network, the elements of the distribution vector, $\underline{\beta}$, computed using equation (3.33) are shown in Table 3.1, and the participation factors of the generating units are shown in Table 3.2.

Using multiple load flow computations, plots of variation of load bus voltages are obtained as the total *MVA* load (S_{TOTAL}) is increased. The corresponding bus *MVA* are increased according to

Table 3.1 : Load Distribution Vector ($\underline{\beta}$)

Bus No.	β_i
3	0.2666
4	0.1735
5	0.1321
7	0.0
9	0.0939
10	0.0820
11	0.0408
12	0.1003
13	0.0672
14	0.0436

Table 3.2: Generators Participation Factors ($\underline{\gamma}$)

Unit No.	γ_i
2	0.4444

$$S_i^{n+1} = S_i^n + \beta_i (\Delta S_{TOTAL}) \quad i \in J_L \quad (3.35)$$

$$n = 0, 1, 2, \dots$$

where n is the step count and ΔS_{TOTAL} is the step increase in the total MVA load. At each increment in S_{TOTAL} , both open- and short-circuit (complementary) load flow solutions are obtained, i.e., multisolutions of the load flow equations are determined at each step [60]. Figures 3.2a and 3.2b show two such plots for buses 3 and 12. As noted in [13], the open- and short-circuit solutions should coincide at the limit. However, as this limit is approached, the Newton-Raphson-based load flow solution method did not converge. The limit has been obtained by graphical extrapolation (shown in broken lines). It is this limit that will be determined directly by the proposed method.

Table 3.3 shows the system condition at the limit obtained by the proposed method. The corresponding stability margin SM_1 is also shown. It will be observed that the critical condition obtained by the proposed method corresponds to the limit of the curves, obtained by multiple load flow and extrapolation, in figure 3.2a and 3.2b. The optimization method requires much less computational effort than the multiple load flow method. The proposed method takes 1.716 CPU seconds for computations while a single load flow computation for the system takes 0.429 CPU seconds. A good number of load flow computations is required to plot the curves. Also, nonconvergence of load flow computations close to the critical

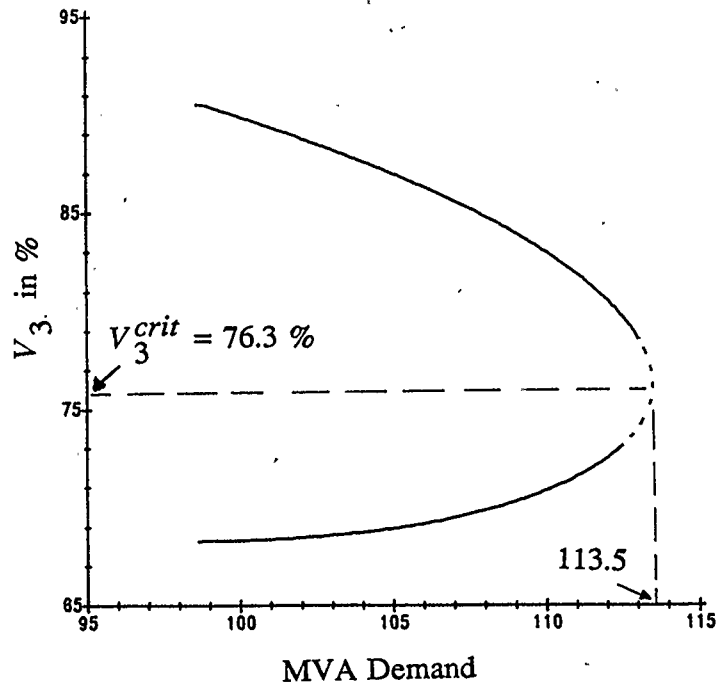


Figure 3.2a: Voltage Versus MVA Load at Bus 3 (pf constant)

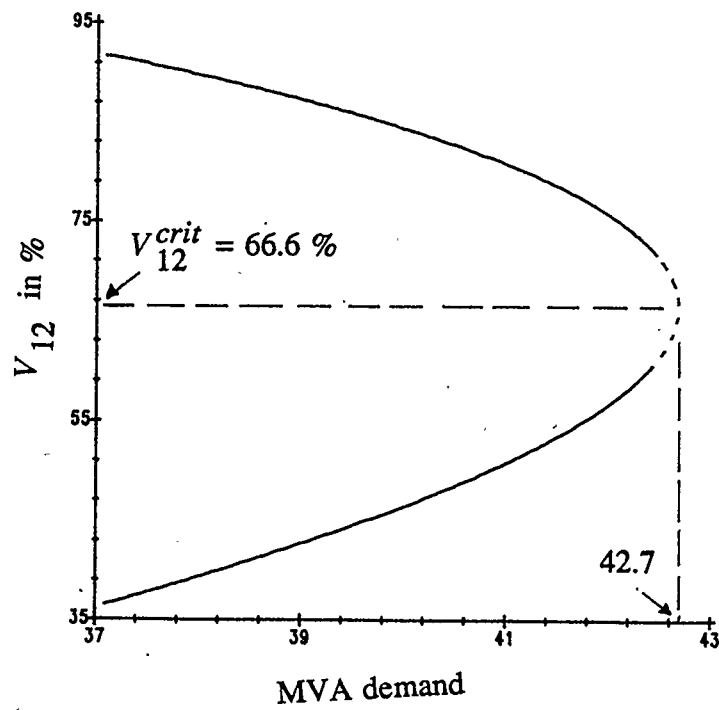


Figure 3.2b: Voltage Versus MVA Load at Bus 12 (pf constant)

Table 3.3: System Condition At The Voltage Stability Limit
(Load MVA Independent of Bus Voltage)

Bus	Bus Voltage		Bus Power*	
	Mag.	Ang.**	MW	MVAR
1	1.060	0.00	409.1	278.4
2	0.9251	-7.3	70.0	50.0
3	0.7629	-22.7	-111.3	-22.4
4	0.7602	-20.6	-68.3	-28.2
5	0.7850	-18.2	-56.2	-1.9
6	0.7509	-39.8	0.0	24.0
7	0.7535	-32.3	0.0	0.0
8	0.8059	-32.3	0.0	24.0
9	0.7214	-38.9	-34.9	-19.6
10	0.6987	-42.0	-34.3	-6.9
11	0.7040	-42.3	-15.9	-6.9
12	0.6656	-48.5	-42.6	-1.9
13	0.6949	-44.9	-27.8	-6.9
14	0.6762	-44.2	-17.6	-5.9
$SM_1 = 0.1535$				

* -ve for loads

** in degrees

point may be a problem.

Next, an outage condition is considered. A heavily loaded line between buses 14 and 15 (figure III.1) is tripped and the proposed method is applied to determine the system critical state assuming the same β and same initial operating condition. Table 3.4 shows the system condition at the stability limit and the corresponding stability margin SM_2 . In this case, the stability margin is negative, which means that with line 1-5 out, the network cannot sustain (or supply) the specified initial system demand. No steady state operating point exists under this condition and system collapse would occur.

It should be observed from Tables 3.3 and 3.4 that the MW and MVAR limits on the generator and the synchronous condensers have been limited to their respective maximum values. The importance of limiting the generator outputs to their specified production capabilities is demonstrated by recomputing the security margins for the base case and the outage condition considered previously with these limits ignored. Table 3.5 shows the system state at the critical point and the corresponding security margin, SM_3 , for the base case (no outage condition) with the MW and MVAR limits on the generators and synchronous condensers ignored. It is apparent that SM_3 (being greater than SM_1) gives a false indication of system security. Also, Table 3.6 shows the system state at the critical point for the contingency condition (line 1-5 out) with the MW and MVAR limits on the generator and synchronous condensers ignored. The corresponding SM_4 (greater

Table 3.4: System Condition At The Stability Limit
(With line outage)

Bus	Bus Voltage		Bus Power*	
	Mag.	Ang.**	MW	MVAR
1	1.060	0.0	307.6	188.9
2	0.9070	-8.7	70.0	50.0
3	0.7595	-23.6	-85.7	-17.3
4	0.7352	-24.8	-52.6	-21.7
5	0.7360	-24.7	-43.3	-1.5
6	0.7577	-41.1	0.0	24.0
7	0.7577	-34.4	0.0	0.0
8	0.8099	-34.4	0.0	24.0
9	0.7367	-39.5	-26.8	-15.1
10	0.7198	-41.9	-26.4	-5.3
11	0.7234	-42.5	-12.3	-5.3
12	0.6962	-47.3	-32.8	-1.5
13	0.7173	-44.7	-21.4	-5.3
14	0.7035	-43.7	-13.6	-4.5
$SM_2 = -0.0991$				

* -ve for loads

** in degrees

Table 3.5: System Condition At The Voltage Stability Limit
(Generators MW and MW Limits Ignored)

Bus	Bus Voltage		Bus Power*	
	Mag.	Ang.**	MW	MVAR
1	1.060	0.00	409.1	278.4
2	1.045	-9.80	483.7	696.6
3	0.6001	-45.90	-213.2	-43.0
4	0.6616	-42.2	-130.8	-54.1
5	0.6978	-37.9	-107.7	-3.6
6	1.0700	-78.6	0.	359.9
7	0.8337	-64.2	0.	0.
8	1.0900	-64.2	0.	158.6
9	0.7934	-73.9	-66.8	-37.6
10	0.7952	-79.0	-65.6	-13.1
11	0.8992	-80.2	-30.6	-13.1
12	0.9354	-87.0	-81.7	-3.6
13	0.9563	-83.3	-53.2	-13.1
14	0.8087	-81.9	-33.7	-11.3
$SM_3 = 0.5582$				

* -ve for loads

** in degrees

than SM_2) also gives a false indication of system security. In fact the value of SM_4 , being positive, shows quite incorrectly that the system can survive that outage condition.

It is apparent that in order to obtain realistic security margins of a system to the collapse point, the system generating units' MW and MVAR production capabilities must be taken into account.

3.7.1.1 Effect of Voltage Dependence of Loads

The results in section 3.7.1 were obtained assuming that the MVA loads are independent of their respective bus voltages. Referring to Section 3.4, equation (3.14) and (3.15)

$$p_i = q_i = 0, \quad i \in J_L$$

in equations (3.17) and (3.18). However, it is known that most system loads have characteristics differ from the constant MVA type. Effects of the voltage dependence of loads have been studied briefly by assuming that the static load characteristics may be modelled as in equations (3.14) and (3.15).

Table 3.7 shows the system critical state and the corresponding stability margin SM_5 when $p_i = q_i = 2$, $i \in J_L$. This situation corresponds to the constant impedance representation of the system loads. When compared with results in Table 3.3, it can be seen that the stability margin SM_5 is higher in this case.

Table 3.6: System Condition At The Stability Limit
(With line outage and Generator limits Ignored)

Bus	Bus Voltage		Bus Power*	
	Mag.	Ang.**	MW	MVAR
1	1.060	0.0	307.6	188.9
2	1.045	-15.2	428.2	753.3
3	0.6730	-47.5	-178.9	-36.1
4	0.6819	-51.9	-109.8	-45.2
5	0.6948	-52.6	-90.4	-3.0
6	1.0700	-83.3	0.	303.2
7	0.8662	-69.9	0.	0.
8	1.0900	-69.9	0.	138.5
9	0.8410	-77.7	-56.0	-31.5
10	0.8444	-82.0	-55.1	-11.0
11	0.9303	-83.8	-25.6	-11.0
12	0.9611	-90.0	-68.6	-3.0
13	0.9780	-86.8	-44.6	-11.0
14	0.8564	-84.7	-28.3	-9.5
$SM_4 = 0.4735$				

* -ve for loads

** in degrees

Table 3.7: System Condition At Voltage Stability Limit
(Impedance Load Representation)

Bus	Bus Voltage		Bus Power*	
	Mag.	Ang.**	MW	MVAR
1	1.060	0.0	402.0	271.6
2	0.9285	-7.1	70.0	50.0
3	0.7719	-21.9	-106.5	-21.5
4	0.7648	-20.2	-66.2	-27.4
5	0.7887	-17.9	-55.3	-1.9
6	0.7524	-39.6	0.0	24.0
7	0.7554	-32.0	0.0	0.0
8	0.8077	-32.0	0.0	24.0
9	0.7224	-38.7	-36.1	-20.3
10	0.6993	-41.9	-34.8	-7.0
11	0.7045	-42.2	-16.4	-7.0
12	0.6770	-48.3	-42.7	-1.9
13	0.6937	-44.8	-28.4	-7.0
14	0.6771	-44.0	-17.6	-5.9
$SM_5 = 0.2085$				

* -ve for loads

** in degrees

In general, let

$$p_i = q_i = n \quad (3.38)$$

Figure 3.3 shows a plot of SM against n , n varying from 0 to 2. It will be observed that as n increases from zero, the corresponding stability margin increases. It should be observed that in this example the constant power representation of loads (loads independent of bus voltage) is the most severe load model from voltage stability viewpoint.

3.7.2 System Two: 28-Bus Network (Figure III.3)

The elements of the distribution vector β and the generator participation vector γ are shown in Tables 3.8 and 3.9 respectively.

Table 3.10 shows the the system critical state and the corresponding security margin SM_6 obtained using the proposed method.

It should be observed that, unlike the situation in the 14-bus example in section 3.7.1, the system voltage magnitudes in this example approach normal operating values. Hence, as mentioned by several investigators, voltage magnitudes alone may not provide sufficient information to predict the security of power systems from collapse.

Figure 3.4a and 3.4b shows the voltage variations at load buses 4 and 5 obtained using multiple load flow computations. Again due to convergence prob-

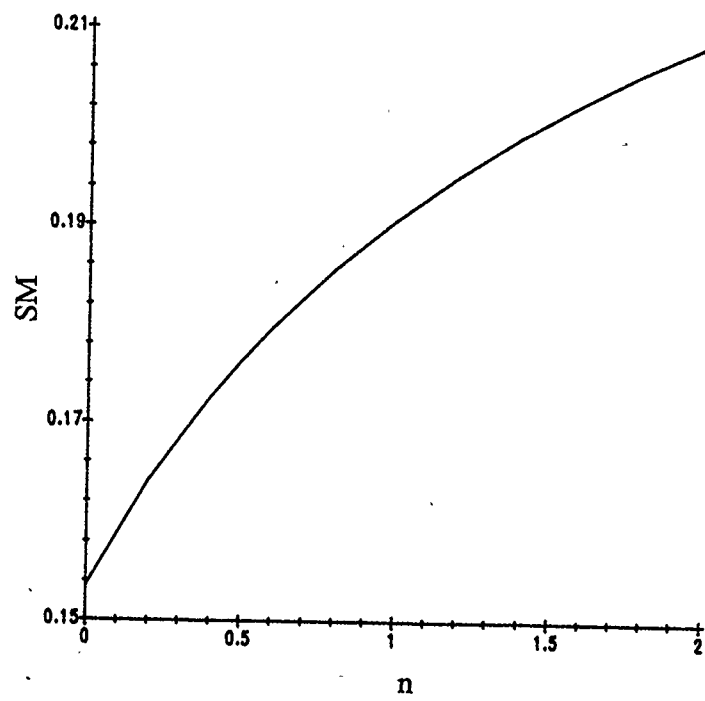


Figure 3.3: SM Versus Load Exponent (14-Bus System)

Table 3.8 : Load Distribution Vector (β)

Bus No.	β_i^*
2	0.0681
3	0.1180
4	0.1695
5	0.1705
6	0.1667
7	0.0573
8	0.0652
9	0.0272
10	0.0530
11	0.0386
12	0.0659

* only non-zero values shown

Table 3.9: Generators Participation Factors (γ)

Unit No.	γ_i
24	0.1507
26	0.1356
27	0.2110
28	0.2028

Table 3.10: System Condition at the Voltage Stability Limit: 28-Bus Network

Bus	Bus Voltage		Bus Power	
	Mag.	Ang.**	MW	MVAR
1	1.0500	0.0	1298.3	267.0
2	0.9089	-52.2	-147.8	-50.9
3	0.9050	-56.8	-270.0	-22.4
4	0.9124	-55.2	-388.2	-26.5
5	0.9045	-60.4	-391.3	-2.0
6	0.9838	-23.4	-381.1	-34.6
7	0.9808	-15.0	-131.4	-3.1
8	0.9814	-22.4	-137.6	-59.1
9	0.9896	-11.6	-62.0	-7.0
10	0.9309	-338.2	-120.2	-18.0
11	0.9275	-41.1	-76.4	-44.8
12	0.9881	-25.7	-144.6	-53.0
13	0.9660	-18.0	0.0	0.0
14	0.9490	-27.5	0.0	0.0
15	0.9280	-35.3	0.0	0.0
16	0.9258	-33.2	0.0	0.0
17	0.9916	-11.7	0.0	0.0
18	0.9820	-14.0	0.0	0.0
19	0.9936	-6.3	0.0	0.0
20	0.8958	-52.4	0.0	0.0
21	0.9003	-46.7	0.0	0.0
22	0.8964	-48.9	0.0	0.0
23	0.9017	-44.5	0.0	0.0
24	1.0500	-8.4	201.9	140.0
25	1.0500	5.9	440.0	71.5
26	1.0500	-22.1	58.8	40.2
27	1.0500	-20.3	405.2	244.5
28	1.0500	-31.2	166.7	200.0
$SM_6 = 0.01863$				

* -ve for loads

** in degrees

lems of the load flow analysis method, the limits of the curves have been obtained by graphical extrapolation as shown by broken lines in the figures 3.4a and 3.4b. It should be noted that the critical condition obtained by the proposed method (Table 3.10) corresponds to the limits indicated in these curves.

A contingency condition is considered next. The line between buses 14 and 15 (figure III.3) is outaged and the proposed method is applied to determine the system critical state assuming β and γ remain unchanged. Table 3.11 shows the system critical state for this situation computed using the proposed method. The corresponding security margin, SM_7 , is less than the security margin associated with the base case condition (i.e., $SM_7 < SM_6$). SM_7 is negative, indicating that the system voltages would collapse if the line between bus 14 and bus 15 is outaged due to a disturbance.

In general, as may be expected, the effect of line outages is to reduce the load supply capability of the network, and hence reduce the system security margin.

3.7.2.1 Effect of Voltage Dependence of Loads : 28-Bus System

In order to investigate the effect of the voltage dependence of the MVA load on the security margin, SM , in the 28-bus example system, we let

$$n = p_i = q_i, \quad i \in J_L.$$

Figure 3.5 shows a plot of the security margin, SM , against n , which varies

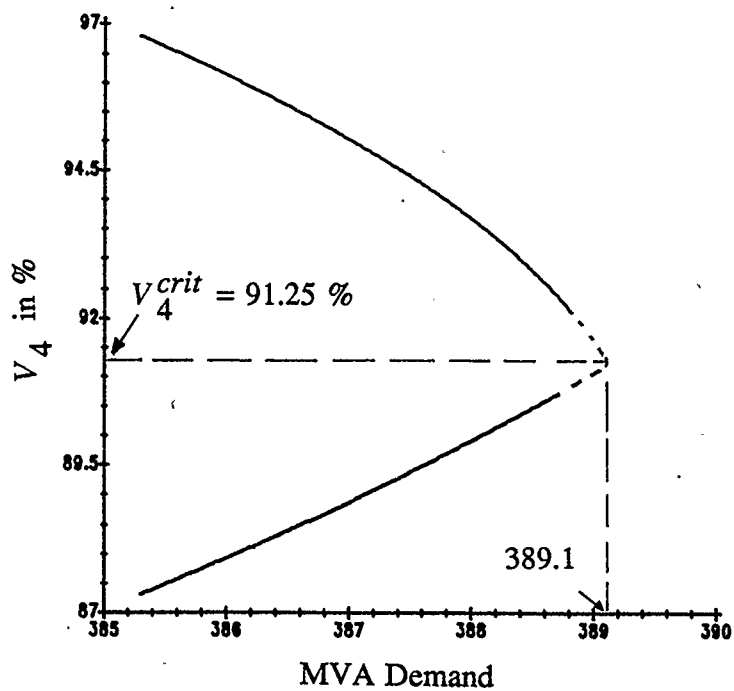


Figure 3.4a: Voltage Versus MVA Load at Bus 4 (pf constant)

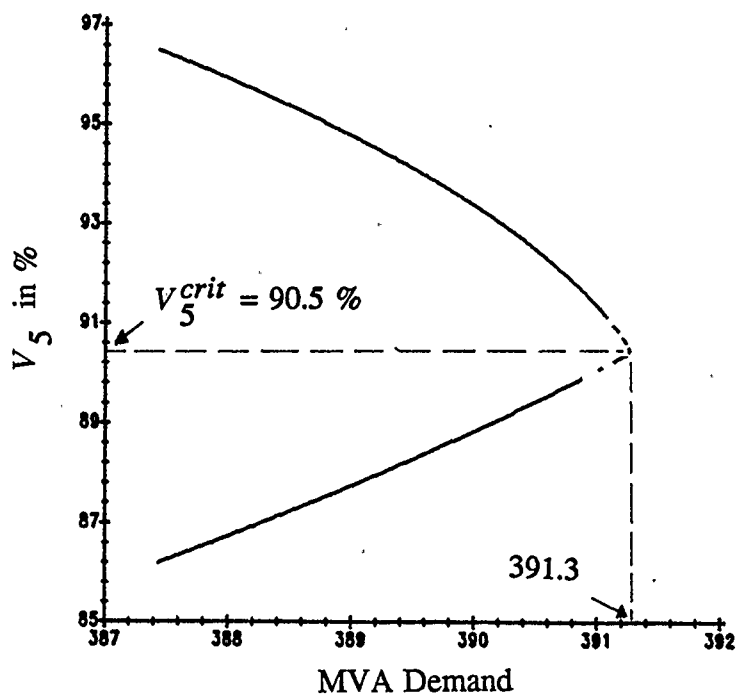


Figure 3.4b: Voltage Versus MVA Load at Bus 5 (pf constant)

Table 3.11: System Condition at the Voltage Stability Limit: 28-Bus Network
(With Line Outage)

Bus	Bus Voltage		Bus Power	
	Mag.	Ang.**	MW	MVAR
1	1.0500	0.0	1118.7	223.7
2	0.8997	-48.4	-138.0	-47.6
3	0.9009	-54.9	-252.3	-20.9
4	0.9215	-56.1	-362.7	-24.8
5	0.9172	-60.9	-365.6	-1.9
6	0.9910	-22.8	-356.0	-32.4
7	0.9833	-15.0	-122.8	-2.9
8	0.9927	-21.9	-128.5	-55.2
9	0.9939	-11.2	-57.9	-6.7
10	0.9277	-41.8	-112.3	-17.1
11	0.9301	-44.6	-71.4	-41.9
12	0.9902	-25.2	-132.3	-49.5
13	0.9602	-19.0	0.0	0.0
14	0.9632	-15.2	0.0	0.0
15	0.9270	-40.6	0.0	0.0
16	0.9207	-37.1	0.0	0.0
17	0.9896	-12.1	0.0	0.0
18	0.9843	-14.0	0.0	0.0
19	0.9953	-6.2	0.0	0.0
20	0.9047	-53.5	0.0	0.0
21	0.9050	-48.3	0.0	0.0
22	0.8895	-47.3	0.0	0.0
23	0.8891	-41.0	0.0	0.0
24	1.0500	-8.6	213.0	144.4
25	1.0500	6.0	440.0	68.1
26	1.0500	-20.8	68.8	37.2
27	1.0500	-8.3	390.0	203.5
28	1.0500	-35.9	181.6	200.0
$SM_{\gamma} = -0.0469$				

* -ve for loads

** in degrees

between 0 and 2. From figure 3.5, it is apparent that in this case, as in the 14-bus example, as the MVA loads become more voltage dependent the security margin, SM , tends to increase.

3.8 CONCLUSIONS

A methodology to determine the voltage stability limit of a multimachine power system has been described. The methodology formulates the problem as an optimization problem of maximizing the system total MVA load. The resulting nonlinearly constrained optimization problem is solved using the sequential quadratic programming algorithm. With this formulation, difficulties related to singularity of the Jacobian matrix associated with the load flow equations, and convergence of the load flow solution around the voltage stability limit, are avoided. The method accommodates device constraints and limitations in system controls (e.g. generator VAR limits and limits on transformer tap settings).

A stability margin SM , which may serve as a measure of the security of the system as far as voltage collapse is concerned, is defined. This index gives an explicit indication of the distance to voltage collapse in terms of actual total system load.

Modifications to the general formulation are presented taking into consideration exponential voltage dependence of system loads (steady state).

The computational requirements of the proposed method is about the same as that for the well-known optimal power flow computation for the economic dispatch

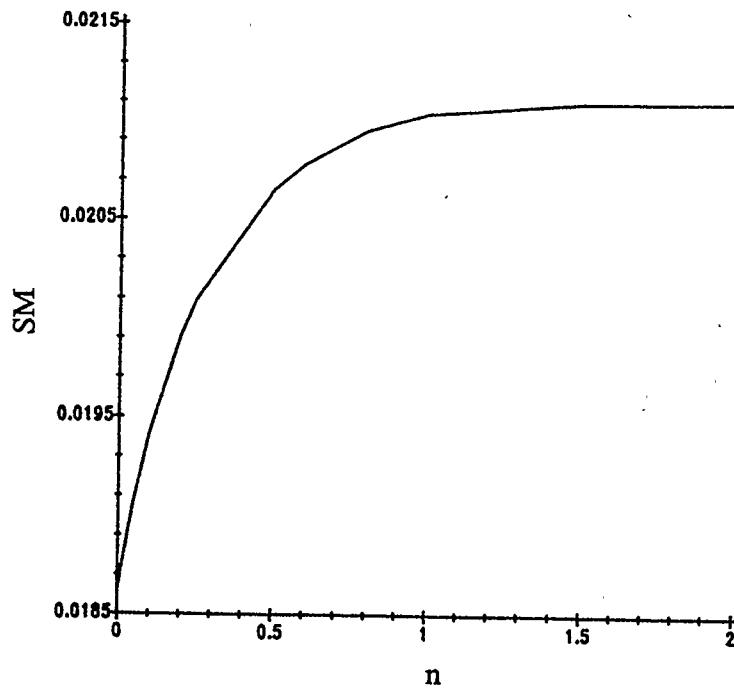


Figure 3.5: SM Versus Load Exponent (28-Bus System)

of system generation.

Results of application of the proposed method to two example networks are presented and discussed.

CHAPTER 4

IDENTIFYING STRONG AND WEAK SPOTS IN A POWER SYSTEM FROM VOLTAGE STABILITY VIEWPOINT

4.1 INTRODUCTION

As noted previously in this thesis, the problem of declining voltages under heavy loading conditions in a transmission system, and loss of voltage stability following a major system disturbance, have been experienced with greater frequency and severity in France [5], Belgium [6], Japan [8], the United States [7], and recently in the Ontario Hydro system in Canada [9].

Calvaer mentioned in [6] that a system may be voltage unstable if it includes at least one voltage unstable bus. It is also mentioned in [34] that the experience in France and Italy suggests that a practical control algorithm should identify critical buses in the network and maintain control on voltages at these buses in order to alleviate the vulnerability of the system to collapse. In addition, since voltage collapse may originate from the system critical bus, this might be the best location to apply countermeasures, like switching operations or load shedding, in order to save the rest of the system. Load shedding is regarded as a last measure control action. The question is, how can the critical bus in a network be identified?

The critical bus or the "weak" spot in a transmission system is, electrically, the most remote bus from point of constant voltage, (or point of controllable voltage). For a simple radial system which includes a generating unit serving a number of load points along a transmission line (Figure 4.1), the critical bus is easily determined as the most remote bus from the generating unit in both electrical and physical terms. However, identifying the critical buses or areas in a practical size interconnected system is not so simple.

In [31], Kessel et. al. proposed a method of identifying the critical bus in a network based on certain voltage stability indices. These indices assess the proximity of load supply at each bus to the load flow feasibility limit. The bus with the largest index is said to be the critical bus in the network. One drawback of this method is that it fails to take into consideration the operating constraints of system equipment, for example the VAR limits of the generators. As mentioned before, this is an important consideration because, when a generator reaches its VAR limit, the terminal voltage can no longer be controlled. Under this condition, the machine model has to be modified resulting in a change in the system performance pattern.

Schlueter proposed a method in [41] to determine the weak areas in a transmission system. The method has been adapted from the literature on determining coherent groups of machines which are aggregated to form a dynamic equivalent for transient stability studies. A voltage control area is then defined as a set of PQ and PV buses that are "coherent" in terms of voltage deviations for

any set of real or reactive power disturbances. The voltage control areas identified using the coherency algorithm applied to the reactive power/voltage Jacobian matrix are believed to have weak boundaries in terms of transferring reactive power.

In this chapter, two methods are proposed for identifying the weak spots in transmission systems. The methods are extensions of the approach proposed in Chapter 3 of this thesis for determining the static voltage stability limit in multimachine power systems. The first method is based on the relative change in the bus voltages going from an initial operating state to the voltage stability limit. The second method is based on the sensitivity parameters computed at the voltage stability limit.

4.1 METHOD ONE - RELATIVE VOLTAGE CHANGE METHOD

Let V_i^{init} and V_i^{limit} be the voltage magnitudes at bus i at the initial operating state and the voltage stability limit respectively. The system state at the voltage stability limit is determined using the method proposed in Chapter 3 of this thesis. A voltage change index is defined for each load bus as

$$VC_i = \frac{V_i^{init} - V_i^{limit}}{V_i^{limit}}, \quad i \in J_L \quad (4.1)$$

where

J_L is the set of all load buses.

As mentioned previously, the "weak" or critical bus in the network is the most (electrically) remote bus from the point of constant or controllable voltage. It is expected that the critical bus would be the worst affected (voltage-wise) because of a shortage of local VARs or VARs transferred or imported from a remote source. This is a typical scenario in reported cases of voltage collapse problems [11]. Based on this expectation, it is anticipated that for a specified operating regime, going from an initial operating point to the voltage stability limit, the critical bus would experience the largest voltage change (or drop), i.e., the largest index VC_i defined by equation (4.1). Therefore if bus k is the critical bus, then

$$VC_k = \max_{i \in J_L} \{ VC_i \} \quad (4.2)$$

Based on the index VC_i , the system buses may be arranged in order of "weakness", the weakest bus corresponding to the one with the largest index.

The voltage change index defined in equation (4.1) to identify the critical bus in a network may be extended to identify the weakest area in a power network. In this context, an area would consist of a set of connected buses in a geographical region.

Let K be an area with n_K connected load buses, where $K \in S_A$, S_A is the set of all areas. An index, AVC_K , is defined for all areas in S_A as

$$AVC_K = \frac{\sum_{i \in K} VC_i}{n_K}, \quad K \in S_A \quad (4.3)$$

AVC_K is simply the average voltage change for the buses in area K . Again, it is expected that the weakest area would experience the largest average voltage change. Thus, if area J is the the weakest area, then

$$AVC_J = \max_{K \in S_A} \{ AVC_K \} \quad (4.4)$$

Using this index, areas in the system may be ordered on the basis of "weakness", the weakest area corresponding to the one with the largest index, AVC_J .

4.3 METHOD TWO - SENSITIVITY METHOD

This method of identifying the critical bus and weak areas in a power network is based on the sensitivity of the objective function, which is the total maximum load S_T , that the system can supply stably for a given distribution vector $\underline{\beta}$ (reference Chapter 3).

As mentioned in Chapter 3, the vector $\underline{\beta}$ specifies the direction of increase of the MVA demand vector. β_i , an element of $\underline{\beta}$, is an increase in the load at bus i expressed in per unit of the corresponding system total load increase. In a stable operating regime, an increase $\Delta\beta_i$, in β_i should result in an increase ΔS_i in the MVA demand at bus i and consequently, an increase in the total

MVA load. β_i may be viewed as a mechanism for varying the MVA demand at bus i .

The increase in the MVA demand at bus i , ΔS_i , due to an increase $\Delta\beta_i$, is however dependent on the strength of the network at bus i . The sensitivity parameters,

$$SI_i = \frac{\partial S_T}{\partial \beta_i}, \quad i \in J_L \quad (4.5)$$

therefore may be seen as measures of incremental effectiveness, of load supply at the respective buses. SI_i may thus be used as a "strength index" and interpreted as a measure of the capability of the network to supply additional power (real or reactive) to bus i .

It is apparent that the critical bus in the network will have the minimum strength index, i.e., if bus k is the critical bus in the network, then,

$$SI_k = \min_{i \in J_L} \{ SI_i \} \quad (4.6)$$

Again, using this index, the system buses may be ordered on the basis of "weakness", the weakest bus corresponding to that with the smallest strength index.

This definition of strength index may also be extended to identify weak areas in a network. For this purpose, an index ASI_K is defined for each area as

$$ASI_K = \frac{\sum_{i \in K} SI_i}{n_K}, \quad K \in S_A \quad (4.7)$$

ASI_K is the average strength index for the buses in the area. The weakest area is the area with the smallest average strength index. Thus if area J is the weakest area, then

$$ASI_J = \min_{K \in S_A} \{ ASI_K \} \quad (4.8)$$

This index (ASI_J) may be used to order the system areas on the basis of weakness.

It should be noted that this method of identifying the system critical bus and weak areas depends on the computation of the sensitivity parameter, SI_i , $i \in J_L$ at the voltage stability limit. Although the maximum total load S_T depends on the choice of the distribution vector $\underline{\beta}$, the relationship is not explicit and makes the direct computation of the sensitivity parameters defined in equation (4.5) rather difficult. However, as shown in the next section, the Lagrange multipliers associated with binding constraints at the solution point of an optimization problem have useful sensitivity interpretations. Of particular interest are the Lagrange multipliers associated with the elements of the vector $\underline{\beta}$ in the optimization problem (3.13) to determine the system voltage stability limit.

It will be recalled that the elements of the vector $\underline{\beta}$ are specified and are not included as variables in the optimization problem. For the purpose of determining the sensitivity of the objective function with respect to the elements of $\underline{\beta}$, an additional constraint set,

$$\beta_i = \beta_i^{spec}, \quad i \in J_L \quad (4.9)$$

must be included in the optimization problem (3.13). β_i^{spec} is the specified value of β_i .

Next, it is shown how the Lagrange multipliers at the solution point are used to evaluate the required sensitivity parameters.

4.3.1 Interpretation of The Lagrange Multipliers

In order to provide an interpretation of the Lagrange multipliers [68], the optimization problem (3.13) including the constraint set (4.9) above is written in compact form as,

minimize

$$f(\underline{x}) \quad (4.10)$$

subject to,

$$(1) \quad c_j(\underline{x}) = b_j, \quad j = 1, \dots, m_e$$

$$(2) \quad c_j(\underline{x}) \geq b_j, \quad j = m_{e+1}, \dots, m$$

$$(3) \quad \underline{x}^l \leq \underline{x} \leq \underline{x}^u$$

where

\underline{x} is an n -dimensional vector of variables,

\underline{x}^l and \underline{x}^u are the lower and upper limits on \underline{x} respectively, and

all functions are continuously differentiable.

Let the t -dimension vector \hat{c} be the vector of constraints that are binding at the solution of the optimization problem (4.10), i.e., constraints that satisfy

$$\hat{c}_j(\underline{x}^*) = \hat{b}_j, \quad j = 1, 2, \dots, t \quad (4.11)$$

The effect of a change in \hat{b}_j on the optimal value of the objective function, $f(\underline{x}^*)$ may be expressed as,

$$\begin{aligned} \frac{\partial f(\underline{x}^*)}{\partial \hat{b}_j} &= \sum_{i=1}^n \frac{\partial f(\underline{x}^*)}{\partial x_i} \cdot \frac{dx_i}{d\hat{b}_j} \\ &= \nabla f(\underline{x}^*)^T \left[\frac{dx}{d\hat{b}_j} \right] \end{aligned}$$

$$= \underline{g}(\underline{x}^*)^T \left[\frac{dx}{d\hat{b}_j} \right] \quad (4.12)$$

where

$$\nabla f(\underline{x}^*) = \underline{g}(\underline{x}^*) \quad (4.13)$$

The Kuhn-Tucker first order optimality condition [65] requires that,

$$\underline{g}(\underline{x}^*) = \hat{A}(\underline{x}^*)^T \underline{\lambda}^* \quad (4.14)$$

where $\hat{A}(\underline{x}^*)$ is the $t \times n$ Jacobian matrix of $\hat{c}(\underline{x}^*)$, i.e.,

$$\hat{A}(\underline{x}^*) = \left[\nabla \hat{c}_1, \nabla \hat{c}_2, \dots, \nabla \hat{c}_t \right]^T,$$

and $\underline{\lambda}^*$ is the of vector Lagrange multipliers associated with the binding constraint set (4.11) at the solution point.

Combining equations (4.12) and (4.14), we have,

$$\begin{aligned} \frac{\partial f(\underline{x}^*)}{\partial \hat{b}_j} &= \underline{\lambda}^{*T} \hat{A}(\underline{x}^*) \left[\frac{dx}{d\hat{b}_j} \right] \\ &= \sum_{j=1}^t \lambda_j^* \nabla \hat{c}_j^T \left[\frac{dx}{d\hat{b}_j} \right] \end{aligned} \quad (4.15)$$

From the j^{th} constraint of equation (4.11), we have

$$\frac{d(\hat{b}_j - \hat{c}_j(x^*))}{d\hat{b}_k} = \frac{d\hat{b}_j}{d\hat{b}_k} - \sum_{i=1}^n \frac{\partial \hat{c}_j(x^*)}{\partial x_i} \cdot \frac{dx_i}{d\hat{b}_k} = 0$$

or

$$\nabla \hat{c}_j(x^*)^T \frac{dx}{d\hat{b}_k} = \begin{cases} 1 & k = j \\ 0 & k \neq j \end{cases} \quad (4.16)$$

Combining equations (4.15) and (4.16), we have,

$$\frac{\partial f(x^*)}{\partial \hat{b}_j} = \lambda_j^* \quad (4.17)$$

It is apparent from equation (4.17) that the Lagrange multipliers at the optimal point provide a relative measure of the sensitivity of the objective function to changes in the constraints, i.e., they indicate how tightly the constraints are binding.

The above result is applied to the optimization problem (3.13) including the constraints set (4.9). Of particular interest are the Lagrange multipliers associated with the constraint set (4.9). Using equation (4.18), we have

$$SI_i = \frac{\partial S_T}{\partial \beta_i} = -\lambda_{\beta_i}^* \quad i \in J_L \quad (4.18)$$

where $\lambda_{\beta_i}^*$ is the Lagrange multiplier associated with the element β_i of the vector $\underline{\beta}$.

4.3.2 Evaluating The Lagrange Multipliers

The optimization problem (3.13) is solved using the Sequential Quadratic Programming (SQP) algorithm which is discussed in Chapter 3 of this thesis. At each major iteration, k , of the SQP algorithm, estimates of the optimal solution \underline{x}_k and the Lagrange multipliers $\underline{\lambda}_k$ are computed. At the k^{th} iteration, let \hat{c}_k be the vector of constraints that are believed to be active at the optimal point \underline{x}^* , and \hat{A}_k be the corresponding Jacobian matrix. The first order Kuhn-Tucker optimality condition shown in equation (4.14) requires that at the optimal solution, \underline{x}^* , the gradient of the objective function must equal a linear combination of the gradients of the active constraints. This condition suggests that the vector $\underline{\lambda}_L$ that solves the linear least-square problem

$$\underset{\underline{\lambda}}{\text{minimize}} \quad \|\hat{A}_k^T \underline{\lambda} - g_k\|_2^2 \quad (4.19)$$

would provide an estimate $\underline{\lambda}_k$ of the multipliers of the optimization problem.

Let

$$H = \hat{A}_k^T$$

in the problem (4.19). The vector $\underline{\lambda}_k$ which is the vector of minimum Euclidean length that is the solution of the problem (4.19) is given as

$$\underline{\lambda}_k = H^+ g_k \quad (4.20)$$

where the $t \times n$ matrix H^+ is the pseudo-inverse of the $n \times t$ matrix H .

The pseudo-inverse is written as

$$H^+ = (H^T H)^{-1} H^T; \quad (4.21)$$

however, it is not computed in this form. A convenient way of finding H^+ is based on singular value decomposition.

The real matrix H may be written as

$$H = U \Sigma V^T, \quad (4.22)$$

where

U is an $n \times n$ orthonormal matrix,

V is a $t \times t$ orthonormal matrix, and

Σ is an $n \times t$ diagonal matrix

$$\Sigma = \text{diag}(\sigma_1, \dots, \sigma_t)$$

with $\sigma_i \geq 0$ for all i .

The pseudo-inverse of H is then evaluated as,

$$H^+ = V \Omega U^T \quad (4.23)$$

where Ω is a $t \times n$ diagonal matrix

$$\Omega = \text{diag}(\omega_i)$$

with

$$\omega_i = \begin{cases} 1/\sigma_i & \text{if } \sigma_i \neq 0 \\ 0 & \text{if } \sigma_i = 0 \end{cases} \quad (4.24)$$

As the SQP algorithm progresses, \underline{x}_k converges to \underline{x}^* , and $\underline{\lambda}_k$ converges to $\underline{\lambda}^*$. SI_i , $i \in J_L$ can therefore be obtained using equation (4.18).

4.4 NUMERICAL EXAMPLES

Results of application of the proposed methods of identifying the system critical bus and weak areas to some example systems are presented in this section. The first system is a simple radial network which includes one generating unit and four load buses (Figure 4.1). By design, the critical bus in this network would be the physically most remote bus from the generating unit. The network is chosen for analysis in order to demonstrate the proposed methods. The second system is the AEP 14-bus network which includes two generating units, three synchronous condensers, and twenty transmission lines/transformers. The third system is a 20-bus network which includes six generating units and twenty-seven transmission lines/transformers.

In evaluating the voltage stability limits for these examples, only the reactive demands are assumed to increase, i.e., MW demands remain constant. Also, for

each of the example systems, the elements of the distribution vector β are chosen as,

$$\beta_i = \frac{P_{Li}}{\sum_{j \in J_L} P_{Lj}} \quad (4.25)$$

where

P_{Li} is the MW demand at bus i .

4.4.1 Radial System

Figure 4.1 shows a one line diagram of the four bus radial system. The line data for this system are given in Table 4.1.

Table 4.2 indicates the initial system state obtained by load flow analysis and the system state at the voltage stability limit evaluated using the optimization method described in Chapter 3. In Table 4.3 the calculated system strength indices, i.e., VC's and SI's, for each of the load buses in the system are presented.

By the design of this network, bus 4 is the critical bus in the network. As may be observed in Table 4.3, both the VC and the SI indices correctly pick bus 4 as the critical bus in the system. System buses may be ordered on the basis of "weakness" (from the weakest to the strongest) using these indices as

$$\{ 4, 3, 2 \}, \quad (4.25)$$

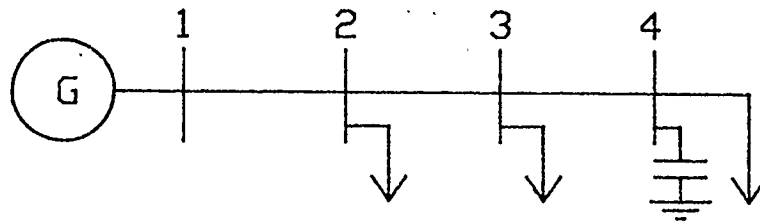


Figure 4.1: 4-Bus Radial Network

Table 4.1: Line and Transformer Data (Radial Network)

Line No	Line Conn.	Impedance		Charging p.u.
		R	X	
1	1-2	0.010	0.060	0.180
2	2-3	0.006	0.080	0.140
3	3-4	0.020	0.120	0.220

Table 4.2: Initial and Limiting System States (Radial Network)

Bus	Initial State				Voltage Stability Limit			
	Bus Voltage		Bus Power*		Bus Voltage		Bus Power*	
	Mag	Ang**	MW	MVAR	Mag	Ang**	MW	MVAR
1	1.050	0.0	254.4	52.1	1.050	0.0	268.9	285.4
2	1.000	-8.0	-90.0	-30.0	0.865	-8.3	-90.0	-64.8
3	0.990	-15.3	-65.0	-15.0	0.723	-19.6	-65.0	-40.1
4	0.986	-21.9	-90.0	-15.0	0.597	-33.1	-90.0	-49.8

* negative for loads

** in degrees

Table 4.3: Bus Strength Indices (Radial Network)

Bus	VC_i	SI_i
2	0.156	1.212
3	0.369	0.672
4	0.652	0.000

which can be judged by the structure of this network to be the correct order. It should be noted that both indices (SI and VC) provide the same ordering of the buses.

4.4.2 14-Bus System.

The bus and line data for this system are given in Appendix III. Table 4.4 shows the system initial operating state and the state at the voltage stability limit computed using the optimization method described in Chapter 3. It should be noted that the VAR outputs of the generators and synchronous condensers have been limited to their respective specified maximum values.

Table 4.4: Initial and Limiting System States (14-Bus Network)

Bus	Initial State				Voltage Stability Limit			
	Bus Voltage		Bus Power*		Bus Voltage		Bus Power*	
	Mag	Ang**	MW	MVAR	Mag	Ang**	MW	MVAR
1	1.060	0.0	338.7	85.0	1.060	0.0	366.9	290.5
2	1.000	-6.6	40.0	50.0	0.921	-6.4	40.0	50.0
3	0.911	-16.7	-94.2	-19.0	0.745	-18.9	-94.2	-38.3
4	0.920	-15.5	-57.8	-23.9	0.750	-17.1	-57.8	-35.7
5	0.932	-14.0	-47.6	-1.6	0.777	-15.1	-47.6	-11.4
6	0.978	-25.3	0.0	24.0	0.713	-34.6	0.0	24.0
7	0.963	-21.7	0.0	0.0	0.728	-27.5	0.0	0.0
8	1.005	-21.7	0.0	24.0	0.782	-27.5	0.0	24.0
9	0.953	-24.9	-29.5	-16.6	0.684	-33.6	-29.5	-22.6
10	0.940	-26.4	-29.0	-5.8	0.656	-36.4	-29.0	-11.7
11	0.946	-26.5	-13.5	-5.8	0.662	-36.6	-13.5	-8.6
12	0.928	-29.3	-36.1	-1.6	0.615	-41.9	-36.1	-9.0
13	0.944	-27.7	-23.5	-5.8	0.649	-38.9	-23.5	-10.6
14	0.929	-27.4	-14.9	-5.0	0.631	-38.2	-14.9	-8.1

* negative for loads

** in degrees

Table 4.5: Bus Strength Indices (14-Bus Network)

Bus	VC_i	SI_i
3	0.222	0.662
4	0.227	0.597
5	0.200	0.644
7	0.327	0.337
9	0.394	0.159
10	0.433	0.091
11	0.431	0.086
12	0.511	-0.023
13	0.457	0.034
14	0.473	0.000

Table 4.5 shows the strength indices evaluated for each of the load buses. Using the VC indices, the system buses may be ordered on the basis of strength (weakest to strongest) as follows:

$$\{ 12, 14, 13, 10, 11, 9, 7, 4, 3, 5 \} \quad (4.26)$$

Also using the SI indices, the system buses are ordered as follows (weakest to strongest):

$$\{ 12, 14, 13, 11, 10, 9, 7, 4, 5, 3 \} \quad (4.27)$$

It should be noted from (4.26) and (4.27) that both indices pick bus 12 as the critical bus in the network. It should also be noted that the indices produce the practically identical order of the system buses as far as "weakness" is concerned. The differences between the two sequences (4.26) and (4.27) are the positions for buses 10 and 11 which are interchanged and positions for buses 4 and 5 that are also interchanged. The strength indices for the interchanged positions are quite close and within the tolerance of the computation. For example, VC_{10} and VC_{11} differ by 0.002.

Because of the additional constraint that

$$\sum_{i \in J_L} \beta_i = 1,$$

it follows that the last of the constraint set specified by equation (4.9) is an extra

(redundant) equation. It is therefore assigned a Lagrange multiplier value of zero since its inclusion in the constraint set does not affect the final value of the objective function. Consequently, in this example, $\lambda_{\beta_{14}} = 0.0 = SI_{14}$. As mentioned previously, the Lagrange multipliers give relative measures of the sensitivity of the objective function with respect to the constraint function. The Lagrange multipliers for the rest of the constraints specified by equation (4.9) are therefore relative to the preassigned zero value and may therefore be positive or negative. The result of this is that positive and negative values of the SI_i indices may result as happened in this example.

For a given network, the weakest bus and bus ordering based on weakness determined above depend on the distribution and power factors of the initial MVA load and on the expected (given) pattern of increase from the initial load as specified by the distribution vector β . Changes in these specified parameters will result in a different ordering of the buses.

Next, the network is partitioned into three geographical areas as shown in Figure 4.2. Each area consists of connected buses. Table 4.6 shows the areas' strength indices ASI and AVC evaluated for each area. It should be observed that area A is picked by both the ASI and the AVC indices as the weakest area. The indices also produce identical ordering of the areas as far as weakness is concerned.

Table 4.6: Area Strength Indices (14-Bus Network)

Area	AVC_K	ASI_K
A	0.222	0.662
B	0.410	0.161
C	0.362	0.254

4.4.3 20-Bus System

The data for this system is given in Appendix III. Table 4.7 shows the system states at the initial operating point and at the voltage stability limit. In Table 4.8 the system load buses strength indices SI and VC are shown. Based on the VC indices the system load buses are ordered from the weakest to the strongest as follows:

$$\{ 7, 12, 11, 10, 19, 9, 6, 18, 5, 17, 16, 4, 14, 15 \} \quad (4.28)$$

Similar ordering based on the SI indices yields

$$\{ 7, 12, 11, 10, 9, 6, 19, 5, 18, 17, 16, 4, 14, 15 \} \quad (4.29)$$

Again, it is observed from (4.28) and (4.29) that both the VC and SI indices pick bus 7 as the critical (or weakest) bus in the network in terms of meeting a demand for reactive power. It is also apparent that these two indices produce practically identical ordering of the buses as far as weakness is concerned. The differences in

Figure 4.7: Initial and Limiting System States (20-Bus Network)

Bus	Initial State				Voltage Stability Limit			
	Bus Voltage		Bus Power*		Bus Voltage		Bus Power*	
	Mag	Ang**	MW	MVAR	Mag	Ang**	MW	MVAR
1	1.050	0.0	416.6	273.0	1.060	0.0	498.8	947.3
2	1.020	3.4	384.0	45.1	1.020	3.1	384.0	600.0
3	1.020	3.4	384.0	45.1	1.020	3.1	384.0	600.0
4	1.011	1.3	0.0	0.0	0.956	1.4	0.0	0.0
5	0.977	-4.6	0.0	0.0	0.800	-5.7	0.0	0.0
6	0.962	-5.7	-153.0	-80.0	0.768	-7.4	-153.0	-156.7
7	0.937	-9.4	-563.0	-430.0	0.653	-13.4	-563.0	-712.2
8	1.020	-1.4	308.0	400.0	0.882	-1.5	308.0	400.0
9	0.977	-5.2	0.0	0.0	0.778	-6.5	0.0	0.0
10	0.953	-7.5	-174.0	-77.0	0.712	-10.2	-174.0	-164.2
11	0.973	-7.1	0.0	0.0	0.722	-9.5	0.0	0.0
12	0.947	-9.1	-715.0	-381.0	0.662	-13.0	-715.0	-739.3
13	0.995	-7.1	410.0	600.0	0.738	-9.1	410.0	600.0
14	1.029	-1.5	0.0	0.0	0.982	-1.6	0.0	0.0
15	1.031	-1.1	0.0	0.0	0.994	-1.1	0.0	0.0
16	0.983	-4.7	0.0	0.0	0.833	-5.6	0.0	0.0
17	0.978	-5.4	-171.0	-75.0	0.818	-6.5	-171.0	-160.7
18	0.966	-5.6	0.0	0.0	0.782	-7.1	0.0	0.0
19	0.958	-7.6	-142.0	-68.0	0.747	-9.8	-142.0	-139.2
20	0.961	-7.7	51.0	80.0	0.730	-10.1	51.0	80.0

* negative for loads

** in degrees

Table 4.8: Bus Strength Indices (20-Bus Network)

Bus	VC_i	SI_i
4	0.057	2.343
5	0.221	0.011
6	0.253	-0.489
7	0.436	-4.078
9	0.256	-0.791
10	0.340	-2.379
11	0.348	-2.602
12	0.430	-2.936
14	0.049	5.513
15	0.037	5.882
16	0.181	1.932
17	0.196	1.783
18	0.236	0.187
19	0.282	0.0

the above two sequences are in the fifth to ninth positions where the strength indices are quite close in magnitude.

Next the network is partitioned into three geographical areas as shown in Figure 4.3, each area consisting of interconnected buses. Table 4.9 shows the strength indices ASI and AVC computed for each area in the network. It is noted that area A has been picked as the weakest area in the network by both indices ASI and

Table 4.9: Area Strength Indices (20-Bus Network)

Area	AVC_K	ASI_K
A	0.367	-2.776
B	0.163	2.550
C	0.211	-0.204

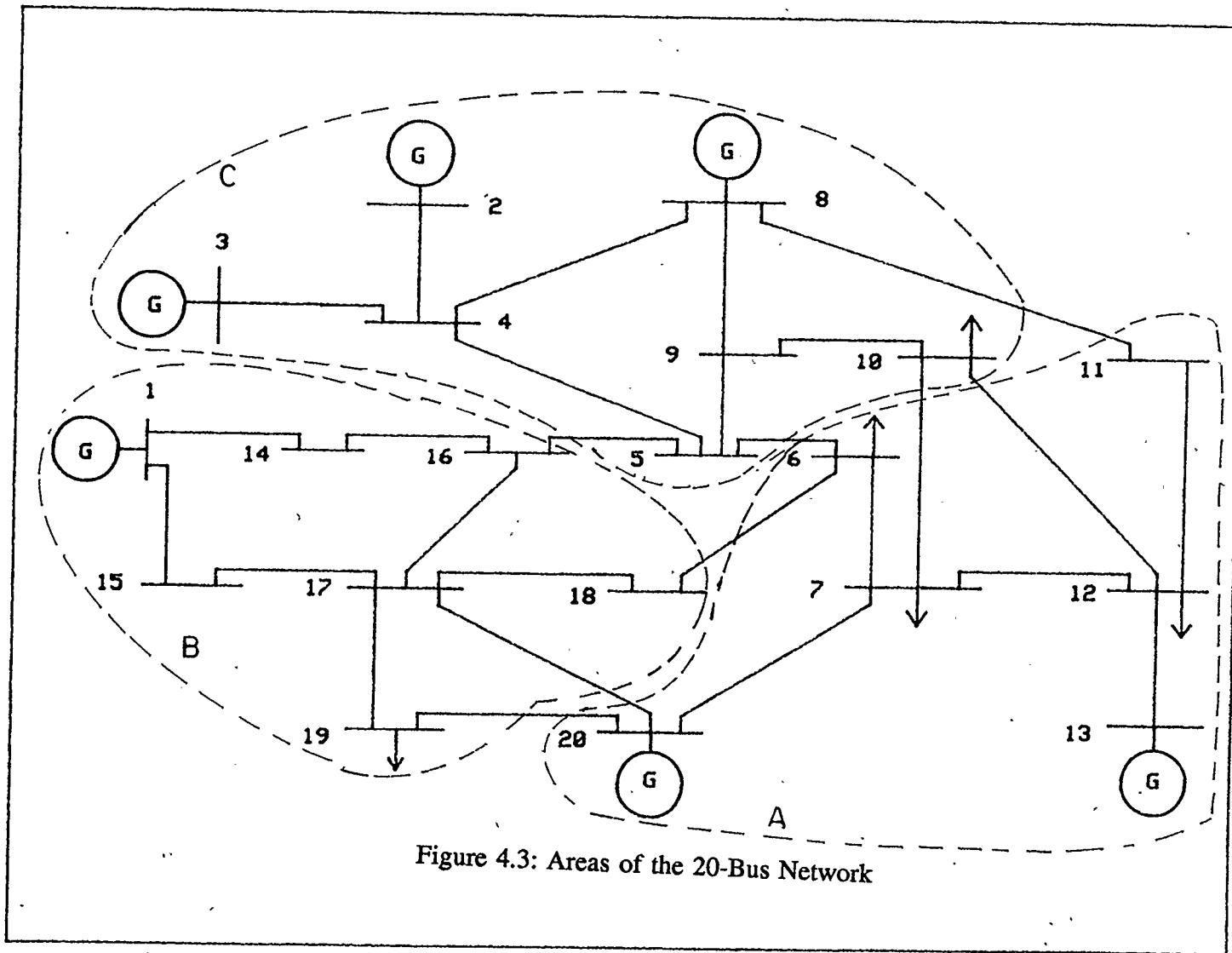


Figure 4.3: Areas of the 20-Bus Network

AVC. That the area A is the weakest area in this case is not so surprising since, as may be observed from Table 4.8, the local generating units, 13 and 20, in this area are delivering their maximum VAR outputs, and additional VARs have to be transported from the remote source at bus 1.

4.5 CONCLUSIONS

In this chapter, two methods of identifying the critical or weakest bus, and the weakest area of a power system are proposed. The methods take advantage of the optimization method described in Chapter 3 to determine the system voltage stability limit accurately and directly, taking into consideration the limits on system VAR supply. These methods are expected to yield more realistic results than previously proposed methods, which do not consider equipment limitations. The computational requirements for each of the two methods are comparable to those of the optimization method to determine the voltage stability limit.

The methods have been applied to 3 example systems. For these examples, the two proposed methods produce practically identical results.

CHAPTER 5

VAR PLANNING FOR POWER SYSTEM SECURITY

5.1 INTRODUCTION

The purpose of distributed system VAR planning has primarily been to provide enough reactive power to correct unacceptable pre- and post-contingency voltage levels. Numerous studies have been conducted in this area. Some of these studies are listed in references [46-55].

An objective in VAR planning is usually to minimize the investment cost of the reactive supply facilities required. However, as noted in Chapter 1 of this thesis, increased loading and exploitation of power transmission networks appears to have created a special voltage security problem, namely voltage instability or collapse [5-45]. System voltages might collapse if the network is unable to meet a given load demand. It is also noted by some investigators [10,14,16] that the inability to meet a load demand may be attributed to inadequate VAR support or transmission capability. Some work has been reported regarding identification of the most beneficial locations for VAR support, designed to enhance the system's security from voltage collapse [14,41].

In this chapter, an integrated method of identifying dispersed VAR supply is proposed for the dual purpose of maintaining voltage profiles within specified lim-

its, and increasing the security margin of anticipated operating conditions with respect to voltage collapse. The objective is to minimize the cost of the VAR supply required for a given security margin in the event of occurrence of any one of a set of specific contingencies.

5.2 SECURITY

5.2.1. Concept

In this section, the concept of voltage security as interpreted in this thesis will be discussed by examining a simple power system.

Figure 5.1 shows a simple system including an impedance load $\bar{Z}_R = Z_R / \phi$ supplied by a constant voltage source \bar{V}_1 through a transmission line of impedance $\bar{Z}_L = Z_L / \xi$ and a load tap changing (LTC) transformer of off-nominal turns ratio $t:1$. Figure 5.2 shows the variation of the receiving end voltage V_R against the MVA demand S_R , at constant power factor. The point A (where $V_R = V_R^{crit}$) represents the system critical state. The voltage stability condition derived in Chapter 2 of this thesis, i.e.,

$$\frac{|\bar{Z}_L|}{|\bar{Z}_R|} < 1,$$

implies that the upper segment ($V_R > V_R^{crit}$) is the stable operating regime.

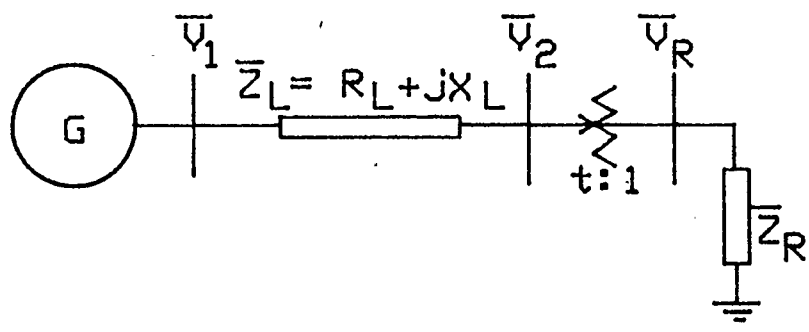


Figure 5.1: Simple System

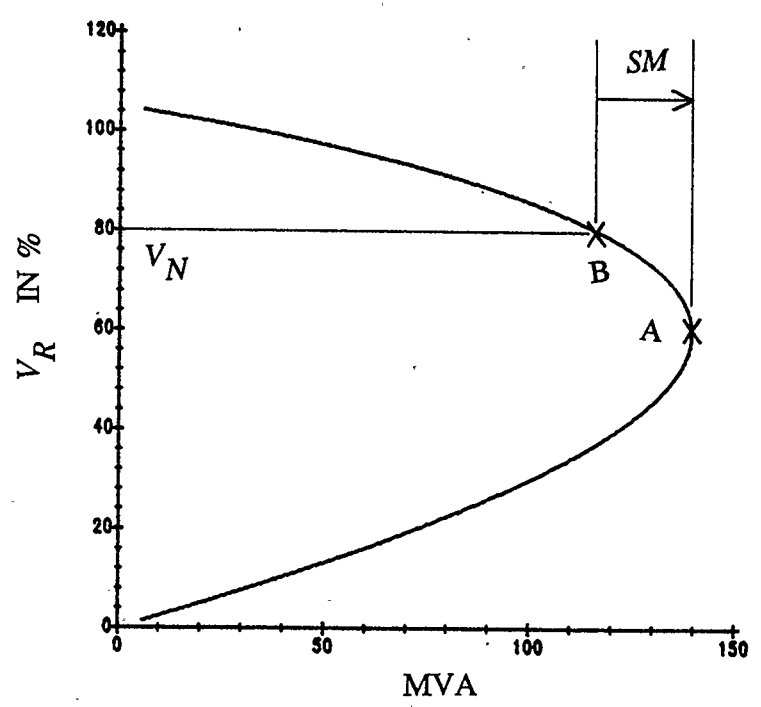


Figure 5.2: At-Load Voltage Variations
(Load pf = 0.93)

For operation at a stable operating point, B, it is desirable that

- (i) the voltage magnitude V_N be within a specified margin i.e.

$$V_N^{\min} \leq V_N \leq V_N^{\max}$$

and

- (ii) the operating point B lies a certain distance from the point corresponding to the critical state. This distance can be identified in terms of a security margin, SM , so that

$$SM \geq SM^{spec}$$

where SM^{spec} represents the minimum permissible margin.

Power system operation is said to be secure if the system can sustain a disturbance without violating the operating limits (i) and (ii) above. The degree of security that can be planned into a power system is limited by costs. Technical requirements are also important considerations in deciding the values of V_N^{\min} , V_N^{\max} and SM^{spec} .

As has been noted [25,28], voltage magnitude alone may not be a reliable indication of how far an operating point is from the collapse point. Hence, satisfying the voltage magnitude constraint does not guarantee that the security margin requirement is satisfied. One way by which both the voltage magnitude and the

security margin, SM , may be modified to some extent is through reactive power (VAR) compensation. Electrically, the VAR compensation referred to in this discussion is provided by rotating or static components connected between a bus and ground.

5.2.2 Effect of VAR Compensation

Figure 5.3 shows the same simple system as before with a capacitor of admittance jb at the receiving end. The capacitor constitutes (static) VAR compensation.

Figure 5.4 is a plot of the receiving end voltage against the MVA demand with $b = 0$ and $b = 0.25$ pu. It is evident that installing a VAR source at the receiving end improves the operating voltage V_N and also the security margin from SM^o to SM^f .

For practical size power networks (more than just two buses), deciding on locations and amounts of VAR to install in order to meet the voltage level and security requirements while minimizing the VAR supply costs is not simple. The best locations for a possible set of reactive sources will depend on system structure and operating conditions. Also, load distribution, contingencies, and system control variables like the generator voltages and transformer taps, and their respective limits, need to be taken into account. These aspects are included in the VAR supply planning methodology for a general multi-bus network proposed in this chapter.

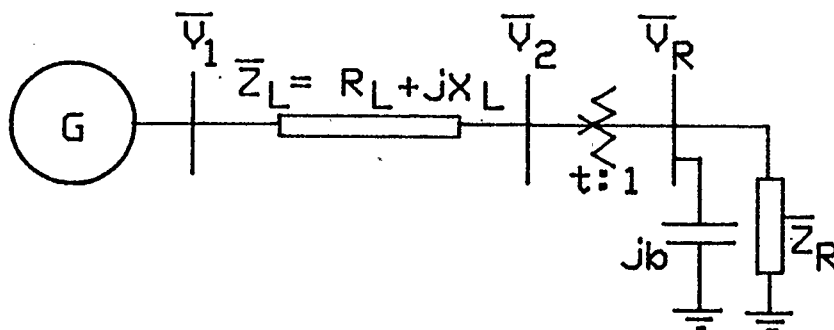


Figure 5.3: Simple System with Compensation

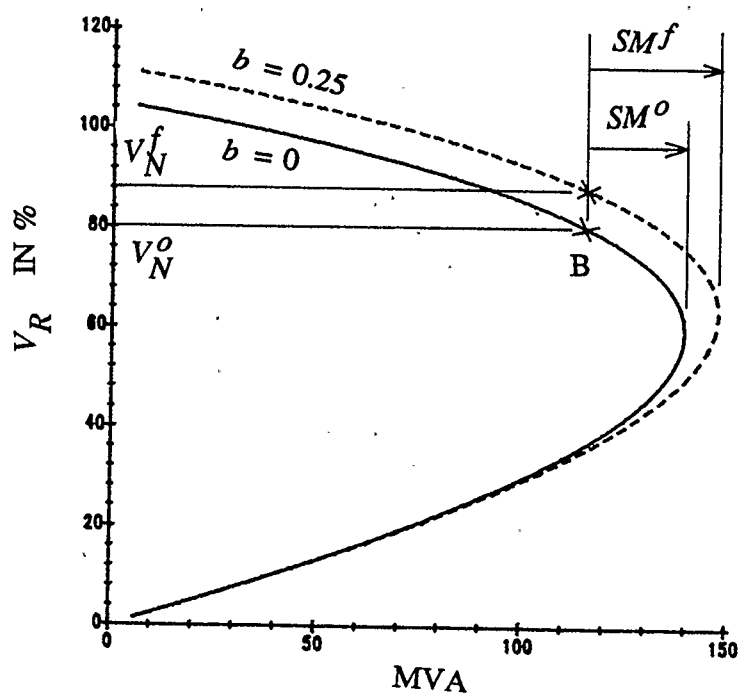


Figure 5.4: At-Load Voltage Variations (with Compensation)
(Load pf = 0.93)

5.3 SECURITY ASSESSMENT

In order to determine whether or not the power system meets the voltage level and security requirements it is necessary to determine both the voltage magnitudes and the security margins for the operating conditions anticipated.

The voltage magnitudes may be determined by solving the load flow equations for the system. The well-known Newton-Raphson solution algorithm is employed for this purpose.

To evaluate the security margin, SM , it is necessary to determine the system critical condition (voltage stability limit). The method proposed in Chapter 3 of this thesis to determine the static voltage stability limit in multimachine power systems is used for this purpose. A security margin, SM , is subsequently defined for each of the anticipated contingency conditions in terms of actual power margin to collapse (equation 3.19).

In the event that a voltage magnitude at an expected operating point is outside the specified limits, and/or SM is less than required, additional VAR injections may be considered.

5.4 VAR SUPPLY - FORMULATION

Consider the object in dispersed reactive power supply planning as that of minimizing the cost of the necessary VAR sources needed to achieve a bus voltage distribution within a specific range, and security margins at or above a specified

minimum value. This objective may be realized by formulating the problem as the following optimization problem:

minimize

[Total cost of dispersed VAR supply]

such that:

- (1) all voltages are within specified limits, and
- (2) the security margin (SM) is equal to or greater than some specified value.

The mathematical modeling of the objective function and the associated constraints are discussed next.

5.4.1 VAR Supply Costs

The cost of VAR installation at a bus is considered to have two components, one fixed and one variable [52]. The fixed cost is independent of the number of the VARs installed. The variable cost is proportional to the size of the added VAR. The i -th bus VAR cost can therefore be modeled as

$$Cost = d_i + s_{ci}q_{ci} + s_{ri}q_{ri} \quad (5.1)$$

where

s_{ci} and s_{ri} are unit costs of capacitive and inductive sources

respectively,

q_{ci} and q_{ri} are the added capacitive and inductive VAR's

d_i is the fixed VAR installation cost for bus i .

The total cost of VAR expansion may then be modeled as

$$\text{Total Cost} = \sum_{i \in C} (d_i + s_{ci}q_{ci} + s_{ri}q_{ri}) a_i \quad (5.2)$$

where a_i is a 0 - 1 decision variable. $a_i = 1$ if the i^{th} bus is selected for VAR installation, otherwise $a_i = 0$. C is the set of candidate buses consisting of buses to be considered for VAR injection. Based on engineering judgement, many of the system buses may be excluded from the candidate set.

Physical and/or environmental considerations may limit the size of the VAR facility that may be installed at a bus. Therefore, the size is constrained by

$$\begin{aligned} 0 &\leq q_{ci} \leq a_i q_{ci}^{\max} \\ 0 &\leq q_{ri} \leq a_i q_{ri}^{\max} \end{aligned} \quad (5.3)$$

5.4.2 Voltage Magnitude Constraint

As mentioned above, the system voltages for an expected operating condition may be determined using the load flow equations. The goal of having the system

voltage magnitudes for a particular operating condition within specified limits may therefore be realized by including the load flow equations as constraints in the optimization problem. The new VAR sources should be included in the load flow equations. Bounds on the system voltage magnitudes and transformer taps are also included as constraints. The resulting constraint set can be expressed as

$$\begin{aligned}
 P_i^N + P_i(\underline{V}^N, \underline{\delta}^N, \underline{t}^N) &= 0 \\
 Q_i^N + Q_i(\underline{V}^N, \underline{\delta}^N, \underline{t}^N) - q_{ci} + q_{ri} &= 0, \quad i \in J_L \\
 P_{Gj}^{\min} \leq P_{Gj}(\underline{V}^N, \underline{\delta}^N, \underline{t}^N) \leq P_{Gj}^{\max} & \quad (5.4) \\
 Q_{Gj}^{\min} \leq Q_{Gj}(\underline{V}^N, \underline{\delta}^N, \underline{t}^N) \leq Q_{Gj}^{\max}, & \quad j \in J_G \\
 \underline{V}^{\min} \leq \underline{V}^N \leq \underline{V}^{\max} \\
 \underline{t}^{\min} \leq \underline{t}^N \leq \underline{t}^{\max}
 \end{aligned}$$

where

\underline{V}^N is the vector of voltage magnitudes at normal operating condition

$\underline{\delta}^N$ is the vector of voltage angles at normal operating condition

\underline{t}^N is the vector of tap settings at normal operating condition

P_i^N and Q_i^N are the specified MW and MVAR demands at bus i , normal operating condition

P_{Gj} and Q_{Gj} are the MW and MVAR outputs of generating unit j

J_L is the set of load buses

J_G is the set of generator buses.

5.4.3 Security Margin Constraints

In addition to having the system voltage magnitudes at the given operating point within specified limits, it is also required that the operating point be some safe margin away from collapse (the critical point). This margin is specified by SM in equation (3.19), i.e.,

$$SM \geq SM^{spec} \quad (5.5)$$

where SM^{spec} is the specified minimum margin to the critical point, ($0 < SM^{spec} < 1$).

Combining equation (3.19) with (5.5) we have,

$$S_i^{limit} \geq S_i^{initial} + \frac{SM^{spec}}{1 - SM^{spec}} \beta_i \sum_{j \in J_L} S_j^{initial} \quad (5.6)$$

It is assumed that the power factor of the MVA demand at bus i is constant at pf_i , $i \in J_L$. Decomposing equation (5.6) into real and imaginary parts, and including generator MW and MVAR limits and the new VAR sources, the security margin constraints may be written as

$$\begin{aligned} P_i(\underline{V}^L, \underline{\delta}^L, \underline{t}^L) &\geq c_i \\ Q_i(\underline{V}^L, \underline{\delta}^L, \underline{t}^L) - q_{ci} + q_{ri} &\geq d_i, \quad i \in J_L \\ P_{Gj}^{\min} &\leq P_{Gj}(\underline{V}^L, \underline{\delta}^L, \underline{t}^L) \leq P_{Gj}^{\max} \\ Q_{Gj}^{\min} &\leq Q_{Gj}(\underline{V}^L, \underline{\delta}^L, \underline{t}^L) \leq Q_{Gj}^{\max}, \quad j \in J_G \\ \underline{t}^{\min} &\leq \underline{t}^L \leq \underline{t}^{\max} \end{aligned} \quad (5.7)$$

where

$$\begin{aligned} c_i &= pf_i \left[S_i^{initial} + \frac{SM^{spec}}{1 - SM^{spec}} \beta_i \sum_{j \in J_L} S_j^{initial} \right] \\ d_i &= (1 - pf_i^2)^{1/2} \left[S_i^{initial} + \frac{SM^{spec}}{1 - SM^{spec}} \beta_i \sum_{j \in J_L} S_j^{initial} \right] \end{aligned}$$

\underline{V}^L is the vector of voltage magnitudes of the critical point

$\underline{\delta}^L$ is the vector of voltage angles at the critical point

\underline{t}^L is the vector of tap settings at the critical point.

5.4.4 Overall Problem Formulation

The overall problem of VAR supply distribution may now be written as

minimize

$$\sum_{i \in C} (d_i + s_{ci} q_{ci} + s_{ri} q_{ri}) a_i$$

subject to:

- (i) $a_i = 0$ or 1
- (ii) $0 \leq q_{ci} \leq a_i q_{ci}^{\max}$
- (iii) $0 \leq q_{ri} \leq a_i q_{ri}^{\max}$, $i \in C$
- (iv) Equation set (5.4) (5.8)
- (v) Equation set (5.7).

This is a mixed-integer nonlinear programming (MINP) problem. The only known solution method for this class of problems is the combinatorial programming method. According to that method the problem is solved for all possible combinations of 0's and 1's in the candidate set. The method is inefficient for problems of the size associated with practical power systems. A two-stage algorithm to obtain a near-optimal solution has therefore been developed.

5.5 A TWO-STAGE SOLUTION ALGORITHM

A near-optimal solution may be obtained by decomposing the MINP problem into two subproblems. The first subproblem installs VARs such that the variable component of the cost function is minimized. The second subproblem optimizes the fixed component of the cost function by minimizing the number of buses where VARs were installed according to the relation of the first subproblem.

5.5.1 First Stage Solution

The first-stage subproblem is established by fixing the values of the decision variables a_i , $i \in C$, at 1. The resulting problem may be stated as follows:

minimize

$$\sum_{i \in C} (s_{ci} q_{ci} + s_{ri} q_{ri})$$

such that:

- (i) $0 \leq q_{ci} \leq q_{ci}^{\max}$
- (ii) $0 \leq q_{ri} \leq q_{ri}^{\max}, \quad i \in C$ (5.9)
- (iii) Equation set (5.4)
- (iv) Equation set (5.7).

This is a non-linear programming (NCP) problem. Efficient methods exist today for solving this class of problems even for large-scale systems [64].

The solution of the first stage is the minimum amount of VARs that needs to be installed in order to satisfy voltage levels and the security constraint. However, this solution does not necessarily correspond to minimum investment cost of the dispersed VAR supply because the number of VAR supply locations is not minimized. The results obtained are passed on to the second-stage subproblem.

5.5.2 Second Stage Solution

The purpose of this stage is to minimize the number of VAR supply locations while maintaining system voltages within specified limits and maintaining a security margin greater than (or equal to) SM^{spec} . The equations for the second stage of the algorithm are obtained by linearizing the equations of MINP around the solution point obtained in the first stage subproblem with some modifications. Bearing in mind that the problem of minimizing the number of locations where VARs are to be installed is equivalent to maximizing the number of locations

omitted for VAR installation in the candidate set, the second stage subproblem is formulated as follows:

maximize

$$\sum_{i \in C} d_i k_i - s_{ci} \Delta q_{ci} - s_{ri} \Delta q_{ri}$$

subject to:

- (i) $k_i = 0$ or 1 , $i \in C$
- (ii) $H_i \underline{\Delta \delta}^N + N_i \underline{\Delta V}^N + D_i \underline{\Delta t}^N = 0$
- (iii) $J_i \underline{\Delta \delta}^N + L_i^N \underline{\Delta V}^N + E_i \underline{\Delta t}^N + q_{ci} k_i - \Delta q_{ci} - q_{ri} k_i + \Delta q_{ri} = 0$, $i \in J_L$
- (iv) $\Delta P_{Gj}^{\min} \leq (H_j \underline{\Delta \delta}^N + N_j \underline{\Delta V}^N + D_j \underline{\Delta t}^N) \leq \Delta P_{Gj}^{\max}$
- (v) $\Delta Q_{Gj}^{\min} \leq (J_j \underline{\Delta \delta}^N + L_j \underline{\Delta V}^N + E_j \underline{\Delta t}^N) \leq \Delta Q_{Gj}^{\max}$, $j \in J_G$
- (vi) $F_i \underline{\Delta \delta}^L + G_i \underline{\Delta V}^L + R_i \underline{\Delta t}^L \geq 0$ (5.10)
- (vii) $M_i \underline{\Delta \delta}^L + S_i \underline{\Delta V}^L + T_i \underline{\Delta t}^L + q_{ci} k_i - q_{ri} k_i - \Delta q_{ci} + \Delta q_{ri} \geq 0$, $i \in J_L$
- (viii) $\Delta P_{Gj}^{\min} \leq (F_j \underline{\Delta \delta}^L + G_j \underline{\Delta V}^L + R_j \underline{\Delta t}^L) \leq \Delta P_{Gj}^{\max}$
- (ix) $\Delta Q_{Gj}^{\min} \leq (M_j \underline{\Delta \delta}^L + S_j \underline{\Delta V}^L + T_j \underline{\Delta t}^L) \leq \Delta Q_{Gj}$, $j \in J_G$

$$(x) \quad k_i \Delta q_{ci}^{\max} + \Delta q_{ci} \leq \Delta q_{ci}^{\max}$$

$$(xi) \quad \Delta q_{ci} \geq 0$$

$$(xii) \quad k_i \Delta q_{ri}^{\max} + \Delta q_{ri} \leq \Delta q_{ri}^{\max}$$

$$(xiii) \quad \Delta q_{ri} \geq 0$$

where the parameters of the sensitivity vectors $H_i, N_i, D_i, J_i, L_i, E_i, F_i, G_i, R_i, M_i, S_i, T_i$ are as defined in section 5.5.3. The decision variable k_i (in the constraint set (i)) is a 0 - 1 variable. k_i is 0 if the i^{th} bus remains a candidate for VAR installation, and is 1 if the i^{th} bus is deleted as a candidate bus. It should be noted that when k_i is 1, Δq_{ci} and Δq_{ri} are zero (combining constraint set (x) and (xi)); also, VARs of size q_{ci} (or q_{ri}) which was installed at the i^{th} bus in the first stage is switched off (i.e. deleted).

This class of optimization problems is known as mixed-integer linear programming. Again, efficient solution methods exist today for solving this class of problems [64].

The procedure outlined not only maximizes the number of buses that are omitted as candidate buses, it also minimizes the VAR additions (Δq_{ci} and Δq_{ri}) at the remaining candidate buses such that the goal regarding voltage level and security is still realized. The final VAR distribution is:

$$\begin{aligned}
 q_{ci}^{final} &= q_{ci} + \Delta q_{ci} \\
 q_{ri}^{final} &= q_{ri} + \Delta q_{ri} \quad i \in C'
 \end{aligned}
 \tag{5.11}$$

where q_{ci} and q_{ri} , $i \in C'$, are the solutions of the first stage problem, and C' is a subset of C . C' is the set of buses for which $k_i = 0$, $i \in C$, i.e., candidate buses where VARs are installed. Also, the final values of the voltages (magnitudes and angles) at the normal operating point may be obtained as,

$$\begin{aligned}
 \underline{V}^{Nf} &= \underline{V}^N + \Delta \underline{V}^N \\
 \underline{\delta}^{Nf} &= \underline{\delta}^N + \Delta \underline{\delta}^N \\
 \underline{t}^{Nf} &= \underline{t}^N + \Delta \underline{t}^N
 \end{aligned}
 \tag{5.12}$$

where \underline{V}^N , $\underline{\delta}^N$, and \underline{t}^N are the solution of the first stage subproblem. Final values, \underline{V}^{Lf} , $\underline{\delta}^{Lf}$, and \underline{t}^{Lf} are obtained in the same way. More accurate values of q_{ci}^{final} and q_{ri}^{final} , $i \in C'$, and the voltages and tap positions, may be obtained by setting $a_i = 1$, $i \in C'$ and solving subproblem 1 (first stage) again.

The limits on the dependent and independent variables are set as follows:

Variable $\Delta \underline{x}^N$

$$\underline{\Delta x}^N = (\underline{\Delta V}^N, \underline{\Delta \delta}^N, \underline{\Delta t}^N)$$

$$\underline{\Delta V}^{Nmin} = \underline{V}^{Nmin} - \underline{V}^N, \quad \underline{\Delta V}^{Nmax} = \underline{V}^{Nmax} - \underline{V}^N$$

$$\underline{\Delta t}^{Nmin} = \underline{t}^{Nmin} - \underline{t}^N, \quad \underline{\Delta t}^{Nmax} = \underline{t}^{Nmax} - \underline{t}^N$$

Variable $\underline{\Delta x}^L$

$$\underline{\Delta x}^L = (\underline{\Delta V}^L, \underline{\Delta \delta}^L, \underline{\Delta t}^L)$$

$$\underline{\Delta V}^{Lmax} = \underline{V}^{Lmax} - \underline{V}^L$$

$$\underline{\Delta t}^{Lmin} = \underline{t}^{Lmin} - \underline{t}^L, \quad \underline{\Delta t}^{Lmax} = \underline{t}^{Lmax} - \underline{t}^L$$

Variables ΔP_{Gi} and ΔQ_{Gi} , $i \in J_G$

$$\Delta P_{Gi}^{\max} = P_{Gi}^{\max} - P_{Gi}, \quad \Delta P_{Gi}^{\min} = P_{Gi}^{\min} - P_{Gi}$$

$$\Delta Q_{Gi}^{\max} = Q_{Gi}^{\max} - Q_{Gi}, \quad \Delta Q_{Gi}^{\min} = Q_{Gi}^{\min} - Q_{Gi}$$

Variables Δq_{ci} and Δq_{ri}

$$\Delta q_{ci}^{\max} = q_{ci}^{\max} - q_{ci}, \quad \Delta q_{ri}^{\max} = q_{ri}^{\max} - q_{ri}$$

5.5.3 Sensitivity Vectors

As mentioned previously, the row sensitivity vectors $H_i, N_i, D_i, J_i, L_i, E_i, F_i, G_i, R_i, M_i, S_i, T_i$ are obtained by linearizing the nonlinear equations for

the MW and MVAR injections at bus i around the solution obtained from the first stage subproblem.

Assuming a system of n buses and r LTC transformers with bus 1 as the slack bus, the row vectors are evaluated as,

$$\begin{aligned}
 H_i &= \left[\frac{\partial P_i}{\partial \delta_2^N}, \frac{\partial P_i}{\partial \delta_3^N}, \dots, \frac{\partial P_i}{\partial \delta_n^N} \right] \\
 N_i &= \left[\frac{\partial P_i}{\partial V_1^N}, \frac{\partial P_i}{\partial V_2^N}, \dots, \frac{\partial P_i}{\partial V_n^N} \right] \\
 D_i &= \left[\frac{\partial P_i}{\partial t_1^N}, \frac{\partial P_i}{\partial t_2^N}, \dots, \frac{\partial P_i}{\partial t_r^N} \right] \\
 J_i &= \left[\frac{\partial Q_i}{\partial \delta_2^N}, \frac{\partial Q_i}{\partial \delta_3^N}, \dots, \frac{\partial Q_i}{\partial \delta_n^N} \right] \\
 L_i &= \left[\frac{\partial Q_i}{\partial V_1^N}, \frac{\partial Q_i}{\partial V_2^N}, \dots, \frac{\partial Q_i}{\partial V_n^N} \right] \\
 E_i &= \left[\frac{\partial Q_i}{\partial t_1^N}, \frac{\partial Q_i}{\partial t_2^N}, \dots, \frac{\partial Q_i}{\partial t_r^N} \right], \quad i \in J_L \cup J_G.
 \end{aligned} \tag{5.13}$$

The elements of these vectors are evaluated as shown in Appendix II of this thesis.

The sensitivity vectors $F_i, G_i, R_i, M_i, S_i, T_i$ are evaluated in the same way as

shown in equation (5.13) except that the linearization is performed around $(\underline{V}^L, \underline{\delta}^L, \underline{t}^L)$.

5.5.4 Steps in the Digital Solution

The steps in the digital solution of the VAR supply problem by the proposed two-stage algorithm is summarized in Figure 5.5.

The first stage subproblem, which is a nonlinear optimization problem, is solved using a routine in the Numerical Algorithm Group software package [66] which solves that class of problems. The second-stage subproblem, which is a mixed-integer linear program, is solved using the APEXIV software package [69]. APEXIV require that the output be supplied in the so-called MPS (Mathematical Programming System) standard form.

5.6 CONSIDERATION OF CONTINGENCIES

The previous analyses only consider a single system operating regime. It may be desirable to plan VAR support such that the system voltage levels and SM requirements remain satisfied in the event of any one of a collection of contingencies occurring. In this section a method to achieve this preventive planning goal is described. The method is indicated by flow chart in Figure 5.6.

Procedure A reads the base case data and data for the change cases. Procedure B assesses the voltage levels and SMs for all cases using the algorithm

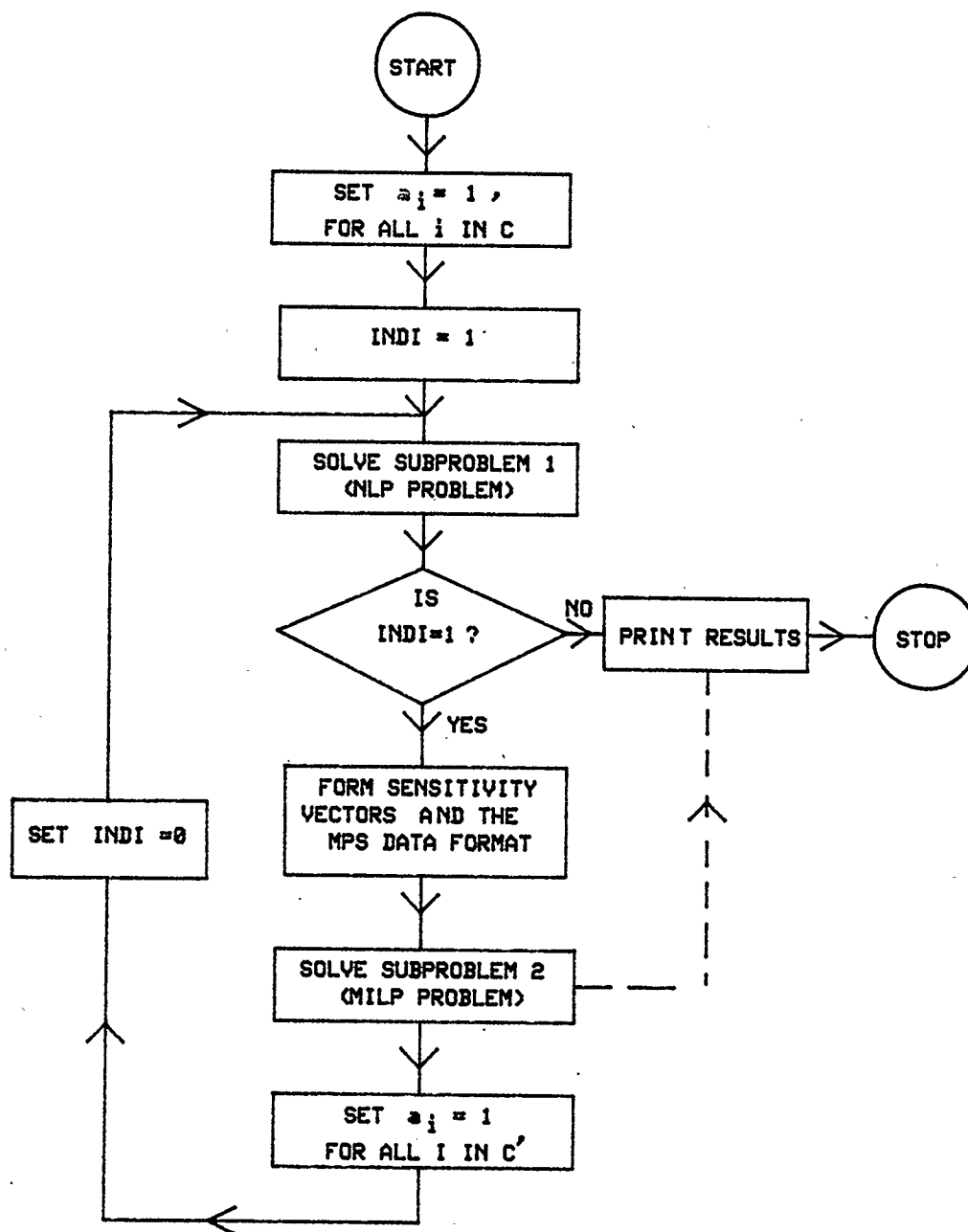


Figure 5.5: Flowchart of Basic Solution Method

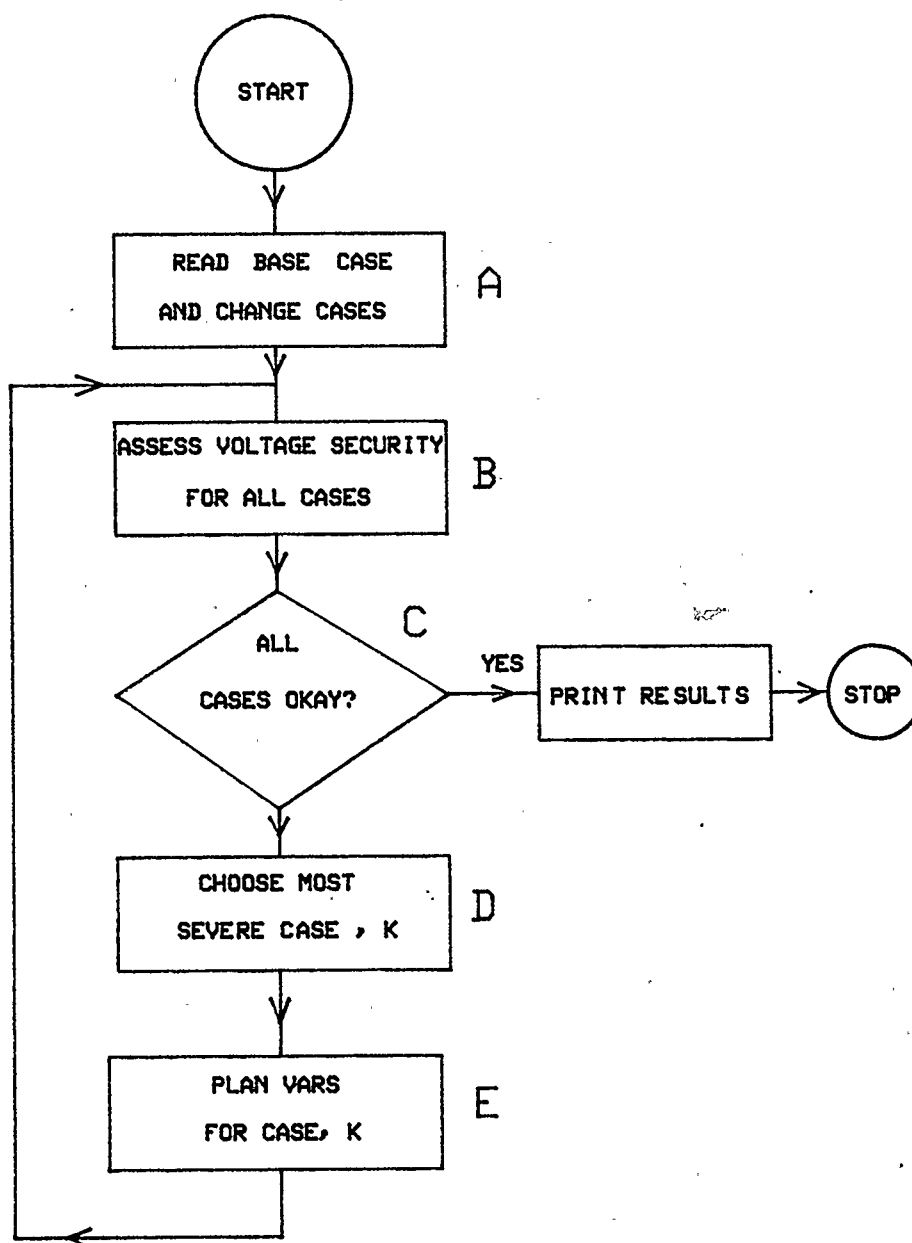


FIGURE 5.6: Flowchart of VAR Supprt Planning Considering Contingencies

described in section 5.3 of this Chapter. Procedure C checks if all cases meet the voltage level and SM requirements. If they do, the algorithm prints results and terminates; otherwise it proceeds to D. Procedure D chooses the most severe contingency case. This is done on the basis of the security margin index, SM . The most severe case is chosen to be the one with the smallest value of SM . In procedure E, VAR support is determined for this most severe case. The algorithm is repeated starting from procedure B.

The final result is a VAR support plan to satisfy voltage level and security margin constraints for the selected system states.

5.7 RESULTS

The results of application of the proposed methods to the AEP 14-bus network [67] are now presented. The 14-bus system has two generators, three synchronous condensers, and twenty transmission lines/transformers. System data are shown in Appendix III of this thesis.

The base case and five contingency cases are considered. The contingencies are as listed in Table 5.1. The required voltage level and security margin condition for all system states is shown in Table 5.2.

Table 5.3 shows the computed security margins SM and voltage magnitudes for each of the system states using procedure B (Figure 5.6). It will be noted that some of the system states have margins (SM) that are lower than the required SM^{spec} and that all the states have bus voltage magnitudes lower than the

Table 5.1. Contingency List

System States	Line Outage
(Base Case) 1	---
2	1 → 2 (one of two lines)
3	1 → 5
4	2 → 4
5	6 → 13
6	9 → 14

Table 5.2. Specified Security Limits

Variable	Limit
v^{\min}	0.95
v^{\max}	1.05
SM^{spec}	15%

minimum required. VAR support is therefore considered for the network.

State 3 with SM of -7.69% is the most severe operating state and is therefore selected for VAR support. It should be observed that since the SM is negative, no steady state operating point exists for this state for the specified initial conditions. Load flow analysis for this case is not convergent. The relevant parameters for VAR allocation are shown in Table 5.4.

Table 5.5 presents the solution of the first stage subproblem. It may be observed that the voltage magnitudes are within specified limits and the SM value

Table 5.3. System Voltages and SM before VAR Allocation

	VOLTAGE MAGNITUDES					
Bus	State 1	State 2	State 3	State 4	State 5	State 6
1	1.0600	1.0600	-	1.0600	1.0600	1.0600
2	1.0017	0.9267	-	0.9838	0.9936	0.9992
3	0.9107	0.8255	-	0.8384	0.8959	0.9069
4	0.9201	0.8390	-	0.8140	0.9014	0.9157
5	0.9319	0.8564	-	0.8435	0.9171	0.9250
6	0.9784	0.8871	-	0.8664	0.9593	0.9560
7	0.9629	0.8730	-	0.8471	0.9292	0.9610
8	1.0050	0.9190	-	0.8944	0.9727	1.0032
9	0.9527	0.8581	-	0.8312	0.9118	0.9514
10	0.9400	0.8439	-	0.8174	0.9019	0.9350
11	0.9461	0.8509	-	0.8266	0.9164	0.9328
12	0.9282	0.8505	-	0.8077	0.8602	0.8991
13	0.9443	0.8486	-	0.8259	0.8162	0.9080
14	0.9288	0.8313	-	0.8055	0.8466	0.8566
<i>SM</i>	17.3%	7.6%	-7.7%	6.2%	12.1%	14.8%

Table 5.4. VAR Support Parameters

Parameter	Values
d_i	10 units *
s_{ci}	1 unit *
s_{ri}	1 unit *
q_{ci}^{\max}	75 MVAR
q_{ri}^{\max}	75 MVAR
$i \in C$	C is set of all load buses

* Fictitious monetary units

is satisfied. However, 9 of the possible 10 locations have been identified for VAR installation. It is desirable to consider a reduced number of locations. The results of the first stage analysis are therefore passed on to the second stage subproblem which minimizes the number of locations. The results of the second stage analysis is shown in Table 5.6. It is apparent that the number of locations has been reduced from 9 to 2. However, total MVAR installed has increased from 135.4 to 140.3, i.e., 3.4%. Total cost of the VAR support facilities are down from 225.4 to 160.4 units, a cost reduction of 28.8%. The system voltage limits and security requirements remain satisfied. The final system voltages and SM's after the VAR allocation are as shown in Table 5.7.

The computations in the above example were performed on the CDC 860 mainframe computer. The first stage subproblem required 30.9 CPU seconds and the second stage 7.5 CPU seconds.

Table 5.5. Results of Solution of First-Stage Subproblem

Bus	Voltage Mag.	MVAR Allocated (all capacitive)
3	0.9506	12.0
4	0.9688	30.5
5	0.9675	15.4
7	1.0256	0.0
9	1.0497	32.2
10	1.0430	8.3
11	1.0437	9.5
12	1.0229	7.0
13	1.0391	13.2
14	1.0376	7.3
SM = 15 %		
TOTAL MVAR = 135.4		
TOTAL COST = 225.4 Units		

Table 5.6. Results After Solution of Second Stage Subproblem

Bus	Voltage Mag.	MVAR Allocated
3	0.9512	0.0
4	0.9833	70.3
5	0.9677	0.0
7	1.0103	0.0
9	1.0500	70.0
10	1.0343	0.0
11	1.0308	0.0
12	1.0063	0.0
13	1.0228	0.0
14	1.0197	0.0
SM = 15%		
TOTAL MVAR = 140.3		
TOTAL COST = 160.4 Units		

Table 5.7. System Voltages and SM after VAR Allocation

	VOLTAGE MAGNITUDES					
Bus	State 1	State 2	State 3	State 4	State 5	State 6
1	1.0600	1.0600	1.0600	1.0600	1.0600	1.0600
2	1.0450	1.0446	1.0139	1.0450	1.0448	1.0289
3	0.9943	0.9946	0.9512	0.9868	0.9950	0.9791
4	1.0294	1.0303	0.9833	1.0192	1.0310	1.0168
5	1.0187	1.0191	0.9677	1.0091	1.0188	1.0001
6	0.9995	1.0046	1.0508	1.0086	1.0674	1.0398
7	0.9908	0.9965	1.0103	0.9882	1.0002	1.0007
8	0.9842	0.9910	1.0200	0.9862	0.9928	0.9904
9	1.0274	1.0329	1.0498	1.0258	1.0423	1.0499
10	1.0064	1.0119	1.0343	1.0065	1.0306	1.0326
11	0.9908	0.9962	1.0308	0.9953	1.0364	1.0247
12	0.9548	0.9602	1.0063	0.9636	0.9872	0.9886
13	0.9742	0.9795	1.0228	0.9819	0.9524	0.9967
14	0.9853	0.9909	1.0197	0.9878	0.9834	0.9506
<i>SM</i>	30.5%	33.1%	15%	22.5%	27.4%	28.3%

5.8 CONCLUSIONS

In this chapter, a new method of determining transmission system reactive power support is presented for maintaining satisfactory voltage levels and achieving a prescribed minimum power system pre- and post-contingency security from voltage collapse. The security requirement is stated as a relative margin, defined in terms of actual and maximum or critical loads at the respective buses. VAR injections are considered in order to achieve satisfactory voltage levels and security

margins. The method minimizes the total investment cost of the VAR facilities assuming any one of a set of contingencies may occur.

Results of application of the proposed method to the AEP 14-bus network have been presented.

CHAPTER 6

CONCLUSIONS AND RECOMMENDATIONS FOR FUTURE WORK

6.1 INTRODUCTION

In this thesis, certain aspects of power systems voltage instability or collapse problems have been discussed. Analytical techniques have been developed for assessing power system security as far as steady state voltage stability is concerned, and also for the planning of new VAR sources for enhanced security. The main contributions of the work reported are summarized in this chapter together with suggestions for further work in this area.

6.2 CONCLUSIONS

A method of computing a practical voltage stability index has been presented. This index serves to determine the voltage stability or otherwise of a given operating point of a power system. The method can easily be incorporated in a load flow analysis program based on the Newton-Raphson method.

Simulation of a process that may lead to system voltage collapse has been discussed and results presented. The simulation is concerned mainly with the action of the LTC transformer and it incorporates load-voltage characteristics of the exponential type. System performance following a disturbance is simulated.

In the operation or planning of power systems, it is of interest to determine the voltage stability of an operating point as well as the margin to the collapse point or stability limit. In order to evaluate the margin of an operating point to collapse, it is necessary to determine the voltage stability limit. A new method to determine this directly and accurately for a multimachine power system has been introduced. The methodology formulates the problem as one of maximizing the system total *MVA* load. The resulting nonlinearly constrained optimization problem is solved using a sequential quadratic programming algorithm. With this formulation, difficulties related to singularity of the Jacobian matrix associated with the load flow equations and convergence of the load flow solution around the voltage stability limit are avoided. The method accommodates device constraints and limitations in system controls (e.g, generator *VAR* limits and limits on transformer tap settings). Also, the system steady state load-voltage characteristics are taken into consideration.

A stability margin *SM* is defined which may serve as a measure of the security of the system as far as voltage collapse is concerned. This index gives an explicit indication of the distance to voltage collapse in terms of actual total system load.

The critical or weakest bus in a power network is the bus most severely affected electrically because of a shortage of reactive power. A collapse of system voltages will likely originate from the critical bus. It is desirable therefore necessary to identify the critical bus in the network and maintain control of the voltage

at this bus in order to alleviate the vulnerability of the entire system to collapse. Two methods of identifying the critical or weakest bus, and the weakest area, of a power system are proposed. Both methods incorporate the optimization algorithm used to determine the system voltage stability limit accurately and directly, taking into account the limits on system VAR supply. These methods are expected to yield more realistic results than previously proposed methods which do not consider equipment limitations.

The problems of voltage level and voltage collapse in a transmission system are closely linked with the inadequacy of VAR supply. These problems may be solved at the planning stage by installing VAR sources at key buses in the network. A method has been introduced to determine transmission system VAR support for the dual purpose of:

- (i) maintaining satisfactory voltage levels, and
- (ii) achieving a prescribed minimum power system pre- and post-contingency security margin from voltage collapse.

The method minimizes the total investment cost of the VAR facilities.

6.3 RECOMMENDATION FOR FURTHER WORK

The research work reported in this thesis provides a basis for further investigations some of which are enumerated below.

- (a) Methods need to be developed for identifying all possible single and multiple line outage, loss of generation contingencies, and changes in operating conditions (unit commitment, generation dispatch, load level) that may cause voltage collapse. The information will be useful in determining power transfer capability requirements from a system security standpoint.
- (b) The methods suggested in the thesis for identifying the weakest bus in a network need to be developed further to identify the boundaries of a of an electrically weak area.
- (c) Some research effort should be directed at the development of suitable preventive measures to maintain voltage controllability and reactive reserve in the local control areas subject to a range of operating conditions. These controls would increase system security and reduce long term operating costs compared.
- (d) Finally, research is required to develop corrective measures that attempt to restore normal operation if a voltage collapse trend has been initiated inadvertently. Corrective control would attempt to limit or avert load shedding, islanding and local blackouts.

REFERENCES

- [1] H.M. Rustebakke (Ed.), *Electric Utility Systems and Practices*, John-Wiley & Sons, 1983.
- [2] P.M. Anderson and A. A. Fouad, *Power System Control and Stability*, The Iowa State University Press, 1980.
- [3] R. T. Byerly and E. W. Kimback (Ed.), *Stability of Large Electric Power Systems*, IEEE Press, 1974.
- [4] S. H. Horowitz (Ed.) *Protective Relaying for Power Systems* IEEE Press, 1980.
- [5] R.F. Wolff, "French Shutdown Meaningful to US", *Electrical World*, July 15, 1979.
- [6] A. Calvaer, " Voltage Stability and Voltage Collapses" *CIGRE Report*, Paper 38.02, April 1985.
- [7] A. Costi, L. Shu and R. A. Schlueter, "Power Systems Voltage Stability and Controllability", *Proceedings of the International Symposium on Circuits and Systems*, San Jose, CA, May 1986.
- [8] S. Abe, Y. Fukunaga, A Isono, and B. Kondo, "Power Systems Voltage Stability", *IEEE Trans. on Power Apparatus and Systems*, Vol-PAS 101, No. 10, Oct. 1982, pp 3830-3840.

- [9] M. B. Awad, S. Mantenuto and V. F. Carvalho, "Curtailment of a Voltage Instability Problem in Eastern Ontario", Presented to Transmission & Station Planning & and Operation Subsection, Canadian Electric Association, Toronto, March 1986.
- [10] B. M. Weedy and B. R. Cox, "Voltage Stability of Radial Power Links", *Proc. IEE*, Vol 115, April 1968, pp 528-536.
- [11] W. R. Lachs, "Dynamic Study of Extreme System Reactive Power Deficit", *IEEE Trans. on Power Apparatus and Systems*, Vol-PAS 104, No. 9, Sept. 1985.
- [12] T. J. E. Miller (Ed.) *Reactive Power Control In Electric Systems*, John-Wiley, 1982.
- [13] Y. Tamura, H. Mori, and S. Iwamoto, "Relationship Between Voltage Stability and Multiple Load Flow Solutions in Electric Power Systems" *IEEE Trans. on Power Apparatus and Systems*, Vol-PAS 102, May 1983, pp 1115-1125.
- [14] A. Tiranuchit and R.J. Thomas, "A Posturing Strategy Against Voltage Instabilities in Electric Power Systems", *IEEE/PES 1987 Winter Meeting*, New Orleans, Louisiana, Paper No. 87 WM 095-3, Feb. 1987.
- [15] F. Mercede, J-C Chow, H. Yan and R Fischl, "A Framework to Predict Voltage Collapse in Power Systems", *IEEE/PES Winter Meeting*, Paper 88 WM 189-3, NY, New-York, Feb 1988.

- [16] H. G. Chiang and F. F. Wu, "On Voltage Stability", *Proceedings of the IEEE International Symposium on Circuits and Systems*, San Jose, CA, May 1986, pp 1339-1342.
- [17] G.J. Berg, "Assessment of critical Voltage and Load Margins in VAR-Compensated Power Transmission Systems", *Electric Power System Research*, Vol. 12, 1987, pp. 63-69.
- [18] V.A. Venikov, V.A. Stroeve, V.I. Idelchick, and V.I. Tarasov, "Estimation of Electric Power System Steady-State Stability in Load-Flow Calculation", *IEEE Trans. on Power Apparatus and Systems*, Vol-PAS 94, No. 3, May/June 1975, pp. 1034-1038.
- [19] W. R. Lachs, "Voltage Collapse in EHV Power Systems", IEEE PES Winter Meeting, Paper No. A 78 057-2, 1978.
- [20] W. R. Lachs, "System Reactive Power Limitations" IEEE PES Winter Meeting, Paper No. A 79 015-9, 1979.
- [21] W. R. Lachs, "Insecure Systems Reactive Power Balance Analysis and Counter Measures", *IEEE Trans. on Power Apparatus and Systems*, Vol-PAS 104, No. 9, Sept. 1985.
- [22] S. Abe and A Isono, " Determination of Power System Voltage Instability, Parts 1 and 2", *The Trans. of IEE of Japan*, Vol. 96-B , April 1976, pp 171-186.

- [23] J. Crispy, "The Influence of the Regulating Transformers and the Excitation of Alternators on System Voltages and Stability", *CIGRE*, Paris, Paper 323, 1962.
- [24] S. Abe and A. Isono, "Determination of Power Systems Voltage Stability, Part 3 : Dynamical Approach ", *Electrical Engineering in Japan*, Vol. 103, 1983, pp 57-63.
- [25] C. Barbier and J-P. Barret, "An Analysis of Voltage Collapse on a Transmission System", *RGE*, T. 89, No. 10, Oct. 1980, pp. 672-690.
- [26] N. Flatabo and T. Carlson, "Evaluation of Reactive Power Reserve in Transmission Systems", *Proc. IFAC Symposium on Planning and Operation of Electric Power Systems* Rio de Janeiro, 1985.
- [27] T. Nagao, "Voltage Collapse at Load Ends of Power Systems", *Electrical Engineering in Japan*, Vol. 95, No. 4, 1975.
- [28] J. Carpentier, R. Girard, and E. Scano, "Voltage Stability Indicators Computed from an Optimal Load Flow", *Proc. of 8th Power System Computational Conf.*, Helsinki, 1984, pp. 671-678.
- [29] S. Abe, N. Hamada, A. Isono, and K. Okuda, "Load Flow Convergence in the Vicinity of a Voltage Stability Limit", *IEEE Trans. on Power Apparatus and Systems*, Vol-PAS 97, No. 6, Nov./Dec. 1978, pp. 1983-1993.
- [30] C.C. Liu and F.F. Wu, "Steady-State Voltage Stability Regions of Power Systems", *Systems & Control Letters*, No. 6, 1985, pp. 23-31.

- [31] P. Kessel and H. Glavitch, "Estimating the Voltage Stability of Power Systems", *IEEE Trans. on Power Delivery*, Vol. PWRD-1, No. 3, July 1986, pp. 346-354.
- [32] P. Borresmans, A. Calvaer, J.P. de Reuck, J. Goosens, E. Van Geert, J. Van Hecke, A. Van Ranst, "Voltage Stability - Fundamental Concepts and Comparison of Practical Criteria", *CIGRE Report*, Paper 38-11, 1984.
- [33] J. Jarjis and F.D. Galiana, "Qualitative Analysis of Steady-State Stability in Power Networks", *IEEE Trans. on Power Apparatus and Systems*, Vol-PAS 100, No. 1, Jan. 1981, pp. 318-326.
- [34] H. G. Kwatny, A. K. Pasrija, and L. Y. Bahar, "Static Bifurcation in Electric Power Networks: Loss of Steady-State Stability And Voltage Collapse", *IEEE Trans. on CAS*, Vol. CAS-33, No 10, Oct. 1986, pp 981-991.
- [35] B. K. Johnson, "Extraneous And False Load Flow Solutions", *IEEE Trans. on Power Apparatus and Systems*, Vol-PAS 96, No. 2, Mar. 1977, pp. 524-534.
- [36] A. J. Korsak, "On the Question of Uniqueness of Stable Load Flow Solution" *IEEE Trans. on Power Apparatus and Systems*, Vol-PAS 91, May 1972, pp. 1093-1110.
- [37] J. Medanic, M. Illic-Spong and J. Christensen, "Discrete Models of Slow Voltage Dynamics for Under Load Tap-Changing Transformer Coordination", *IEEE/PES Summer Meeting*, Paper 86 SM 345-3, Mexico City, New Mexico, 1986.

- [38] C. L. De Marco and A. R. Bergen, "A Security Measure for Random load Disturbances in Nonlinear Power System Models", *IEEE Trans. on Circuits and Systems*, Vol. CAS-34, No 12, Dec. 1987, pp 1546-1557.
- [39] R. Fischl, L. Zaragocin, F. Mercede, and H. Yan, "Power Systems Model for Voltage Collapse", *Proceedings of the IEEE International Symposium on Circuits and Systems*, San Jose, CA, May 1986, pp 1015-1018.
- [40] C. Concordia, "Voltage Instability -Definition and Concepts" Panel Session on Voltage Instabilities, IEEE/PES Winter Meeting, NY, New-York, 1988.
- [41] R. A. Schlueter, "Voltage Stability and Security Assessment", Panel Session on Voltage Instabilities, IEEE/PES Winter Meeting, NY, New-York, 1988.
- [42] V. A. Venikov and M. N. Rozonov, "The Stability of a Load" *Izv. Akad. Nauk SSSR (Energetika i Artomaica)*, Vol. 3, 1961, pp 121-125.
- [43] M. Brucoli, F. Rossi, F. Torelli, and M. Trovato, "A Generalized Approach to the Analysis of Voltage Stability in Electric Power Systems", *Electric Power Systems Research*, Vol. 9, 1985, pp 49-62.
- [44] L. Zaragocin, H. Yan, R. O'Connel, F. Mercede and R. Fischl, "A Review of Methods for Predicting Voltage Collapse of Power Systems" *Proc. Eighteenth North American Power Symposium*, 1986, pp 11-20.
- [45] D. S. Kirschen and H. P. Van Meeteran, "MW/Voltage Control in a Linear Programming Based Optimal Power Flow" IEEE/PES Winter Meeting, Paper No 87 WM 058-1, New Orleans, Louisiana, Feb 1987.

- [46] T.H. Lee, O.O. Obadina, E.F. Hill, T.L. Jong and C.T. Pan, "Capacitor Bank Planning for Possible System Contingencies", *IEEE Trans. on Power Apparatus and Systems*, Vol. 104, 1985, pp. 2361-2366.
- [46] H.H. Happ and K.A. Wirgau, "Static and Dynamic VAR Compensation in System Planning", *IEEE Trans. on Power Apparatus and Systems*, Vol. PAS-97, September/October, 1978, pp. 1564-1578.
- [47] R.A. Fernandes, F. Lange, R.C. Burchett, H.H. Happ and K.A. Wirgau, "Large Scale Reactive Power Planning", *IEEE Trans. on Power Apparatus and Systems*, Vol. PAS-102, May 1983, pp. 1083-1088.
- [48] R.M. Malisewski, L.L. Garver and A.J. Wood, "Linear Programming as an Aid in Planning Kilo VAR Requirements", *IEEE Trans. on Power Apparatus and Systems*, Vol. PAS-87, December 1968, pp. 1963-1968.
- [49] S. Ertem and J. R. Tudor "Optimal Shunt Capacitor Allocation by Nonlinear Programming", *IEEE/PES Winter Meeting, New Orleans, LA, 1987, Paper No 87 WM 142-3*.
- [50] R.M. Porter and H.K. Amchin, "VAR Allocation - An Optimization Technique", *PICA Conference Proceedings*, 1971, pp. 310-318.
- [51] A. Hughes, G. Lee, P. Hsiang, R.R. Shoults and M.S. Chen, "Optimal Reactive Power Planning", *IEEE Trans. on Power Apparatus and Systems*, Vol. PAS-100, May 1981, pp. 2189-2196.

- [52] W.M. Lebow, R. Rouhani, R. Nadira, P.B. Usoro, R.K. Mehra, D.W. Sobieski, M.K. Pal and M.P. Bhavaraju, "A Hierarchical Approach to Reactive Volt Ampere (VAR) Optimization in System Planning", *IEEE Trans. on Power Apparatus and Systems*, Vol. PAS-104, August 1985, pp. 2051-2057.
- [53] A. Venkataramana, J. Carr and R.S. Ramshaw, "Optimal Reactive Power Allocation", *IEEE Trans. on Power Systems*, Vol. PWR-2, February 1987, pp. 138-144.
- [54] K. Iba, H. Susuki, K-I. Susuki, K. Susuki, "Practical Reactive Power Allocation/Operation Planning Using Successive Linear Programming", IEEE PES Winter Meeting, New York, February 1987, Paper No. 87, WM. 055-7.
- [55] K. Aoki, M. Fan, and A. Nishikori, "Optimal VAR Planning By Approximation Method for Recursive Mixed-Integer Linear Programming" IEEE PES Winter Meeting, New York, February 1988, Paper No. 88, WM. 145-5.
- [56] O.O. Obadina and G.J. Berg, "Determination of Voltage Stability Limit of Multimachine Power Systems", IEEE/PES Winter Meeting, New York, Feb 1988, Paper No. 88 WM 194-3.
- [57] F. Illiceto and A. Capasso "Dynamic Equivalents of Asynchronous Motor Loads in System Stability Studies" IEEE/PES Winter Meeting, Jan.-Feb 1974, Paper No T 74 117-8.
- [58] J. R. Tudor and W. A. Lewis, "Transmission Losses and Economy of Loading by the Use of Admittance Constants" *IEEE Trans. on Power Apparatus and*

- Systems*, Vol. 82, Oct. 1963, pp 676-683.
- [59] H. H. Happ, "Optimal Power Dispatch" *IEEE Trans. on Power Apparatus and Systems*, Vol 93, May 1974., pp 820-830.
- [60] T. Park and Y. Sekine, "A Method for Analyzing Multisolutions in Power Flow Analysis", *Electrical Engineering in Japan*, Vol. 99, No. 2, 1979, pp. 95-103
- [61] A. J. Calvaer, "On the Maximum Loading of Active Linear Electric Multiports" *Proc. IEEE*, Vol. 71, No. 2, Feb. 1983, pp. 282-283.
- [62] A.J. Wood and B.F. Wollenberg, *Power Generation Operation and Control* John Wiley and Sons, 1984.
- [63] G.J. Berg, "Power System Load Representation", *Proc. IEE*, Vol. 120 (3), 1973, pp. 344-348.
- [64] K. Schittkowski, " Non-linear Programming Codes", *Lectures Notes in Economics and Mathematical Systems*, 183, Springer-Verlag , Berlin, Germany, 1980.
- [65] P.E. Gill, W. Murray, and M. Wright, *Practical Optimization*, Academic Press, 1981.
- [66] Numerical Algorithms Group (NAG), *Fortran Library Manual* Mark 11, Vol 3, 1984.
- [67] L.L. Freris and A.M. Sasson, "Investigation of the Load-Flow Problem", *Proc. IEE*, Vol. 115, No. 10, Oct. 1968, pp. 1450-1460.

- [68] D.P. Bertsekas, *Constrained Optimization and Lagrangian Multiplier Methods*, Academic Press, 1982.
- [69] APEXIV Programming Manual, Control Data Corporation , Minneapolis, MN, USA, 1983.

APPENDIX I

GENERATOR PARTICIPATION FACTORS

A primary objective in the control of power systems is to achieve minimum operating cost. This goal is realized by the economic dispatch of generating units. The objective function in the resulting optimization problem is the total cost of supplying the load. Mathematically, the classic economic dispatch problem may be stated [62],

minimize

$$F_T = \sum_{i \in J_G} F_i(P_i)$$

subject to:

$$\sum_{i \in J_G} P_i = P_R + P_L \quad (I.1)$$

where

F_i is the cost function of generating unit i in \$/hour

P_i is the MW output of unit i

P_R is the total system MW load

P_L is the total system MW losses

J_G is the set of generating units.

Additional equality and inequality constraints may also apply.

For a thermal plant the cost function, $F_i(P_i)$, is known explicitly. In hydro-thermal systems, equivalent cost functions may be assigned to the hydro units. The cost functions for each unit may be expressed as

$$F_i = a_i + b_i P_i + c_i P_i^2 \quad (I.2)$$

Applying the necessary conditions to the Lagrangian of problem I.1 for minimum cost operation, we obtain the coordination equations

$$pn_i \frac{dF_i}{dP_i} = \lambda, \quad i \in J_G \quad (I.3)$$

where

λ is the Lagrangian multiplier

$$pn_i = \frac{1}{1 - \frac{dP_L}{dP_i}} \quad \text{is the penalty factor for unit } i .$$

The solution satisfying the coordination equations is the optimal dispatch of the system generating units $(P_i^0, i \in J_G)$ for the specified bus loads.

Next, assuming a load change, we investigate how much each generating unit needs to be moved (i.e "participate" in the load change) in order that the new

load be served in the most economic way.

For purposes of determining the participation factors, it will be assumed that the penalty factors are approximately equal to 1, [62], i.e.,

$$pn_i \approx 1, \quad i \in J_G$$

For a small change in power output of generating unit i ,

$$\Delta\lambda \approx F_i''(P_i^0)\Delta P_i,$$

i.e.,

$$\Delta P_i = \frac{\Delta\lambda}{F_i''}, \quad i \in J_G \quad (I.4)$$

Let P_D be the total system MW demand, i.e.,

$$P_D = P_R + P_L.$$

Since total change in generation equals the change in total system demand,

$$\Delta P_D = \sum_{i \in J_G} \Delta P_i = \Delta\lambda \sum_{i \in J_G} \left[\frac{1}{F_i''} \right] \quad (I.5)$$

Combining equations (I.4) and (I.5), the participation factors, γ_i^0 , for

each generating unit may be defined as,

$$\gamma_i^o = \frac{\Delta P_i}{\Delta P_D} = \frac{\left[\frac{1}{F_i''} \right]}{\sum_{j \in J_G} \left[\frac{1}{F_j''} \right]}, \quad i \in J_G \quad (1.6)$$

APPENDIX II

DERIVATIVES OF PROBLEM FUNCTIONS

In this appendix, the the evaluation of the first derivatives of the problem functions of the optimization problem NCP1 and NCP2 are shown.

Power Injections P_i, Q_i, S_i

$$P_i(\underline{V}, \underline{\delta}, \underline{t}) = \sum_{j=1}^N V_i V_j Y_{ij} \cos(\delta_i - \delta_j - \phi_{ij})$$

$$Q_i(\underline{V}, \underline{\delta}, \underline{t}) = \sum_{j=1}^N V_i V_j Y_{ij} \sin(\delta_i - \delta_j - \phi_{ij})$$

$$S_i(\underline{V}, \underline{\delta}, \underline{t}) = (P_i^2 + Q_i^2)^{1/2}$$

$i \neq j$

$$\frac{\partial P_i}{\partial \delta_j} = V_i V_j Y_{ij} \sin(\delta_i - \delta_j - \phi_{ij})$$

$$\frac{\partial P_i}{\partial V_j} = V_i Y_{ij} \cos(\delta_i - \delta_j - \phi_{ij})$$

$$\frac{\partial Q_i}{\partial \delta_j} = -V_i V_j Y_{ij} \cos(\delta_i - \delta_j - \phi_{ij})$$

$$\frac{\partial Q_i}{\partial V_j} = V_i Y_{ij} \sin(\delta_i - \delta_j - \phi_{ij})$$

$i = j$

$$\frac{\partial P_i}{\partial \delta_i} = - \sum_{j=1}^N V_i V_j Y_{ij} \sin(\delta_i - \delta_j - \phi_{ij}), \quad j \neq i$$

$$\frac{\partial P_i}{\partial V_i} = \sum_{j=1}^N V_j Y_{ij} \cos(\delta_i - \delta_j - \phi_{ij}) + 2V_i Y_{ii} \cos(\phi_{ii})$$

$$\frac{\partial Q_i}{\partial \delta_i} = \sum_{j=1}^N V_i V_j Y_{ij} \cos(\delta_i - \delta_j - \phi_{ij}), \quad j \neq i$$

$$\frac{\partial Q_i}{\partial V_i} = \sum_{j=1}^N V_j Y_{ij} \sin(\delta_i - \delta_j - \phi_{ij}) + 2V_i Y_{ii} \sin(-\phi_{ii})$$

If bus i is connected to bus j by a load tap-changing (LTC) transformer k , with tap t_k (tap on the i -side), the elements, \bar{Y}_{ij} , \bar{Y}_{ii} and \bar{Y}_{jj} of the bus admittance matrix are affected by t_k as follows:

$$\bar{Y}_{ij} = G_{ij} + jB_{ij} = -(g_{ij} + jb_{ij})/t_k$$

$$\bar{Y}_{ii} = \bar{Y}_{ii}' + (g_{ij} + jb_{ij})/t_k^2$$

$$\bar{Y}_{jj} = \bar{Y}_{jj}' + (g_{ij} + jb_{ij})$$

where

$\bar{y}_{ij} = (g_{ij} + jb_{ij})$ is the primitive admittance of the transformer.

The derivatives of the power injected at the buses i and j with respect to t_k may be evaluated as follows:

$$\frac{\partial P_i}{\partial t_k} = -\frac{e_i}{t_k}(e_j G_{ij} - f_j B_{ij}) - \frac{f_i}{t_k}(f_j G_{ij} + e_j B_{ij}) + 2V_i^2 G_{ij}/t_k^2$$

$$\frac{\partial P_j}{\partial t_k} = -\frac{e_j}{t_k}(e_i G_{ij} - f_i B_{ij}) - \frac{f_j}{t_k}(f_i G_{ij} + e_i B_{ij})$$

$$\frac{\partial Q_i}{\partial t_k} = -\frac{f_i}{t_k}(e_j G_{ij} - f_j B_{ij}) + \frac{e_i}{t_k}(f_j G_{ij} + e_j B_{ij}) - 2V_i^2 B_{ij}/t_k^2$$

$$\frac{\partial Q_j}{\partial t_k} = -\frac{f_j}{t_k}(e_i G_{ij} - f_i B_{ij}) + \frac{e_j}{t_k}(f_i G_{ij} + e_i B_{ij})$$

The derivatives of the MVA power S_i with respect to the variables may be evaluated as

$$\frac{\partial S_i}{\partial \delta_n} = \frac{1}{S_i} \left(P_i \frac{\partial P_i}{\partial \delta_n} + Q_i \frac{\partial Q_i}{\partial \delta_n} \right)$$

The derivatives of S_i with respect to the other variables may be evaluated in the same fashion as shown above.

Objective Function

$$-S_T(\underline{V}, \underline{\delta}, \underline{t}, \underline{\gamma}) = \sum_{j \in J_L} S_j = \sum_{j \in J_L} (P_j^2 + Q_j^2)^{1/2}$$

$$\frac{\partial S_T}{\partial V_i} = \sum_{j \in J_L} \frac{\partial S_j}{\partial V_i}, \quad i = 1, 2, \dots, N$$

The derivatives of S_T with respect to the elements of $\underline{\delta}$ and \underline{t} may be evaluated in the same way. S_T does not depend on the participation factors.

Therefore,

$$\frac{\partial S_T}{\partial \gamma_i} = 0 \quad i = M+1, \dots, N$$

Constraint Functions

$$(1) \beta_i S_T(\underline{V}, \underline{\delta}, \underline{t}, \gamma) - S_i(\underline{V}, \underline{\delta}, \underline{t}, \gamma) = C_i, \quad i \in J_L$$

$$\frac{\partial C_i}{\partial V_j} = \beta_i \frac{\partial S_T}{\partial V_j} - \frac{\partial S_i}{\partial V_j}, \quad i \in J_L, \quad j=1, \dots, N$$

The derivatives of C_i with respect to the elements of $\underline{\delta}$ and \underline{t} is evaluated in the same manner. C_i does not depend on γ , i.e.,

$$\frac{\partial C_i}{\partial \gamma_k} = 0 \quad i \in J_L, \quad k = M+1, \dots, N$$

$$(4) f_i(\underline{V}, \underline{\delta}, \underline{t}, \gamma) = \gamma_i P_D - \gamma_i P_D^{initial} - P_i + P_i^{initial} = 0,$$

$$i = M+1, \dots, N-1$$

where

$$P_D(\underline{V}, \underline{\delta}, \underline{t}, \gamma) = \sum_{j=M+1}^N P_j$$

$$\frac{\partial f_i}{\partial V_j} = \gamma_i \frac{\partial P_D}{\partial V_j} - \frac{\partial P_i}{\partial V_j} \quad j = 1, 2, \dots, N$$

The derivatives of f_i with respect to elements of $\underline{\delta}$ and \underline{t} are evaluated in the same manner.

$$\frac{\partial f_i}{\partial \gamma_i} = P_D - P_D^{initial} \quad i = M+1, \dots, N$$

$$(5) P_i(\underline{V}, \underline{\delta}, \underline{t}, \underline{\gamma}) - pf_i S_i(\underline{V}, \underline{\delta}, \underline{t}, \underline{\gamma}) = K_i, \quad i \in J_L$$

$$\frac{\partial K_i}{\partial V_j} = \frac{\partial P_i}{\partial V_j} - pf_i \frac{\partial S_i}{\partial V_j} \quad i \in J_L, \quad j = 1, 2, \dots, N$$

The derivatives of K_i with respect to $\underline{\delta}$ and \underline{t} are evaluated in the same manner. Again, the participation factors are not involved, i.e.,

$$\frac{\partial K_i}{\partial \gamma_j} = 0 \quad i \in J_L, \quad j = M+1, \dots, N-1$$

APPENDIX III

DATA FOR EXAMPLE SYSTEMS

Data for the three example systems used in this thesis are provided in this appendix. The first of the systems is the AEP 14-bus network [67], the second is a 28-bus sample system given in reference [29], and the third is a 20-bus system given in reference [49].

14-Bus Network

The AEP 14-bus network is as shown in Figure III.1. The system includes two generating units, three synchronous condensers, and twenty transmission lines/transformers. The bus data is shown in Table III.1 and III.2. Table III.3 shows the line/transformer data. Table III.4 shows the data for the generating unit cost functions.

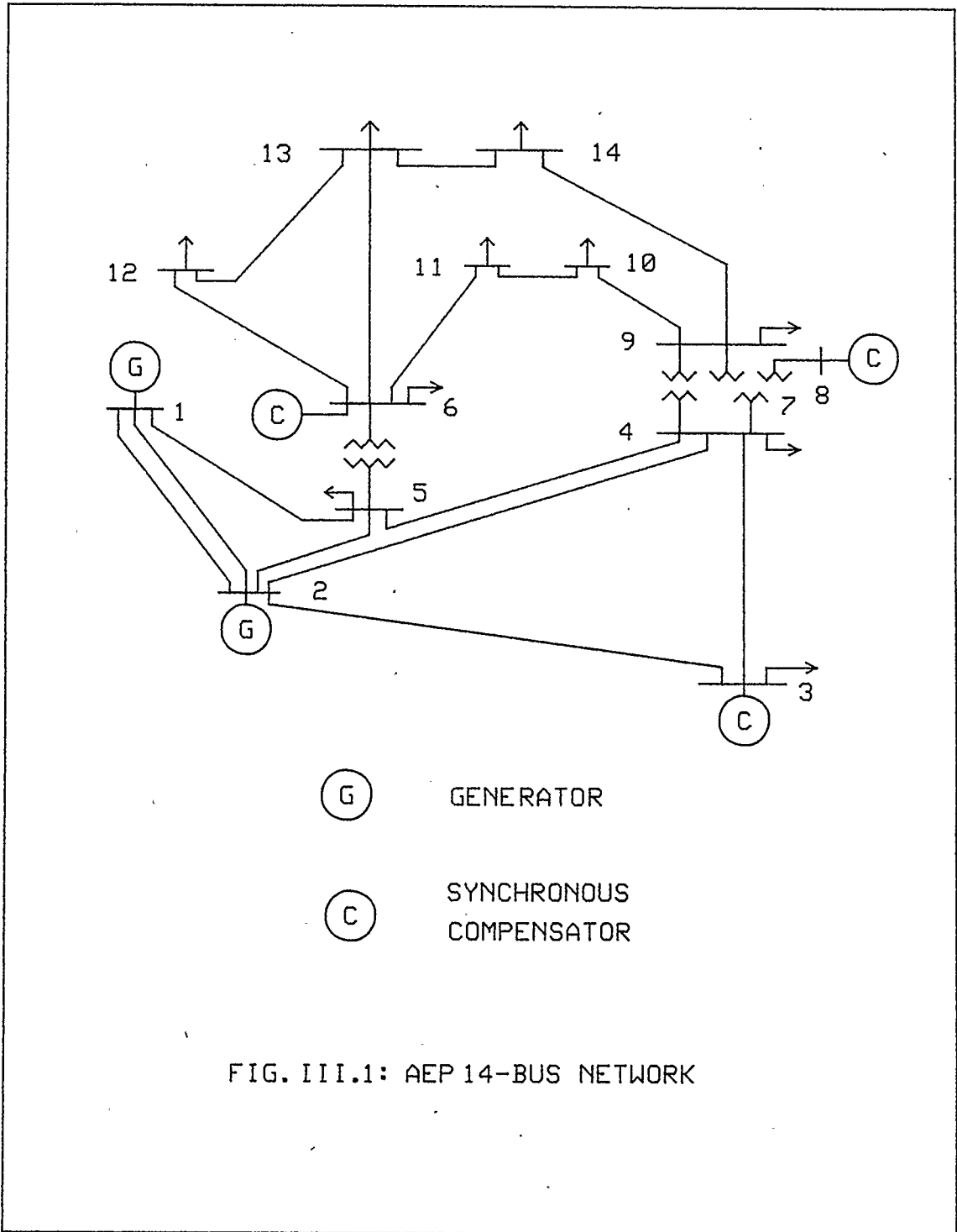


Table III.1. Initial Operating Condition of the 14-bus Network

Bus No.	Bus Voltage		Bus Power*		Static Suscep.
	Mag.	Ang.	MW	MVAR	
1	1.060	0.0	-	-	0.19
2	1.045	0.0	40.0	0.0	
3	1.000	0.0	-94.2	-19.0	
4	1.000	0.0	-57.8	-23.9	
5	1.000	0.0	-47.6	-1.6	
6	1.070	0.0	0.0	0.0	
7	1.000	0.0	0.0	0.0	
8	1.090	0.0	0.0	0.0	
9	1.000	0.0	-29.5	-16.6	
10	1.000	0.0	-29.5	-5.8	
11	1.000	0.0	-13.5	-5.8	
12	1.000	0.0	-36.1	-1.6	
13	1.000	0.0	-23.5	-5.8	
14	1.000	0.0	-14.9	-5.0	

* -ve for loads

Table III.2. Regulated Bus Data

Bus No.	MVAR	Limits	MW	Limits
	Min.	Max.	Min.	Max.
2	-40.0	50.0	30.0	70.0
6	-6.0	24.0	0.0	0.0
8	-6.0	24.0	0.0	0.0

Table III.3 Line and Transformer Data (14-Bus Network)

Line No	Line Conn.	Impedance		Charging p.u.	LTC Tap
		R	X		
1	1-2	0.01938	0.05917	0.0264	
2	1-5	0.05403	0.22304	0.0246	
3	2-3	0.04699	0.19797	0.0219	
4	2-4	0.05811	0.17632	0.0187	
5	2-5	0.05695	0.17388	0.0170	
6	3-4	0.06701	0.17103	0.0173	
7	4-5	0.01335	0.04211	0.0064	
8	4-7	0	0.20912	0	0.978
9	4-9	0	0.55618	0	0.969
10	5-6	0	0.25202	0	0.932
11	6-11	0.09498	0.19890	0	
12	6-12	0.12291	0.25581	0	
13	6-13	0.06615	0.13027	0	
14	7-8	0	0.17615	0	
15	7-9	0	0.11001	0	
16	9-10	0.03181	0.08450	0	
17	9-14	0.12711	0.27038	0	
18	10-14	0.08205	0.19207	0	
19	12-13	0.22092	0.19988	0	
20	13-14	0.17093	0.34802	0	

Table III.4. Cost of Generation *

Unit(i)	c_i	b_i	a_i
1	0.0060	2.0	140
2	0.0075	1.5	120

$$* F_i = a_i + b_i P_i + c_i P_i^2 \quad \text{/hour}$$

28-Bus Network

The 28-bus network taken from reference [29] is shown in Figure III.2. The system includes six generating units, and thirty-two transmission lines. The bus data are shown in Tables III.5 and III.6. Table III.7 shows the line data and Table III.8 the generating units cost functions.

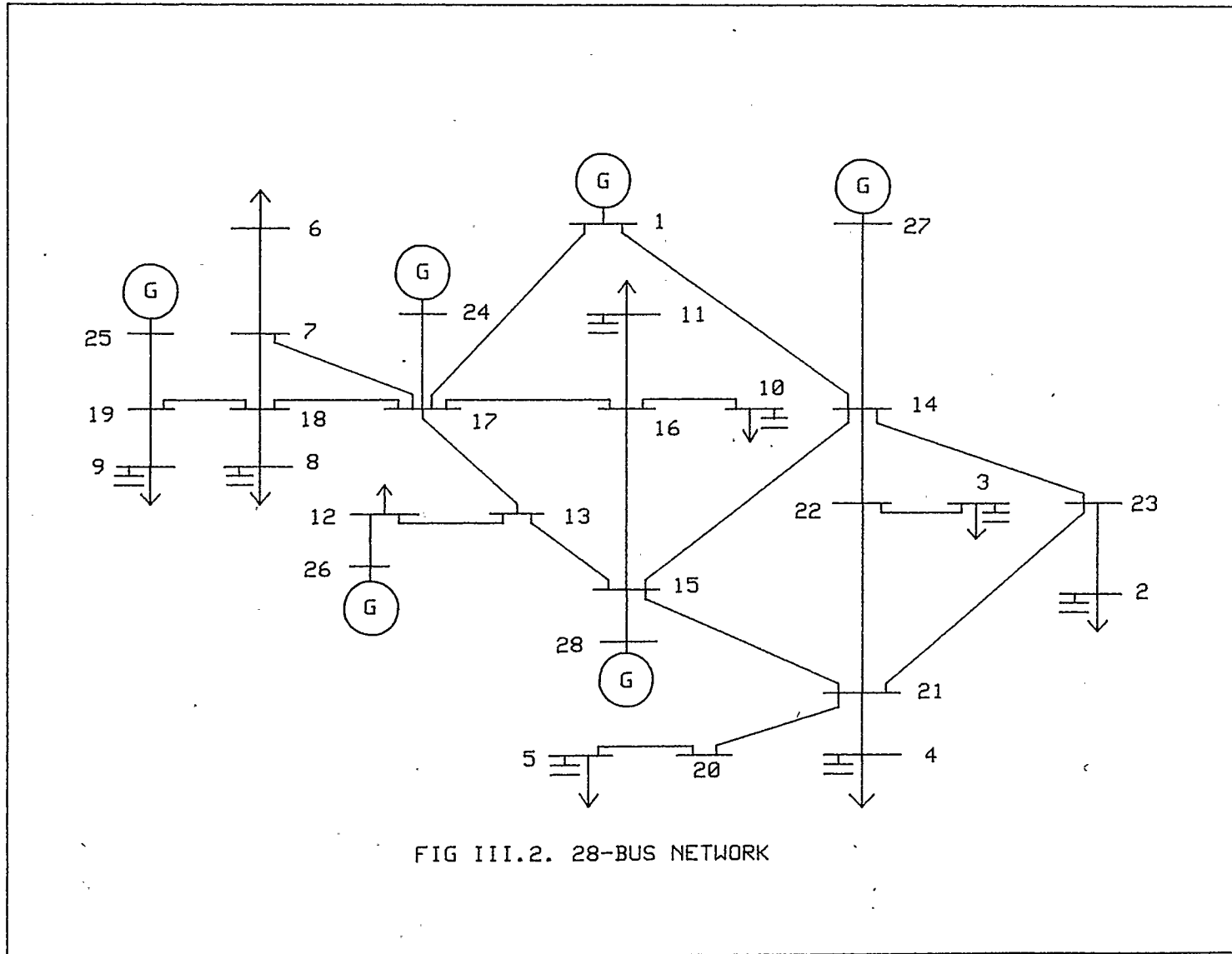


FIG III.2. 28-BUS NETWORK

Table III.5. Initial Operating Condition of the 28-bus Network

Bus No.	Bus Voltage		Bus Power*		Static Suscep.
	Mag.	Ang.	MW	MVAR	
1	1.050	0.0	-	-	
2	1.000	0.0	-145.0	-50.0	1.2169
3	1.000	0.0	-265.0	-22.0	1.4252
4	1.000	0.0	-381.0	-26.0	2.0804
5	1.000	0.0	-384.0	-2.0	1.6965
6	1.000	0.0	-374.0	-34.0	1.5422
7	1.000	0.0	-129.0	-3.0	
8	1.000	0.0	-135.0	-58.0	1.0042
9	1.000	0.0	-60.8	-7.0	0.2080
10	1.000	0.0	-118.0	-18.0	0.6476
11	1.000	0.0	-75.0	-44.0	0.7768
12	1.000	0.0	-139.0	-52.0	0.5868
13	1.000	0.0			
14	1.000	0.0			
15	1.000	0.0			
16	1.000	0.0			
17	1.000	0.0			
18	1.000	0.0			
19	1.000	0.0			
20	1.000	0.0			
21	1.000	0.0			
22	1.000	0.0			
23	1.000	0.0			
24	1.050	0.0	191.0	-	
25	1.050	0.0	440.0	-	
26	1.050	0.0	49.0	-	
27	1.050	0.0	390.0	-	
28	1.050	0.0	152.0	-	

* -ve for loads

Table III.6.: Regulated Bus Data (28-Bus Network)

Bus No.	MVAR Min.	Limits Max.	MW Min.	Limits Max.
24	-100.0	250.0	45.0	350.0
25	-100.0	250.0	100.0	440.0
26	-40.0	60.0	30.0	80.0
27	-200.0	250.0	100.0	440.0
28	-100.0	200.0	60.0	250.0

Table III.7. Cost of Generation* (28-Bus Network)

Unit(i)	c_i	b_i	a_i
1	0.00176	7.081	1285.0
24	0.00350	7.900	400.0
25	0.00227	6.950	750.0
26	0.00389	10.930	200.0
27	0.00250	8.400	325.0
28	0.00260	7.550	313.0

$$* F_i = a_i + b_i P_i + c_i P_i^2 \quad \text{/hour}$$

Table III.8. Line and Transformer Data (28-Bus Network)

Line No	Line Conn.	Impedance		Charging p.u.	LTC Tap
		R	X		
1	2-23	0.0140	0.0700		
2	3-22	0.0078	0.0390		
3	4-21	0.0058	0.0290		
4	5-20	0.0054	0.0270		
5	6-7	0.0070	0.0350		
6	7-17	0.0062	0.0310		
7	7-18	0.0010	0.0050		
8	8-18	0.0196	0.0980		
9	9-19	0.0280	0.1400		
10	10-16	0.0118	0.0590		
11	11-16	0.0294	0.1470		
12	12-13	0.0280	0.1400		
13	12-26	0.0258	0.1290		
14	13-15	0.0220	0.1100		
15	13-17	0.0062	0.0310		
16	14-15	0.0060	0.0300		
17	14-22	0.0296	0.1480		
18	14-23	0.0242	0.1210		
19	14-27	0.0070	0.0350		
20	14-1	0.0200	0.1000		
21	15-16	0.0068	0.0340		
22	15-21	0.0038	0.0190		
23	15-28	0.0112	0.0560		
24	16-17	0.0220	0.1100		
25	17-18	0.0054	0.0270		
26	17-24	0.0070	0.0350		
27	17-1	0.0054	0.0270		
28	18-19	0.0072	0.0360		
29	19-25	0.0104	0.0520		
30	20-21	0.0038	0.0190		
31	21-22	0.0076	0.0380		
32	21-23	0.0128	0.0640		

20-Bus System

The 20-bus network taken from reference [49] is shown in Figure III.3. The system includes six generating units, and twenty-seven transmission lines. The bus data are shown in Tables III.9 and III.10. Table III.11 shows the line data.

Table III.9: Initial Operating Condition of the 20-bus Network

Bus No.	Bus Voltage		Bus Power*		Static Suscep.
	Mag.	Ang.	MW	MVAR	
1	1.050	0.0	-	-	
2	1.020	0.0	384.0	0.0	
3	1.020	0.0	384.0	0.0	
4	1.000	0.0	0.0	0.0	
5	1.000	0.0	0.0	0.0	
6	1.000	0.0	-153.0	-80.0	
7	1.000	0.0	-563.0	-430.0	
8	1.025	0.0	308.0	0.0	
9	1.000	0.0	0.0	0.0	
10	1.000	0.0	-174.0	-77.0	
11	1.000	0.0	0.0	0.0	
12	1.000	0.0	-715.0	-381.0	
13	1.020	0.0	410.0	0.0	
14	1.000	0.0	0.0	0.0	
15	1.000	0.0	0.0	0.0	
16	1.000	0.0	0.0	0.0	
17	1.000	0.0	-171.0	-75.0	
18	1.000	0.0	0.0	0.0	
19	1.000	0.0	0.0	0.0	
20	1.020	0.0	51.0	0.0	

* -ve for loads

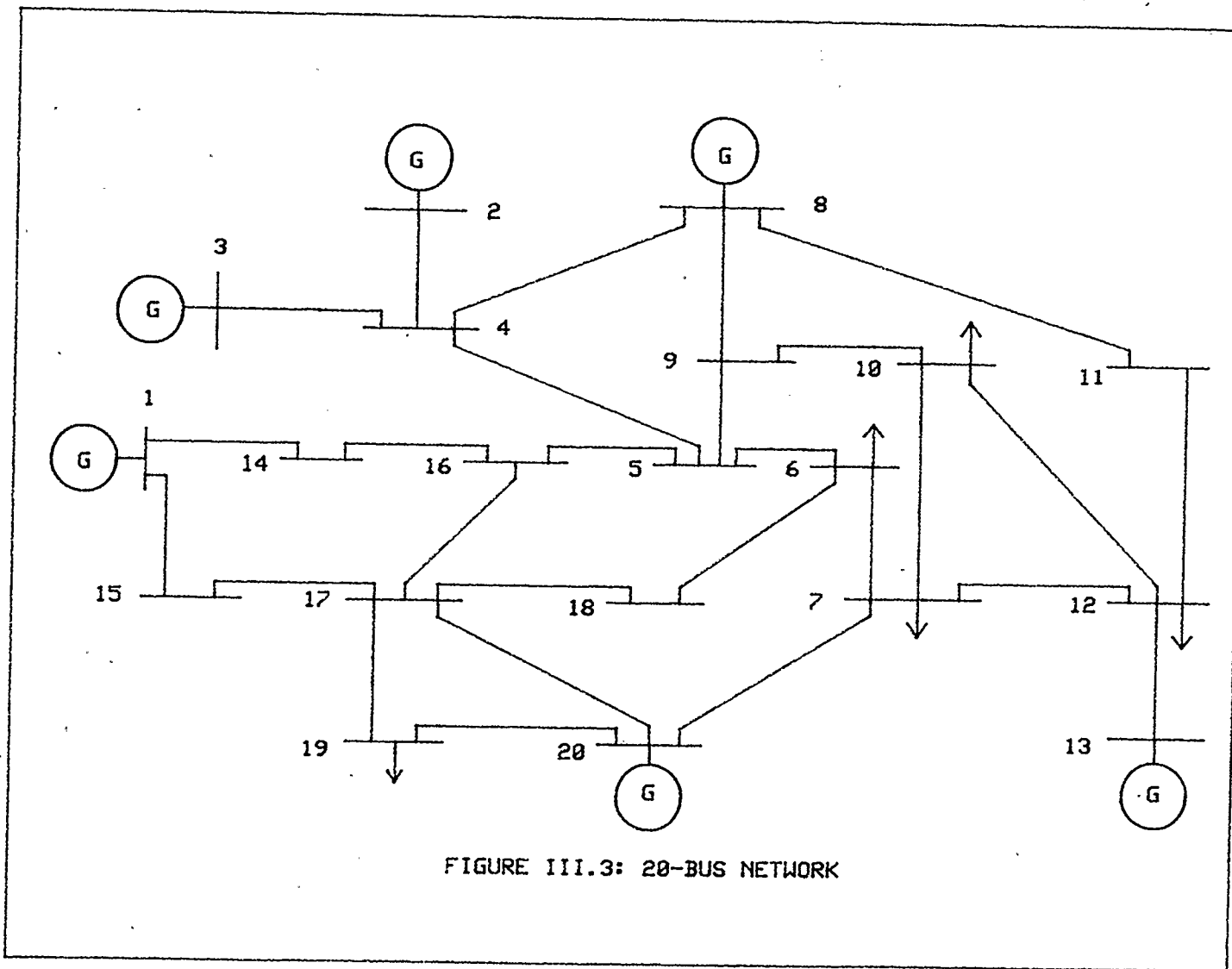


FIGURE III.3: 20-BUS NETWORK

Table III.10.: Regulated Bus Data (20-Bus Network)

Bus No.	MVAR Min.	Limits Max.	MW Min.	Limits Max.
2	-100.0	600.0	150.0	750.0
3	-100.0	600.0	150.0	750.0
8	-100.0	400.0	175.0	550.0
13	0.0	600.0	220.0	700.0
20	0.0	80.0	15.0	100.0

Table III.11. Line and Transformer Data (20-Bus Network)

Line No	Line Conn.	Impedance		Charging p.u.	LTC Tap
		R	X		
1	1-14	0.0015	0.0250		
2	1-15	0.0015	0.0080		
3	2-4	0.0015	0.0100		
4	3-4	0.0015	0.0100		
5	4-5	0.0013	0.0230	7.00	
6	4-8	0.0010	0.0150	1.20	
7	5-6	0.0	0.0050		
8	5-9	0.0008	0.0100	0.95	
9	5-16	0.0030	0.0300	2.50	
10	6-7	0.0030	0.0270	0.30	
11	6-18	0.0010	0.0120	0.03	
12	7-10	0.0040	0.0420	0.10	
13	7-12	0.0003	0.0030	0.09	
14	7-20	0.0027	0.0220	0.30	
15	8-9	0.0020	0.0250	2.00	
16	8-11	0.0030	0.0300	2.50	
17	9-10	0.0	0.0100		
18	10-12	0.0025	0.0225	0.16	
19	11-12	0.0015	0.0100		
20	12-13	0.0015	0.0100		
21	14-16	0.0060	0.0540	0.09	
22	15-17	0.0030	0.0270	0.18	
23	16-17	0.0	0.0100		
24	17-18	0.0035	0.0300	0.07	
25	17-19	0.0030	0.0250	0.06	
26	17-20	0.0060	0.0500	0.12	
27	19-20	0.0030	0.0250	0.06	